

UNIVERSIDAD DE SONORA

DIVISIÓN DE CIENCIAS BIOLÓGICAS Y DE LA SALUD

Departamento de Investigación y Posgrado en Alimentos

Programa de Posgrado en Ciencias y Tecnología de los Alimentos

**Actividad quimioprotectora y posible aplicación nanotecnológica de
lípidos aislados del músculo de camarón de cultivo (*Litopenaeus*
vannamei) y silvestre (*L. stylirostris*)**

TESIS

Como requisito parcial para obtener el grado de:

DOCTOR EN CIENCIAS DE LOS ALIMENTOS

Presenta:

M. C. Joel Said García Romo

APROBACIÓN

Actividad quimioprotectora y posible aplicación nanotecnológica de lípidos aislados del músculo de camarón de cultivo (*Litopenaeus vannamei*) y silvestre (*L. stylirostris*)

M.C. Joel Said García Romo

Dr. Armando Burgos Hernández

Director de la tesis

Dra. Maribel Plascencia Jatomea

Miembro del comité de tesis

Dra. Rosario Maribel Robles Sánchez

Miembro del comité de tesis

Dra. María Guadalupe Burboa Zazueta

Miembro del comité de tesis

Dr. Josué Elías Juárez Onofre

Miembro del comité de tesis

Hermosillo

Febrero de 2020

DERECHOS DE AUTOR

El presente trabajo de tesis se presenta como uno de los requisitos parciales para la obtención del grado de **Doctor en Ciencias de los Alimentos** de la Universidad de Sonora.

Se deposita en la biblioteca del Departamento de Investigación y Posgrado en Alimentos para ponerla a disposición de los interesados. Se permiten citas breves del material contenido en la tesis sin permiso del autor, siempre y cuando se otorgue el crédito correspondiente. Para reproducir, o en su caso referirse a este documento en forma parcial o total, se deberá solicitar la autorización al Coordinador del Programa del Posgrado.

Bajo cualquier otra circunstancia se debe solicitar permiso directamente al autor.

Atentamente

Joel Said García Romo

Dra. Carmen María López Sainz

Coordinadora del Programa de Posgrado

Hermosillo

Febrero de 2020

AGRADECIMIENTOS

Los autores desean agradecer a la Universidad de Sonora por hacer uso de sus instalaciones y por la excelente formación académica durante los 4.5 años de estudio; además, al Consejo Nacional de Ciencia y Tecnología (CONACYT) de México por financiar la investigación (proyecto No. 241133).

CONTENIDO

APROBACIÓN	ii
DERECHOS DE AUTOR	iii
AGRADECIMIENTOS	iv
CONTENIDO	v
INTRODUCCIÓN	1
JUSTIFICACIÓN	6
HIPÓTESIS	7
DESARROLLO DEL TRABAJO DE INVESTIGACIÓN	8
Descripción Del Capítulo I	8
Descripción Del Capítulo II	8
Descripción del capítulo III	8
Descripción Del Capítulo IV	8
Descripción Del Capítulo V	9
CAPÍTULO I	10
Antioxidant, Antihemolysis, and Retinoprotective Potentials of Bioactive Lipidic Compounds from Wild Shrimp (<i>Litopenaeus Stylirostris</i>) Muscle	10
CAPÍTULO II	5
Isolation and Identification of A New Antiproliferative Indolocarbazole Alkaloid Derivative Extracted from Farmed Shrimp (<i>Litopenaeus Vannamei</i>) Muscle	5
CAPÍTULO III	29
An Indolocarbazole Alkaloid Derivative Isolated from <i>Litopenaeus Stylirostris</i> Mediates Anti-Proliferative / Pro-Apoptotic Responses and Induce ROS Production on Human Epithelial Prostate Carcinoma Cells	29
CAPÍTULO IV	55
Evaluation of Anti-Inflammatory-Related Activity of a Bioactive Fraction (Constituted By a Novel Indolocarbazole Alkaloid Derivative, a Polyunsaturated Fatty Acid and an Ester of Phthalic Acid Type) Isolated from <i>Litopenaeus Stylirostris</i>	55
CAPÍTULO V	75
Cytotoxic Evaluation of EPA-Loaded PLGA-PVA Nanoparticles against Human Prostate Carcinoma Cell Line <i>in Vitro</i>	76
CONCLUSIONES GENERALES	100
RECOMENDACIONES	101

INTRODUCCIÓN

El cáncer es la segunda causa de muerte a nivel mundial; en el 2018, causó 9.6 millones de muertes y casi una de cada seis muertes se debe a esta enfermedad (“WHO | Cancer,” 2019) y se prevé un aumento de 22.2 millones de casos nuevos por año para el 2030 (Bray, Jemal, Grey, Ferlay, y Forman, 2012). Sin embargo, muchos tipos de cánceres pueden prevenirse evitando la exposición a factores de riesgo comunes como infecciones por microorganismos, alto consumo de grasas, tabaquismo, factores hereditarios, etc. (Alberts et al., 2010). Aun así, una vez desarrollada esta enfermedad, instituciones académicas y farmacéuticas han desarrollado una serie de compuestos quimioterapéuticos, estos ayudan a retrasar de alguna forma su progresión, pero su ineficacia y efectos adversos son limitaciones para su uso (Buzdar et al., 2005; DeVita & Chu, 2008; Martin et al., 2014). Otro problema en la quimioterapia contra el cáncer, es la resistencia que adquieren ciertas células a la terapia (Austreid, Lonning, & Eikesdal, 2014). Por todo esto, la constante búsqueda de moléculas bioactivas más efectivas y seguras gana importancia con el paso de los años (Livstone, 2019).

Estudios epidemiológicos han ido proporcionando evidencia de la potencia bioactiva de compuestos aislados de fuentes naturales, esto debido a que el 70 % de todos los medicamentos aprobados han sido de productos naturales (Li, 2016). Sin embargo, la búsqueda de nuevos productos bioactivos naturales no es una tarea fácil; hay muchos desafíos a lo largo del proceso de obtención de nuevos medicamentos efectivos y eficientes y a pesar de eso, varias organizaciones han decidido reducir las tasas de mortalidad y morbilidad mediante investigaciones relacionadas con el cáncer (De Kok, Van Breda, & Manson, 2008; Thomson, LeWinn, Newton, Alberts, & Martinez, 2003). Hoy en día la búsqueda de estas nuevas moléculas está enfocada en el medio marino y varios estudios han informado la existencia de posibles compuestos anti-cancerígenos (Lordan, Ross, & Stanton, 2011; Stankevics, Aiub, Maria, Lobo-Hajdu, & Felzenszwalb, 2008). Los productos marinos naturales (MNP) han llamado la atención de los científicos por su potencial aplicación en la industria alimentaria (Claeson & Bohlin, 1997; König & Wright, 1996; Newman, Cragg, & Snader, 2000). Hasta el año 1995, solo aproximadamente 6500 productos naturales marinos habían sido descritos en

archivos científicos; sin embargo, para el 2017, se han informado más de 19000 compuestos (Ciavatta et al., 2017).

El ecosistema marino representa la mayoría de la superficie del planeta y comprende un recurso continuo de compuestos con compuestos anti-cancerígenos, esto debido a condiciones diferentes y a veces extremas, los organismos dentro de este entorno pueden producir metabolitos con características estructurales que los diferencian de los de otras fuentes naturales y muestran un gran potencial biotecnológico (Braekman & Daloze, 1986; Stankevicius et al., 2008). Debido a lo anterior, los organismos marinos han sido considerados fuentes importantes de compuestos anti-cancerígenos y entre estas actividades con gran valor para la prevención o el tratamiento del cáncer están: anti-mutagénica, anti-proliferativa, anti-inflamatoria, anti-tumoral, anti-angiogénica, anti-neoplásica, entre otras (Gerwick & Moore, 2012). Con base en estos argumentos, varios autores apoyan la idea de que los metabolitos secundarios de los organismos marinos son mucho más propensos a producir medicamentos contra el cáncer que otras fuentes (Fahmy, 2013). Dentro de los organismos marinos se incluyen microorganismos como bacterias y hongos, así como de esponjas, algas y ciertos organismos superiores como moluscos, bivalvos, tunicados y crustáceos (Gerwick & Moore, 2012; Montaser & Luesch, 2011; Newman & Cragg, 2014).

Anteriormente, se ha reportado que el camarón (un crustáceo) uno de los mariscos más populares del mundo, contiene posibles compuestos anticancerígenos en su fracción lipídica (López-Saiz et al., 2016; López-Saiz, Suárez-Jiménez, Plascencia-Jatomea, & Burgos-Hernández, 2013; Wilson-Sanchez et al., 2010). Los ejemplos de estos compuestos presentes en el camarón incluyen carotenoides, que se han asociado con la inducción de apoptosis y la promoción del estrés oxidativo en líneas celulares de cáncer (Sila et al., 2013; Sowmya, Arathi, Vijay, Baskaran, & Lakshminarayana, 2017). Además, la hemocianina se ha informado como un inhibidor del crecimiento celular canceroso y un inductor de apoptosis (Zheng et al., 2016) y para ejercer anti-tumoral en estudios *in vivo* (Liu et al., 2017), así como de un triglicérido esterificado con ácidos grasos poliinsaturados con la capacidad de inhibir la proliferación de una línea celular de linfoma murino (López-Saiz et al., 2014).

El camarón blanco (*Litopenaeus vannamei*) es la especie más consumida entre los crustáceos (53 % del total de especies de crustáceos producidos en la acuicultura mundial en 2016), esto debido a que es la especie por excelencia para cultivos en granjas acuícolas; es por ello que es la especie más estudiada, siendo responsable de casi todos los informes de compuestos relacionados con actividad anti-cancerígena (Brito et al., 2018; Da Silva et al., 2015; Liu et al., 2018, 2017; López-Saiz et al., 2016, 2014; Meng et al., 2014; Poonsin et al., 2018; Sinthusamran, Benjakul, Kijroongrojana, Prodpran, & Kishimura, 2018; Wilson-Sanchez et al., 2010). Sin embargo, actualmente el camarón salvaje (*Litopenaeus stylirostris*) es uno de los más consumidos entre las poblaciones cercanas a las bahías (FAO, 2018); así mismo también existe una nula información acerca de la composición química, calidad nutricional y posibles agentes con potencial anti-cancerígeno.

Es por ello, que uno de los objetivos del presente estudio fue estudiar fracciones con potencial quimioprotector, tanto en camarón de cultivo *L. vannamei* como en camarón silvestre *L. stylirostris* y así poder hacer comparaciones entre los compuestos bioactivos presentes entre ambos. Por último, una vez de haber realizado la caracterización biológica es necesario saber que dichos compuestos obtenidos presentan problemas propios de moléculas de carácter lipídico y en general de fármacos de uso terapéutico. Un parámetro problemático está en relación a la concentración terapéutica; a nivel *in vitro* las células responden de cierta manera a estímulos y en la mayoría de las veces cuando se lleva a cabo la caracterización biológica, se buscan concentraciones en las cuales se inhiban el mayor número de células cancerosas; sin embargo, para alcanzar esta inhibición, muchas veces es necesario elevar la concentración del fármaco y así mismo también ser citotóxicas para células no-cancerosas (Shoemaker, 2006). Para esto mismo se determinó un término llamado “bioselectividad”, este se usa para referirse a un compuesto que muestra efectos inhibitorios diferenciales entre líneas celulares cancerosas y no-cancerosas (Ciavatta et al., 2017). Conjuntamente, dejando de lado la bioselectividad, el beneficio exitoso para la salud y las actividades anti-cancerígenas mencionadas anteriormente de los compuestos con actividad quimioprotectores de carácter lipídico se ve obstaculizado por su alta susceptibilidad al deterioro oxidativo (Arab-Tehrany et al., 2012; Romeu-Nadal, Castellote, & López-Sabater, 2004).

Algunos de los parámetros que inducen el deterioro oxidativo son el oxígeno, la luz, el calentamiento, la irradiación UV y, en general, los radicales libres, los cuales aceleran la oxidación de los lípidos, disminuyendo la estabilidad y la vida útil (Johnson & Decker, 2015; Shahidi & Zhong, 2010). La oxidación de los lípidos por los radicales libres no solo ocurre en el medio ambiente, estos ocurren constantemente en el cuerpo humano (Aruoma, 1998); esto significa que si uno de los compuestos con actividad quimioprotectores de carácter lipídico pertenecientes al camarón ingresa al sistema sanguíneo, puede ser oxidado por radicales fisiológicos y luego modificar la homeostasis celular causando efectos adversos para la salud (Lobo, Patil, Phatak, & Chandra, 2010). Por eso que, la baja estabilidad oxidativa de los lípidos requiere una barrera eficaz de protección antioxidante para evitar el deterioro oxidativo (Jacobsen et al., 2001).

Actualmente, en el área de suplementación farmacéutica, algunos fármacos se usan cubiertos con softgel (una cubierta / cápsula), que consiste en una cubierta a base de gelatina que rodea un relleno líquido (Steele & Dietel, 1993); esta cubierta / cápsula resuelve problemas relacionados con la oxidación debido a factores ambientales, además de ayudar a proporcionar una mayor biodisponibilidad ya que algunos fármacos no pueden ser fácilmente absorbidos en el tracto gastrointestinal (Gullapalli, 2010). Sin embargo, una vez que el medicamento ingresa al torrente sanguíneo, los problemas de oxidación de lípidos comienzan por la acción de los radicales libres fisiológicos (Carocho, Morales, & Ferreira, 2018), y es por eso que se requiere una forma de protección del fármaco dentro del sistema sanguíneo.

Hasta este punto, se ha descrito que la ciertos compuestos obtenidos de organismos marinos puede actuar en beneficio de la salud, induciendo un efecto anti-cancerígeno; sin embargo, debido a sus características fisicoquímicas, su débil bioselectividad y su oxidación, puede conducir a efectos contra la salud humana y es por eso que actualmente existen tecnologías emergentes que surgen de estas mismas necesidades, como lo es la nanotecnología. Por definición, la nanotecnología se refiere al estudio de sistemas que se encuentran en el rango dimensional de tamaño de 1 a 1,000 nm (Ferrari, 2005) y existen diferentes sistemas de nanotecnología que están relacionados con el cáncer, esto incluye nano-vectores de administración inyectable, como los liposomas para la terapia del cáncer de mama (Malam, Loizidou, & Seifalian, 2009; Park, 2002), así como sistemas de polímeros biodegradables (Hans

& Lowman, 2002); ejemplos de ellos son: PLGA (Bala, Hariharan, & Kumar, 2004), quitosano (Wang et al., 2011), entre otros.

Es por todo esto, que otro objetivo de este estudio fue evaluar la unión de uno de los lípidos bioactivos presentes en el camarón con actividad anti-cancerígena, a un polímero sintético biodegradable y no tóxico; esto, utilizando una mezcla de polímeros de PLGA-EPA y evaluarlo en un tipo de carcinoma humano con el fin de observar un efecto citotóxico.

JUSTIFICACIÓN

El cáncer se posiciona como una de las enfermedades más mortíferas a nivel mundial y, a pesar de tener hospitales oncológicos y centro de investigaciones, la sociedad científica alienta al constante descubrimiento de nuevas terapias químicas, esto debido al hecho de que actualmente los fármacos son relativamente tóxicos y hasta cierto punto ineficaces, esto se da por un incremento de la resistencia de las células cancerígenas al uso prolongado de los mismos. Estudios epidemiológicos han proporcionado evidencia de la naturaleza bioactiva de compuestos aislados y purificados de fuentes marinas para la inhibición de procesos carcinogénicos y una de estas fuentes de dichos compuestos es el camarón. Así mismo, estos compuestos deberían superar ciertas barreras biológicas antes de ejercer su acción anticarcinogénica (quimioprotectora); es por ello, que la utilización de la nanotecnología pudiera ser una herramienta emergente capaz de acentuar su actividad (haciéndolo menos tóxico y más eficaz).

HIPÓTESIS

Los compuestos lipídicos aislados del músculo de camarón tendrán actividad quimioprotectora, la cual no será eliminada por su encapsulamiento.

DESARROLLO DEL TRABAJO DE INVESTIGACIÓN

El trabajo de investigación está dividido en 5 capítulos, cada uno de ellos representa un artículo publicado, enviado o próximo a enviar para su publicación en revista indizada en el Journal Citation Reports (JCR) del Institute of Scientific Information de la base de datos Thomson-Reuters.

Descripción Del Capítulo I

En este capítulo se evidencia el potencial antioxidante, antihemolítico y retinoprotector de una fracción cromatográfica obtenida a partir de extractos lipídicos del músculo del camarón silvestre (*Litopenaeus stylirostris*) la cual, tras su caracterización químico-estructural, se reveló que esta compuesta por tres principales lípidos: un nuevo indolocarbazole derivado de alcaloide, un ácido graso poliinsaturado omega-3 (ácido eicosapentaenoico) y un éster del tipo ácido ftálico (dioctil ftalato).

Descripción Del Capítulo II

En este capítulo se aisló e identificó de un nuevo el indolocarbazole derivado de alcaloide antiproliferativo, extraído esta vez del músculo de camarón de cultivo (*Litopenaeus vannamei*); el seguimiento biológico descrito se realizó utilizando cinco líneas celulares cancerosas y una no cancerosa, resultado el carcinoma de próstata humano el más sensible de todas ellas.

Descripción del capítulo III

Este capítulo describe como el nuevo indolocarbazole derivado de alcaloide (aislado del músculo de *Litopenaeus stylirostris*), media las respuestas anti-proliferativa / pro-apoptóticas e induce la producción de ROS en células de carcinoma de próstata humano.

Descripción Del Capítulo IV

El capítulo trata sobre la evaluación relacionada con la actividad anti-inflamatoria de la misma fracción bioactiva (aislada de *Litopenaeus stylirostris*) que anteriormente resultó anti-oxidante

y anti-proliferativa / pro-apoptótica y que está constituida por: el indolocarbazole derivado alcaloide, el ácido graso poliinsaturado y el éster del tipo ácido ftálico), resultando el indolocarbazole responsable de la disminución de especies reactivas de nitrógeno (NRS, por sus siglas en Inglés) y de oxígeno (ROS, por su siglas en Inglés), mientras que el ácido graso poliinsaturado resultó ser responsable de disminuir la producción de NO y regular citocinas anti- y pro-inflamatorias.

Descripción Del Capítulo V

Este último capítulo se describe la elaboración de nanopartículas citotóxicas de PLGA-PVA cargadas con ácido graso poliinsaturado omega-3 (ácido eicosapentaenoico) y la evaluación de su potencial antiproliferativo sobre la línea celular de carcinoma de próstata humano, en donde se obtuvo que la actividad biológica del ácido eicosapentaenoico no fue eliminada al ser encapsulado (en comparación de su forma libre).

CAPÍTULO I

Antioxidant, Antihemolysis, and Retinoprotective Potentials of Bioactive Lipidic Compounds from Wild Shrimp (*Litopenaeus Stylirostris*) Muscle

Artículo publicado en: *CyTA – journal of food*

Año: 2020

Antioxidant, Antihemolysis, and Retinoprotective Potentials of Bioactive Lipidic Compounds from Wild Shrimp (*Litopenaeus Stylirostris*) Muscle

Joel Said García-Romo¹, Luis Noguera-Artiaga², Alma Carolina Gálvez-Iriqui¹, Martin Samuel Hernández-Zazueta¹, Daniel Fernando Valenzuela-Cota¹, Ricardo Iván González-Vega¹, Maribel Plascencia-Jatomea¹, María Guadalupe Burboa-Zazueta³, Edgar Sandoval-Petris³, Rosario Maribel Robles-Sánchez¹, Josué Elías Juárez-Onofre⁴, Javier Hernández-Martínez⁵, Hisila del Carmen Santacruz-Ortega⁶, Armando Burgos-Hernández^{1*}.

¹Departamento de Investigación y Posgrado en Alimentos, Universidad de Sonora, 83000 Sonora, Mexico.

²Departamento de Tecnología Agroalimentaria, Universidad Miguel Hernández de Elche, Grupo Calidad y Seguridad Alimentaria, Carretera de Beniel, km 3,2. 03312-Orihuela, Alicante, Spain.

³Departamento de Investigaciones Científicas y Tecnológicas, Universidad de Sonora, 83000 Sonora, Mexico.

⁴Departamento de Física, Universidad de Sonora, 83000 Sonora, Mexico.

⁵Unidad de Servicios de Apoyo en Resolución Analítica, Universidad Veracruzana, 91190 Veracruz, Mexico

⁶Departamento de Investigación en Polímeros y Materiales, Universidad de Sonora, 83000 Sonora, Mexico.

* Corresponding Author. Tel.: + 526-622-592-208; Fax: + 526-622-592-209.

E-Mail: armando.burgos@unison.mx

Abstract

The oxidative stress damage on cells is an example of roles in the pathogenesis of different degenerative diseases and the search of compounds that can slow this oxidation is continuous. The aim of this work was to obtain bioactive fractions from wild shrimp (*Litopenaeus stylirostris*) muscle, in order to evaluate their protective capacity and chemo-structurally characterize them. ABTS and DPPH, and FRAP assays suggested that bioactive fractions possess free radical-scavenging capacity, and

reducing power, respectively. An inhibitory effect observed on AAPH-induced hemolysis and results from a H₂O₂-derived radicals-scavenging assay (retinoprotective), suggest that these fractions can exert their protective activity in human cells. UV-Vis, fluorescence, ¹³C-, ¹H-NMR, and ESI-MS studies performed on the most bioactive fraction, suggest that their main components are eicosapentaenoic acid, dioctyl phthalate, and a possibly novel indolocarbazole alkaloid derivative. These results suggest that these compounds are good candidates to further investigations as possible chemoprotective agents.

Keywords: Protective activity; antioxidant activity; ROS scavenger; chemoprevention; hemolysis.

Introduction

Whiteleg shrimp (*Penaeus vannamei*) is the most consumed species among crustaceans (53 % of total crustacean species produced in world aquaculture in 2016); however, currently wild shrimp (*Litopenaeus stylirostris*) is one of the most consumed among populations close to bays (FAO 2018). Even though information about chemical composition and nutritional quality of *L. stylirostris* (about 19 % protein, 2 % lipids, 1.2 % ashes, and 0.7 % fiber) (Bing & Wang, 2006; Ramirez & Herrera, 1991) has been reported, still scarce studies exist on the health-promoting properties (e.g. antioxidants, antimutagens, antiproliferative, etc.) that shrimp biomolecules might have.

Natural antioxidants have received considerable interest from the food industry due to concerns about the safety of synthetic antioxidants. Marine natural products (MNP) have attracted the attention of scientists for their potential application in the food industry (Claeson & Bohlin, 1997; König & Wright, 1996; Newman, Cragg, & Snader, 2000). Until 1995, about 6500 MNP's had been isolated; however, more than 19000 compounds have been reported up to date (Ciavatta et al., 2017). However, the marine environment has also been in the spotlight due to a wide range of biological activities associated to MNP and their potential therapeutic applications (Pawlik, 1993), among them are the antioxidants.

Among the sources of MNP with antioxidant properties are blue-green algae, which contain significant amounts of antioxidant carotenoids (Singh, Kate, & Banerjee, 2005), polysaccharides evaluated *in vivo* (De Almeida et al., 2011); Further, Belcastro, Marino, Russo, and Toscano (2006) reported the isolation of molecules with antioxidant potential from a fungal species, while Shindo and co-workers (2007) found bioactive molecules in marine bacterial species. However, higher marine organisms (cephalopods, fin-fish, crustaceans, etc.) may also be considered as potential source of bioactive compounds; as an example shrimp is a widely consumed seafood that has been studied for this purpose.

Various types of MNP in shrimp have been reported (da Silva et al., 2015; López-Saiz, Suárez-Jiménez, Plascencia-Jatomea, & Burgos-Hernández, 2013; Seymour, Li, & Morrissey, 1996; Sowmya & Sachindra, 2012). Among these types of bioactive compounds are peptides with ferrous ion chelating activity and radical scavenging activity (Sinthusamran, Benjakul, Kijroongrojana, Prodpran, & Kishimura, 2018), hydrolysates (Latorres, Rios, Saggiomo, Wasielesky, & Prentice-Hernandez, 2018), and caroteno-proteins (López-Saiz et al., 2014; Poonsin et al., 2018). Shrimp has also been reported as a source of astaxanthin, α -tocopherol, and polyunsaturated fatty acid (Gómez-Guillén, Montero, López-Caballero, Baccan, & Gómez-Estaca, 2018), all of them with chemical antioxidant capability as tested *in vitro*. However, questions on whether these *in vitro* antioxidant compounds have the capability of acting on protecting cells against oxidative stress-induced damages arise. Since many of the shrimp species-derived compounds with antioxidant activity as tested *in vitro*, are of lipid nature, the hypothesis of the present research work is that the antioxidant molecules present in *L. stylirostris*, yet to be fully characterized chemically, will be capable of showing chemoprotective activity in cellular models.

Based on the above, the aim of the present study was to obtain bioactive fractions from wild shrimp (*Litopenaeus stylirostris*) muscle, in order to evaluate their protective capacity, and identify the molecules responsible for this bioactivity.

Materials and methods

Testing species

Wild shrimp was obtained from Hermosillo coast (Kino bay), Sonora, Mexico (28°48'37.1"N 111°55'43.4"W) during the spring of 2018, transported in ice to the University of Sonora Seafood Laboratory, where was de-headed, peeled, and shrimp muscle were packed, and stored at -20 °C until analysis.

Sample preparation

A total sample of 1.2 kg of shrimp muscle was separated into 100 g – portions. Chloroform-soluble extracts were prepared according to López-Saiz et al. (2014). This extract was dissolved in 30 mL chromatographic grade (Sigma-Aldrich, St. Louis, MO, USA) ethyl acetate and stirred in a magnetic starred (IKA C-MAG HS 4, IKA – Werke GmbH & Co. KG, Staufen, Germany) for 12 h at room temperature at 500 rpm. Subsequently, it was filtered under vacuum to remove the suspended particles.

Column chromatography

In order to perform the fractionation procedure, 15 g of silica gel 60 (0.040-0.063 mm, Merck KGaA, Darmstadt, Germany) were impregnated with the shrimp muscle-extract. As a stationary phase, silica gel of the same characteristics was used to pack a 4 cm (id) x 27 cm glass chromatography column with 1 L of chromatographic grade (Sigma-Aldrich, St. Louis, MO, USA) hexane. The mobile phase consisted of chromatographic grade hexane (Hx) and ethyl acetate (AcOEt) in different proportions; the polarity of the mobile phase was gradually increased until 100 % chromatographic grade methanol was used. Eluents were obtained every 250 mL in glass bottles and their contents were monitored using TLC (Thin Layer Chromatography) testing plates coated with TLC Silica gel 60 F₂₄₅ (Merck KGaA, Darmstadt, Germany) to allow observation of bands at 254 and 365nm UV light (TLC was eluted with the same solvent system with which the open column was eluted). Eluents showing similar contents were combined, evaporated under reduced pressure at 35 °C, and dried under N₂ stream (each combination represented one fraction).

Antioxidant activity

In order to evaluate the antioxidant activity of the bioactive fraction (using fraction concentrations of 20 mg/mL and downwards), chemical (ABTS, DPPH, and FRAP assays) and cellular (antihemolysis and intracellular ROS scavenging assays) assays were performed to assess the chemical capability of inhibiting oxidation and the capacity of reducing oxidative cellular damage, respectively.

ABTS assay [2, 2'-azino-bis (3-ethylbenzothiazoline-6-sulfonic acid)]

This assay was carried out according to Loarca-Piña, Mendoza, Ramos-Gómez, and Reynoso (2010). A 20-μL aliquot of each fraction, previously dissolved in DMSO, was combined with 230 μL of the ABTS solution and were incubated for 30 min. Absorbance values were obtained at 730 nm (Benchmark Microplate Reader; Bio-Rad, Hercules, CA, USA). Positive control contained all the reaction reagents except the fractions.

DPPH assay (1, 1-diphenyl-2-picrylhydrazyl)

This test was performed according to Loarca-Piña et al., 2010. A 20-μL aliquot of each fraction, previously dissolved in DMSO, was combined with 200 μL of the DPPH (150 μM) solution (prepared in 80 % methanol), and was incubated for 30 min. Absorbance values were obtained at 520 nm (Benchmark Microplate Reader; Bio-Rad, Hercules, CA, USA).

Ferric reducing antioxidant power (FRAP) assay

FRAP assay was done according to Benzie and Strain (1996) with some modifications (the technique was adapted to microplate and our equipment, a scan was performed, and the region where it absorbs the most is 638 nm). First, stock solutions were prepared in acid condition, which included 300 mM sodium acetate buffer (pH 3.6), 20 mM FeCl₃·6H₂O, and 10 mM TPTZ (2, 4, 6-tripyridyl-s-triazine) in 40 mM

HCl. These solutions were mixed in a 10:1:1 ratio to prepare the working solution. A 20- μ L aliquot of the bioactive fraction was combined with 280 μ L of the FRAP solution, placed into wells, and incubated for 30 min at room temperature. Absorbance values were obtained at 638 nm (Thermo Fisher Scientific Inc. Multiskan GO, NY, USA).

For all of the assays above, a Trolox curve was made and all of the results were expressed as μ M TE/g testing fraction.

AAPH assay [2, 2'-azobis- (2-methylpropionamidine)]

The antihemolysis activity was determined as described by Hernández-Ruiz et al. (2018). Human erythrocytes were washed three times with a phosphate buffered saline (PBS) solution at pH 7.4. A suspension of 2 % human erythrocytes is prepared in PBS. In a test tube, 100 μ L of the erythrocyte suspension, 100 μ L of fraction (at different concentrations), and 100 μ L of 40 mM AAPH were combined. Test tubes were incubated at 37 °C under agitation (Labquake Tube Shaker, Thermo Fisher Scientific Inc., MA, USA) at 30 rpm at darkness for 3 h. After incubation, the reaction mixture was diluted with 1 ml of PBS and centrifuged at 2000 $\times g$ for 10 min (Thermo Biofuge Stratos, Thermo Fisher Scientific Inc., Mass, USA). The absorbance of the supernatant was measured at 540 nm (Thermo Fisher Scientific Inc. Multiskan GO, NY, USA).

MTT [3-(4, 5-Dimethylthiazol-2-yl)-2, 5-Diphenyltetrazolium Bromide assay on ARPE-19 cell line

The retinoprotective activity was determined as described by Liu et al., (2017). Human retinal pigment epithelial (ARPE-19) cells line were cultured in Dulbecco's modified Eagle's medium (Sigma-Aldrich, St. Louis, MO, USA), supplemented with 10 % heat-inactivated fetal bovine serum (FBS) (Corning, NY, USA), and grown at 37 °C in an atmosphere of 5 % CO₂ (VWR 2325 Water-Jacketed CO₂ Incubator, Pa, USA). This assay (MTT) was carried out using the Roche cell proliferation kit I (Cat. No. 11-465-007-001, Roche Diagnostics GmbH, Mannheim, Germany) according to the manufacturer instructions,

and was used to i) to determine the H_2O_2 concentration to be applied in the study on *protection against H_2O_2 -induced oxidative cell damage activity* and ii) in that on the *protective activity against H_2O_2 -induced cell injury*.

Briefly, 1×10^4 cells/well were suspended in 100 μ L on DMEM at 10 % of SFB; they were seeded in each well of a flat 96-well microtitration plate. After incubation time, the mixture containing 100 μ L of culture medium at 10 % of SFB was combined with 100 μ g/mL of each fraction in diluted (0.5 % v/v) DMSO (4 and 24 h before H_2O_2 stimuli). Later, wells were washed two times with 100 μ L PBS and 100 μ L of 10 mM H_2O_2 in culture medium were added, and the mixture was incubated for 30 min. Negative control cell cultures were incubated only in medium (containing DMSO 0.5 % v/v) and positive control cell cultures were incubated only in 10 mM H_2O_2 in culture medium.

Phalloidin–tetramethylrhodamine B isothiocyanate and 4', 6-Diamidino-2 phenylindole dilactate fluorescence cell staining on ARPE-19 cell line

In order to observe the effect of the bioactive fraction against H_2O_2 -induced cell injury on tested cell line, internal cell morphological/structural aspects were observed following cell-staining procedures after the addition of fractions (Wankun et al., 2011). Cells were seeded onto 96-well microtitration plates, incubated for a period of 24 h at 37 °C in an atmosphere of 5 % CO_2 (VWR 2325 Water-Jacketed CO_2 Incubator, Pa, USA), and treated with bioactive fraction and H_2O_2 . Cells were fixed with 3.7 % formaldehyde in PBS per 15 min and further permeabilized with 0.2 % Triton X-100 in PBS for 15 min. Then, cells were stained either with phalloidin–tetramethylrhodamine B isothiocyanate (Phalloidin) (Sigma-Aldrich, MFCD00278840) or 4', 6-diamidino-2-phenylindole, dilactate (DAPI) (Sigma-Aldrich, D9564), in order to visualize cell structural issues such as F-actin microtubules or nuclear DNA, respectively. In order to performed observations, the microtitration plates were mounted on an inverted epifluorescence microscope (Leica DMI8, Leica-Microsystems, Wetzlar, Germany) equipped with fluorescence filters (546/10 RHOD excitation filter and emission 585/40, 350/50 DAPI excitation filter

and 460/40 emission, and 480/40 excitation FITC filter and 527/30 emission), a cooled monochromatic DFC 450C camera (Leica Microsystems, Wetzlar, Germany) and fluorescence overlay software (LAS AF version 3.1.0, Leica Microsystems CMS GmbH, Mannheim, Germany).

Intracellular ROS scavenging assay on ARPE-19 cell line

Measurements of intracellular ROS levels in ARPE-19 cells were made using 2',7'-dichlorodihydrofluorescein diacetate (DCFH-DA) as described by Halliwell and Whiteman (2004), who reported it as a reliable method for studying intracellular ROS. Cell samples were incubated in the presence of 10 μ M DCFH-DA at 37 °C for 30 min (VWR 2325 Water-Jacketed CO₂ Incubator, Pa, USA) and washed two times with PBS. The intracellular fluorescence was assayed by excitation at 498 nm and emission 530 nm to monitor intracellular ROS (FLUOstar Omega, BMG Labtech Inc., Ortenberg, Germany). Also, for microscopical qualitatively measuring of the effect of bioactive fraction on H₂O₂-induced intracellular ROS production, cells were labeled with DCFH-DA under an inverted fluorescence microscope (Leica DMI8, Leica Microsystems GmbH, Wetzlar, Germany) equipped with fluorescence filters (with same characteristics as those described above) to performed observations.

Ultraviolet–visible (UV-Vis) and fluorescence spectroscopies

The bioactive sample was solubilized in chromatographic-grade methanol and analyzed on an Agilent 8453 diode array spectrophotometer (Agilent Technologies, Inc, Santa Clara, CA, USA) for the UV-Vis, and in a Perkin Elmer LS-50B Luminescence Spectrometer (PerkinElmer, Inc., Waltham, MA, USA) in case of fluorescence spectroscopy. In both determinations, a wavelength-range from 200 to 700 nm (at 25 °C) and 1 cm quartz cuvette were used.

Carbon and proton nuclear magnetic resonance (¹³C-NMR and ¹H- NMR)

Measurements were analyzed using Bruker NMR spectrometry equipment operated at 400 MHz (Bruker, Billerica, MA, USA). Each fraction was dissolved in 500 μ L CDCl₃ (Sigma-Aldrich, Saint Louis, MI, USA), using tetramethylsilane as internal standard, and the resulting mixture was placed into a 5 mm diameter ultra-precision NMR sample tubes at 23 °C. Carbon was measured at 100 and proton at 400 MHz.

Electrospray ionization tandem mass spectrometry (ESI/MS)

The ESI/MS were performed on Agilent 6130 Quadrupole LC/MS (Agilent Technologies, Inc, Santa Clara, CA, USA). The instrument was operated in the negative [M-H]⁻ and positive [M+H]⁺ ion mode. The sample was performed in methanol acetonitrile 50:50, at 300 °C.

Statistical analysis

Data were analyzed using an analysis of variance (ANOVA) with Tukey multiple comparisons test (Tukey's post hoc test), at a 95 % confidence interval, and the level of significance of $P \leq 0.05$, (SPSS). In order to calculate IC₅₀ values (half maximal inhibitory concentration) for biologically active fractions, a Probit analysis was performed using the Number Cruncher Statistical Software (NCSS, LLC., Kaysville, Utah, USA), version 2001, NCSS Statistical Software, U.S.A. All data were presented as the mean value with their indicated standard deviation (mean \pm S.D.).

Results and discussion

Shrimp extraction, fractionation, and yield

Open column chromatography of the extract from shrimp resulted in a total of 18 fractions, A - R, having each different yields (these results of yield in mg are shown in **supplementary material**. Fractions with the highest antioxidant potential were screened using both, chemical and cellular assays.

Chemically (ABTS, DPPH, and FRAP) assayed antioxidant activity

An antioxidant has the capability to, at low concentrations, significantly prevent the oxidation of biomolecules, such as proteins, lipids, carbohydrates, and DNA. At the present study, the antioxidant activity of fractions was calculated using standard curves for ABTS, DPPH, and FRAP assays correlations values (R^2) of 0.9986, 0.8712, and 0.8182 for ABTS, DPPH, respectively.

As shown in **table 1**, among all of the fractions tested, M produced the significantly ($P \leq 0.05$) highest $\mu\text{M TE/g}$ values (21.4 ± 2.4 , 25.2 ± 1.5 , and 166.8 ± 7.2 , for ABTS, DPPH, and FRAP, respectively).

Antioxidant indicator assays determine the capability of a compound (or group of compounds) to interact with a free neutral radical with a single electron not paired in one of its orbitals (McMurry, 2012). Free radicals are unstable and reactive and, due to their need to achieved stability by electron scavenging, they can initiate chain reactions that destroys cell's chemical structures, such as membranes, lipids, proteins, and among others (Avello & Suwalsky, 2006). Based on the above, molecules present in the fraction M might have the capacity to donate protons and electrons (HAT and SET systems), therefore, to act as antioxidant in a cellular model.

Antihemolysis activity

Fractions were also tested on their capacity of inhibiting free-radical-initiated peroxidation, which mediated the hemolysis of human erythrocyte induced by a water-soluble initiator, AAPH. The hemolytic activity of all fractions was screened against human erythrocytes and tested at different fractions. Erythrocytes are susceptible to peroxidation due to accumulation of hemoglobin and polyunsaturated fatty acids (Babu, Shylesh, & Padikkala, 2001). **Table 1** shows that fractions M, L, and E (minimum IC_{50} values of 213 ± 82 , 308 ± 71 , and $315 \pm 24 \mu\text{g/mL}$, respectively) show the higher inhibition of AAPH radicals, which suggests they may contain primary antioxidants that have antihemolysis potential. Under oxidative stress, lipid peroxidation caused by peroxy radicals may promote loss of erythrocyte membrane integrity; when AAPH enters the cytosol, a ROS chain reaction

may occur due to radicals generated by AAPH decomposition (Zheng et al., 2016). Based on the above, components of fraction M may prevent AAPH-induced erythrocyte hemolysis, phenomenon that can be studied by determining their capability of deactivating peroxy radicals through SET and HAT systems.

Results from the antihemolysis study, the activity of fraction M is significantly ($P \leq 0.05$) different from that obtained for the antioxidant control gallic acid (GA) (IC_{50} of $49 \mu\text{g/mL}$). An issue to be highlighted is that, gallic acid is a hydrophilic molecule, therefore, its antioxidant action takes place in the cellular plasma (as an extracellular protector in blood), while the fractions from shrimp are lipophilic; therefore, their action may be more associated to membrane cell protection; and even, they might enter into the cell and also provide intracellular protection) (Nimse & Pal, 2015; Sies, 1997); for this reason, a retinoprotective study was pertinent; these results are presented below.

Retinoprotective against H_2O_2 -induced oxidative cell damage activity

Cellular ROS mainly include H_2O_2 which easily penetrate cell membranes and cause damages to cells (Akhtar, Ahamed, Alhadlaq, & Alshamsan, 2017). Once inside the cell, H_2O_2 can form the hydroxyl radical causing cell damage / injury to structural proteins, enzymes, phospholipid membrane, and DNA (Liochev & Fridovich, 1994).

As shown in **figure 1a**, low concentrations of H_2O_2 did not diminished ARPE-19 cellular viability, possibly due to pathways of oxidative stress regulation. However, H_2O_2 concentration is high, ROS exceeds cellular regulation capacity and damage becomes possible.

In order to know whether the bioactive fractions (BF) protect cells from H_2O_2 -induced damage, cultivated cells were pre-treated with BF and then exposed to H_2O_2 . As shown in **figure 2**, 10 mM H_2O_2 caused 80 - 85 % loss of cellular viability compared to control (untreated) cells, but no significant ($P \leq 0.05$) cytotoxicity was observed in the presence of 100 $\mu\text{g/mL}$ BF alone. On the other hand, when cells were pre-treated with BF and then exposed to H_2O_2 , cell survival rate remarkably increased. The effect of fraction M (fM) outstand from the rest of the fractions when incubated for 24 h (viability of 75 %),

strongly suggesting that fM has the capacity of protecting cells against H₂O₂. Also, as shown in **figure 1b**, cellular viability lower than 90 % was only observed only when fM concentration was 100 µg/mL. This suggest that compounds present in fM might act as chemo-protectors at that concentration and not higher. Is important to mention that the effect of protection against oxidative stress caused by H₂O₂ does not always shows a linear behavior, therefore, it is necessary to carry out further research on this regard (Halliwell, 2012; Noguera-Artiaga et al., 2019).

Retinoprotective effect of fM against H₂O₂-induced cell injury activity

Cell damage / death is initiated when organelles are injured and, knowing which are either affected or protected, may contribute to know the ways by which a molecule is exerts its antioxidant activity. **Figure 3** shows actin and chromatin morphology in cells stained with phalloidin and DAPI, either in the presence or absence of 250 µM H₂O₂; this made possible to visualize the existence (or not) of cellular injury.

Cells treated with H₂O₂ showed evidence of changes in their structure associated to actin microfilaments de-polymerization, volume reduction (cellular shrinkage), membrane blebbing, and damage of phospholipids membrane. In addition, intense fluorescence suggests severe chromatin damage, and pyknotic and fragmented nuclei. However, actin and DNA structure in cells exposed to H₂O₂ but pretreated with fM, were similar to the control. These results suggest that fM possess the capability to attenuate H₂O₂-induced cellular injury.

Fraction M (fM) inhibit H₂O₂-induced intracellular ROS generation

Kietzmann (2010) described oxidative stress as a pathological state of excessive ROS production; additionally, H₂O₂ may induce cellular apoptosis at harmful concentrations (Li et al., 2013). Based on the above, the capability of fM of intracellularly inhibit H₂O₂-induced damage in ARPE-19 cells was investigated. The effect of fM on intracellular ROS levels was determined using the DCFH-DA assay. Briefly, in this assay, non-fluorescent DCFH-DA is enzymatically transformed to non-fluorescent

DCFH, which oxidized by intracellular ROS results in fluorescent DCF which stains the cells (Gomes, Fernandes, & Lima, 2005).

As shown in **figure 4a**, fluorescence intensity increases in cells with H₂O₂ concentration suggesting an increasing intracellular ROS concentration. On the other hand, **figure 4b** shows that fM did not significantly produced ROS in this model. When cells, previously treated with fM at different concentrations, were exposed to 250 μ M H₂O₂, the fluorescence intensity significantly ($P \leq 0.05$) decreased as fM concentration increased (**Figure 4c**), suggesting that components of fM may protect the cell, possibly by directly blocking ROS. Microscopic visualization subjected to the experimental procedures described above was consisting with fluorescence intensity measurements (**Figure 4d**).

Characterization of fM

According to the results, fM was the most chemoprotective fraction, therefore it was selected for chemical / structural characterization. This information is important for the establishment of association between structural aspects and bioactivity.

The UV-Vis analysis (**Supplementary material**) fM has maximum of absorption at 237 and 273 nm with absorbance values of 3.78, 1.25, which are attributed to $\pi \rightarrow \pi^*$ transitions associated to the presence of aromatic compounds; bands with a very low absorbance values 302, 322, and 350 nm are attributed to $n \rightarrow \pi^*$ transition which are produced by aromatics rings having atoms with available electrons such as oxygen and nitrogen. Fluorescence analyses (**Supplementary material**) showed that component of fM had emissions at $\lambda = 352$ nm and 515 nm when they were excited at $\lambda = 315$ and 380 nm respectively.

Table 2 shows ¹³C- and ¹H-NMR signals suggesting that fM are composed of several compounds. Eicosapentaenoic acid (EPA) was found as a majoritarian component, also its signals are in agreement with Tyl et al. (2008). Likewise, characteristic signals of both, patterns of 1, 4 di-substituted

aromatic ring and coupling pattern of the protons of the aromatic ring, signals at $\delta = 7.71$ ppm (*dd*, $J = 5.7, 3.3$ Hz) and 7.53 ppm (*dd*, $J = 5.7, 3.3$ Hz), suggested the presence of dioctyl phthalate (DOP). However, the amount of this compound was too small that no ^{13}C -NMR signals could be determined. Similar results have been reported (Cruz-Ramírez et al., 2015; García-Romo et al., 2018; López-Saiz et al., 2014) also suggesting the presence of DOP.

Finally, ^1H -NMR signals at $\delta = 9.77$ ppm (*s*) corresponding to alcohol groups, $\delta = 7.52$ (*d*), 7.32 (*d*) and 7.13 (*dd*) ppm corresponding to protons belonging to aromatic rings with a substitution, signals at $\delta = 3.7 - 3.4$ (*m*) ppm associated to aliphatic protons and signals at $\delta = 1.14$ (*d*) ppm related to methyl protons, as well as ^{13}C -NMR signals at 116.66, 110.89, and 109.95 associated to carbons belonging to aromatic rings and signals at 71.10, 65.45, and 56.27 associated to carbons belong to aliphatic chains, were obtained. Also, these results indicate that the molecular weight of this molecule is 540.20 m/z; this molecular weight in conjunction with these signals mentioned above, correspond to a new indolocarbazole alkaloids derivative, with mass a of 543 Da and a chemical formula $\text{C}_{28}\text{H}_{25}\text{N}_5\text{O}_7$. In order to confirm the presence of this compound, characterization by mass technique ESI in negative mode was performed (**Supplementary material**).

However, in agreement to evidence showed, the compounds responsible of shrimp muscle lipid extraction for anti-oxidant, anti-hemolytic, and retinoprotective activities are a least three compounds, EPA, a new indolocarbazole alkaloids derivative and DOP.

Conclusions

Based on the results obtained, the fM isolated from the muscle of wild shrimp (*Litopenaeus stylirostris*) contains antioxidants compounds indeed capable of exerting a chemoprotective effect on human cell lines. A possible novel indolocarbazole type of compound possibly is, in great part, responsible of this

activity; however, further investigation is necessary for both, complete biological characterization and full chemical / structural elucidation.

Funding details

Authors wish to thank *Consejo Nacional de Ciencia y Tecnología* (CONACYT) Mexico for financing the project No. 241133, for granting research scholarships, and for funding this project.

Disclosure statement

No potential conflict of interest was reported by the authors.

References

- Akhtar, M. J., Ahamed, M., Alhadlaq, H. A., & Alshamsan, A. (2017). Mechanism of ROS scavenging and antioxidant signalling by redox metallic and fullerene nanomaterials: Potential implications in ROS associated degenerative disorders. *Biochimica et Biophysica Acta (BBA) - General Subjects*, 1861, 802-813.
- Avello, M., & Suwalsky, M. (2006). Radicales libres, antioxidantes naturales y mecanismos de protección. *Atenea (Concepción)*, 161-172.
- Babu, B. H., Shylesh, B. S., & Padikkala, J. (2001). Antioxidant and hepatoprotective effect of *Acanthus ilicifolius*. *Fitoterapia*, 72, 272-277.
- Belcastro, M., Marino, T., Russo, N., & Toscano, M. (2006). Structural and electronic characterization of antioxidants from marine organisms. *Theoretical Chemistry Accounts*, 115, 361-369.
- Benzie, I. F. F., & Strain, J. J. (1996). The ferric reducing ability of plasma (FRAP) as a measure of “antioxidant power”: The FRAP assay. *Analytical Biochemistry*, 239, 70-76.
- Bing, X., & Wang, J. (2006). A comparative study of nutritional quality in the muscle of *Penaeus stylirostris* and *Penaeus vannamei* in the cultured-pond. *Acta Hydrobiologica Sinica*, 30, 458.

- Ciavatta, M. L., Lefranc, F., Carbone, M., Mollo, E., Gavagnin, M., Betancourt, T., Dasari, R., Kornienko, A., & Kiss, R. (2017). Marine mollusk-derived agents with antiproliferative activity as promising anticancer agents to overcome chemotherapy resistance. *Medicinal Research Reviews*, 37, 702-801.
- Claeson, P., & Bohlin, L. (1997). Some aspects of bioassay methods in natural-product research aimed at drug lead discovery. *Trends in Biotechnology*, 15, 245-248.
- Cruz-Ramírez, S., López-Saiz, C., Plascencia-Jatomea, M., Machi-Lara, L., Rocha-Alonzo, F., Márquez-Ríos, E., & Burgos-Hernández, A. (2015). Isolation and identification of an antimutagenic phthalate derivative compound from octopus (*Paraoctopus limaculatus*). *Tropical Journal of Pharmaceutical Research*, 14, 1257.
- da Silva, F. O., Tramonte, V. L. C. G., Parisenti, J., Lima-Garcia, J. F., Maraschin, M., & da Silva, E. L. (2015). *Litopenaeus vannamei* muscle carotenoids versus astaxanthin: A comparison of antioxidant activity and *in vitro* protective effects against lipid peroxidation. *Food Bioscience*, 9, 12-19.
- De Almeida, C. L. F., De S. Falcão, H., De M. Lima, G. R., De A. Montenegro, C., Lira, N. S., De Athayde-Filho, P. F., Rodrigues, L. C., De Souza, M. d. F. V., Barbosa-Filho, & Batista, L. M. (2011). Bioactivities from marine algae of the genus *gracilaria*. *International Journal of Molecular Sciences*, 12, 4550-4573.
- FAO. 2018. The State of World Fisheries and Aquaculture 2018 - Meeting the sustainable development goals. Rome. Licence: CC BY-NC-SA 3.0 IGO. ISBN 978-92-5-130562-1
- García-Romo, J. S., Yépiz-Gómez, M. S., Plascencia-Jatomea, M., Ortega, H. D. C. S.-., Burgos-Hernández, A., León, J. R. G. D., Cinco-Moroyoqui, F. J., & Borboa-Flores, J. (2018). Compounds with *in vitro* antibacterial activity from hydrosol of *Lippia palmeri* and morphometric changes on *listeria monocytogenes*. *Biotechnia*, 20, 35-42.

- Gomes, A., Fernandes, E., & Lima, J. L. F. C. (2005). Fluorescence probes used for detection of reactive oxygen species. *Journal of Biochemical and Biophysical Methods*, 65, 45-80.
- Gómez-Guillén, M. C., Montero, P., López-Caballero, M. E., Baccan, G. C., & Gómez-Estaca, J. (2018). Bioactive and technological functionality of a lipid extract from shrimp (*L. vannamei*) cephalothorax. *LWT - Food Science and Technology*, 89, 704-711.
- Halliwell, B., & Whiteman, M. (2004). Measuring reactive species and oxidative damage in vivo and in cell culture: how should you do it and what do the results mean? *British Journal of Pharmacology*, 142, 231-255.
- Halliwell B. (2012). Free radicals and antioxidants: updating a personal view. *Nutrition Reviews*, 70.5, 257–265, <https://doi.org/10.1111/j.1753-4887.2012.00476.x>
- Hernández-Ruiz, K. L., Ruiz-Cruz, S., Cira-Chávez, L. A., Gassos-Ortega, L. E., de Jesús Ornelas-Paz, J., Del-Toro-Sánchez, C. L., Márquez-Ríos, E., López-Mata, M. A., & Rodríguez-Félix, F. (2018). Evaluation of antioxidant capacity, protective effect on human erythrocytes and phenolic compound identification in two varieties of plum fruit (*Spondias spp.*) by UPLC-MS. *Molecules*, 23.
- Kietzmann, T. (2010). Intracellular redox compartments: Mechanisms and significances. *Antioxidants & Redox Signaling*, 13, 395-398.
- König, G., & Wright, A. (1996). Marine natural products research: current directions and future potential. *Planta Medica*, 62, 193-211.
- Latorres, J. M., Rios, D. G., Saggiomo, G., Wasielesky, W., & Prentice-Hernandez, C. (2018). Functional and antioxidant properties of protein hydrolysates obtained from white shrimp (*Litopenaeus vannamei*). *Journal of Food Science and Technology*, 55, 721-729.
- Li, Z., Dong, X., Liu, H., Chen, X., Shi, H., Fan, Y., Hou, D., & Zhang, X. (2013). Astaxanthin protects ARPE-19 cells from oxidative stress via upregulation of Nrf2-regulated phase II enzymes through activation of PI3K/Akt. *Molecular Vision*, 19, 1656-1666.

- Liochev, S. I., & Fridovich, I. (1994). The role of O_2^- in the production of $HO\cdot$: in vitro and in vivo. *Free Radical Biology and Medicine*, 16, 29-33.
- Loarca-Piña, G., Mendoza, S., Ramos-Gómez, M., & Reynoso, R. (2010). Antioxidant, antimutagenic, and antidiabetic activities of edible leaves from *Cnidoscolus chayamansa* Mc. Vaugh. *Journal of Food Science*, 75, H68-H72.
- López-Saiz, C.-M., Suárez-Jiménez, G.-M., Plascencia-Jatomea, M., & Burgos-Hernández, A. (2013). Shrimp lipids: A source of cancer chemopreventive compounds. *Marine Drugs*, 11, 3926-3950.
- López-Saiz, C.-M., Velázquez, C., Hernández, J., Cinco-Moroyoqui, F.-J., Plascencia-Jatomea, M., Robles-Sánchez, M., Machi-Lara, L., & Burgos-Hernández, A. (2014). Isolation and structural elucidation of antiproliferative compounds of lipidic fractions from white shrimp muscle (*Litopenaeus vannamei*). *International Journal of Molecular Sciences*, 15, 23555-23570.
- Liu, H., Liu, W., Zhou, X., Long, C., Kuang, X., Hu, J., ... & Fan, Y. (2017). Protective effect of lutein on ARPE-19 cells upon H_2O_2 -induced G2/M arrest. *Molecular medicine reports*, 16, 2069-2074.
- McMurry, J. (2012). *Química orgánica* (8 ed.): CENGAGE Learning.
- Newman, D. J., Cragg, G. M., & Snader, K. M. (2000). The influence of natural products upon drug discovery (Antiquity to late 1999). *Natural Product Reports*, 17, 215-234.
- Nimse, S. B., & Pal, D. (2015). Free radicals, natural antioxidants, and their reaction mechanisms. *Rsc Advances*, 5, 27986-28006.
- Noguera-Artiaga, L.; García-Romo, J.S.; Rosas-Burgos, E.C.; Cinco-Moroyoqui, F.J.; Vidal-Quintanar, R.L.; Carbonell-Barrachina, Á.A.; Burgos-Hernández, A. (2019). Antioxidant, Antimutagenic and Cytoprotective Properties of Hydrosos Pistachio Nuts. *Molecules*, 24, 4362.
- Ramirez, A.D. & Herrera C. (1991). Chemical composition and yield of giant prawns (*Macrobrachium rosenbergii*) and white shrimps (*Penaeus sp.*) and production of meal from waste materials. *Ingeniería y Ciencia Química*, 13, 15-19.

- Pawlik, J. R. (1993). *Marine invertebrate chemical defenses*. Paper presented at the Chemical Reviews, 93, 1911-1922.
- Poonsin, T., Simpson, B. K., Benjakul, S., Visessanguan, W., Yoshida, A., & Klomklao, S. (2018). Carotenoprotein from pacific white shrimp (*Litopenaeus vannamei*) shells extracted using trypsin from albacore tuna (*Thunnus alalunga*) spleen: Antioxidant activity and its potential in model systems. *Journal of Food Biochemistry*, 42, e12462.
- Seymour, T. A., Li, S. J., & Morrissey, M. T. (1996). Characterization of a natural antioxidant from shrimp shell waste. *Journal of Agricultural and Food Chemistry*, 44, 682-685.
- Shindo, K., Kikuta, K., Suzuki, A., Katsuta, A., Kasai, H., Yasumoto-Hirose, M., Matsuo, Y., Misawa, N., & Takaichi, S. (2007). Rare carotenoids, (3R)-saproxanthin and (3R,2'S)-myxol, isolated from novel marine bacteria (*Flavobacteriaceae*) and their antioxidative activities. *Applied Microbiology and Biotechnology*, 74, 1350-1357.
- Sies, H. (1997). Oxidative stress: oxidants and antioxidants. *Experimental Physiology: Translation and Integration*, 82, 291-295.
- Singh, S., Kate, B. N., & Banerjee, U. C. (2005). Bioactive compounds from cyanobacteria and microalgae: An overview. *Critical Reviews in Biotechnology*, 25, 73-95.
- Sinthusamran, S., Benjakul, S., Kijroongrojana, K., Prodpran, T., & Kishimura, H. (2018). Protein hydrolysates from pacific white shrimp cephalothorax manufactured with different processes: Compositions, characteristics and antioxidative activity. *Waste and Biomass Valorization*, 1-14.
- Sowmya, R., & Sachindra, N. M. (2012). Evaluation of antioxidant activity of carotenoid extract from shrimp processing byproducts by *in vitro* assays and in membrane model system. *Food Chemistry*, 134, 308-314.
- Tyl, C. E., Brecker, L., & Wagner, K. H. (2008). ¹H NMR spectroscopy as tool to follow changes in the fatty acids of fish oils. *European journal of lipid science and technology*, 110, 141-148.

- Wankun, X., Wenzhen, Y., Min, Z., Weiyan, Z., Huan, C., Wei, D., ... & Xiaoxin, L. (2011). Protective effect of paeoniflorin against oxidative stress in human retinal pigment epithelium *in vitro*. *Molecular vision*, *17*, 3512.
- Zheng, L., Zhao, X., Zhang, P., Chen, C., Liu, S., Huang, R., Zhong, M., Wei, C., & Zhang, Y. (2016). Hemocyanin from shrimp *Litopenaeus vannamei* has antiproliferative effect against hela cell in vitro. *PLOS ONE*, *11*, e0151801.

Table 1. Indicators of antioxidant activity and half maximal inhibitory concentration (IC₅₀) of antihemolysis activity of fractions obtained from wild shrimp (*Litopenaeus stylirostris*) muscle.

Fraction	Antioxidant ($\mu\text{M TE/gf}$)			Antihemolysis IC ₅₀ ($\mu\text{g/mL}$)
	ABTS	DPPH	FRAP	
A	6.4 \pm 0.3 c	437 \pm 101 bcd	15.7 \pm 4.6 ab	437 \pm 101 cd
B	2.7 \pm 2.4 a	779 \pm 64 gh	36.2 \pm 5.7 cd	779 \pm 64 gh
C	1.4 \pm 0.2 a	648 \pm 99 efg	15.9 \pm 1.3 ab	648 \pm 99 efg
D	14.9 \pm 0.4 e	1533 \pm 89 j	75.2 \pm 4.6 g	1533 \pm 89 j
E	15.2 \pm 0.4 e	315 \pm 24 ab	3.3 \pm 1.0 a	315 \pm 24 bc
F	4.7 \pm 0.0 bc	632 \pm 23 defg	67.9 \pm 7.0 efg	632 \pm 23 efg
G	4.2 \pm 0.0 bc	471 \pm 79 bcde	56.3 \pm 3.7 ef	471 \pm 79 cde
H	10.6 \pm 0.6 d	550 \pm 11 cdef	72.0 \pm 8.3 fg	550 \pm 11 def
I	3.3 \pm 0.5 ab	887 \pm 80 h	18.2 \pm 2.9 ab	887 \pm 80 h
J	2.4 \pm 1.5 a	1095 \pm 21 i	11.1 \pm 2.6 ab	1095 \pm 21 i
K	10.1 \pm 0.3 d	871 \pm 69 h	99.5 \pm 9.9 h	871 \pm 69 h
L	1.4 \pm 0.5 a	308 \pm 71 ab	128.1 \pm 8.5 i	308 \pm 71 bc
M	21.1 \pm 2.4 g	213 \pm 82 a	166.7 \pm 7.2 j	213 \pm 82 ab
N	4.7 \pm 1.2 bc	598 \pm 12 cdefg	97.9 \pm 1.5 h	598 \pm 12 defg
O	2.9 \pm 0.6 ab	538 \pm 13 cdef	51.9 \pm 4.9 de	538 \pm 13 def
P	2.6 \pm 0.4 ab	418 \pm 35 bc	112.3 \pm 2.7 hi	418 \pm 35 cd
Q	18.0 \pm 0.2 f	429 \pm 16 bc	8.6 \pm 2.00 ab	429 \pm 16 cd
R	4.7 \pm 1.2 bc	728 \pm 93 fgh	24.17 \pm 5.75 bc	728 \pm 93 fgh
GA				49 \pm 13 a

The value means \pm S.D. of three determinations. Different letters within the same column indicate significant difference ($P \leq 0.05$); Tukey's least significant difference test. In the antihemolysis activity, DMSO was used as a positive control instead of bioactive fractions since resulted in 100 % hemolysis. Fractions were obtained from open column chromatography. TE: Trolox equivalents, gf: gram of fractions. GA: gallic acid.

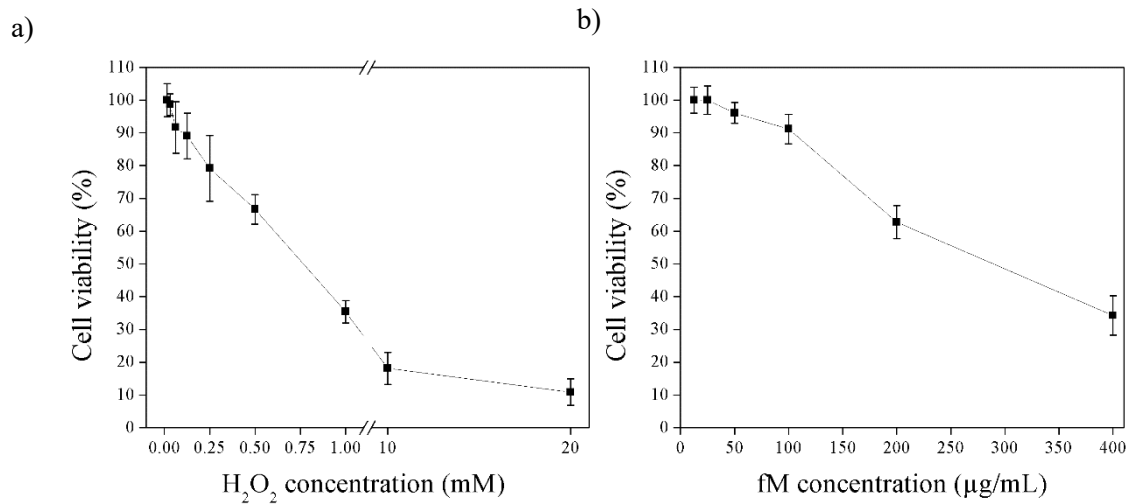


Figure 1. Cell viability of ARPE-19 cells exposed to a) different concentrations of H_2O_2 (0.06 to 20 mM) for 30 min, and b) to different concentrations of fraction M (fM) (12.5 to 400 $\mu\text{g/mL}$) for 24 h. Values represent means from three determinations. Control cell cultures were incubated with DMSO as the vehicle solvent at a maximum concentration 0.5 % and represent 100 % viability.

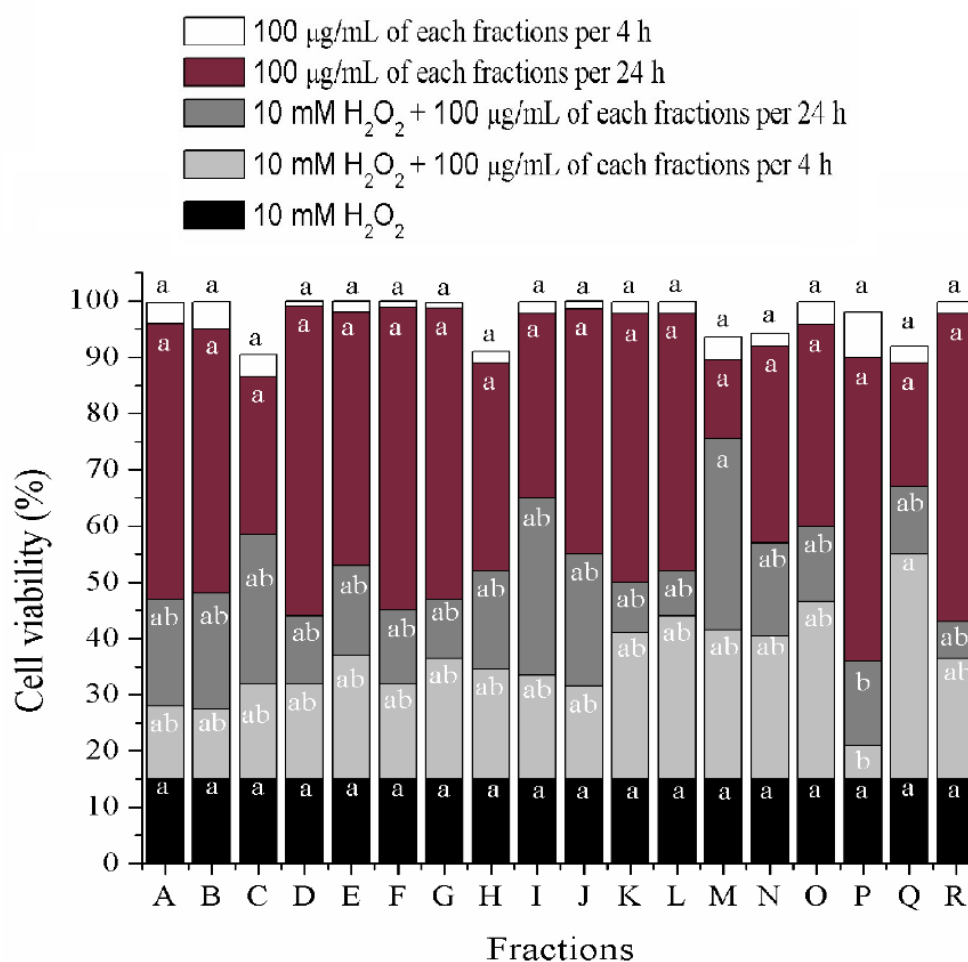


Figure 2. Cell viability of H₂O₂-induced damage ARPE-19 cells, previously exposed to 100 µg/mL of different fractions from wild shrimp (*Litopenaeus stylirostris*) muscle after 4 and 24 h. Values represent means from three determinations. Different letters among bars mean significant differences ($P \leq 0.05$); Tukey's least significant difference test. Fractions were obtained from open column chromatography.

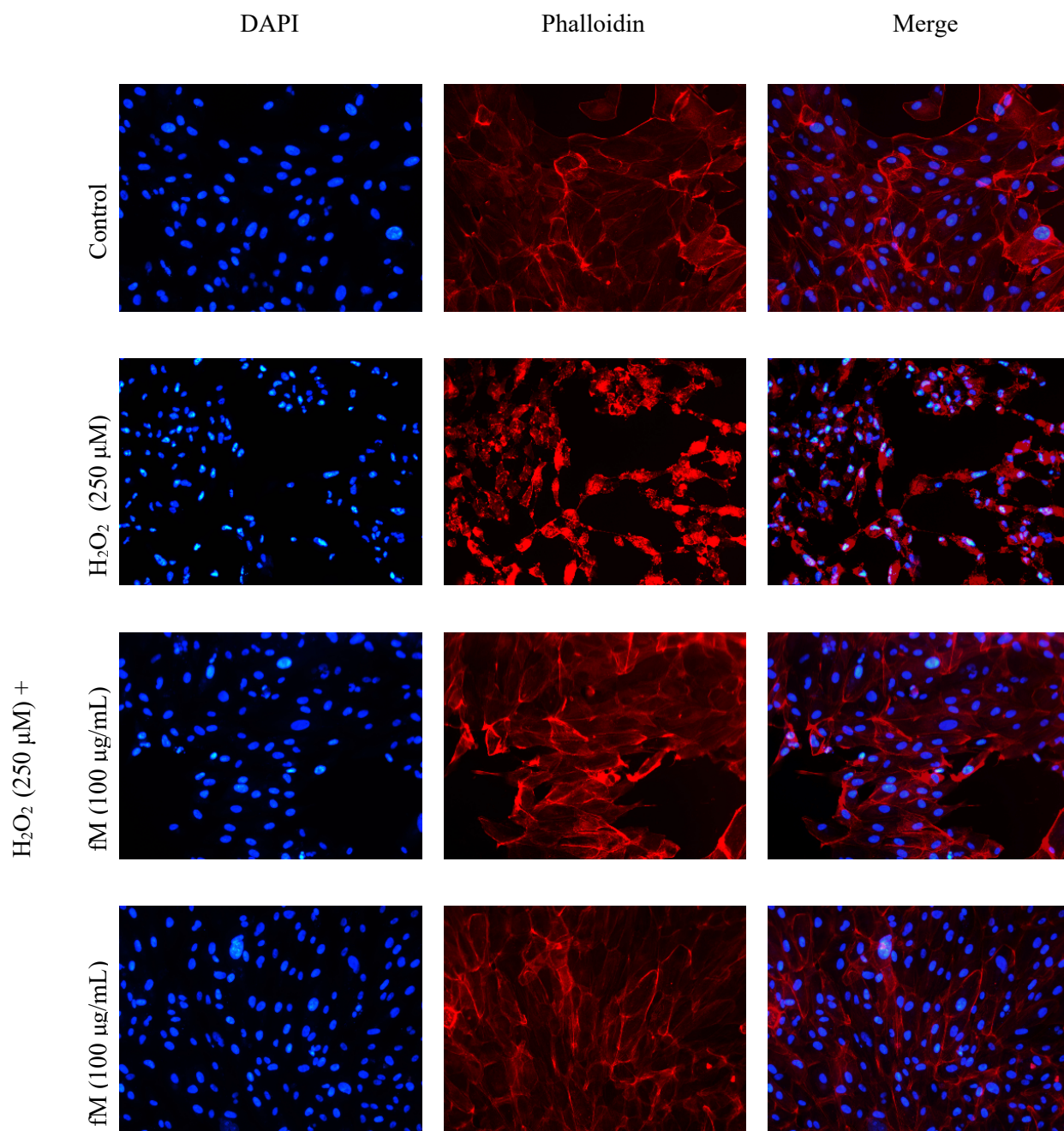


Figure 3. Effect of H₂O₂ on structural cellular aspects of ARPE-19 human cell line, and the retinoprotective effect of fraction M (fM) against H₂O₂-induced cell injury. Cells actin-microfilament cytoskeleton (red-colored) and nuclear DNA (blue-colored), after staining with phalloidin and DAPI, respectively. Observations were made at 20x. Control cells were incubated with DMSO as the vehicle solvent at a maximum concentration 0.5 % and represent no morphologic changes.

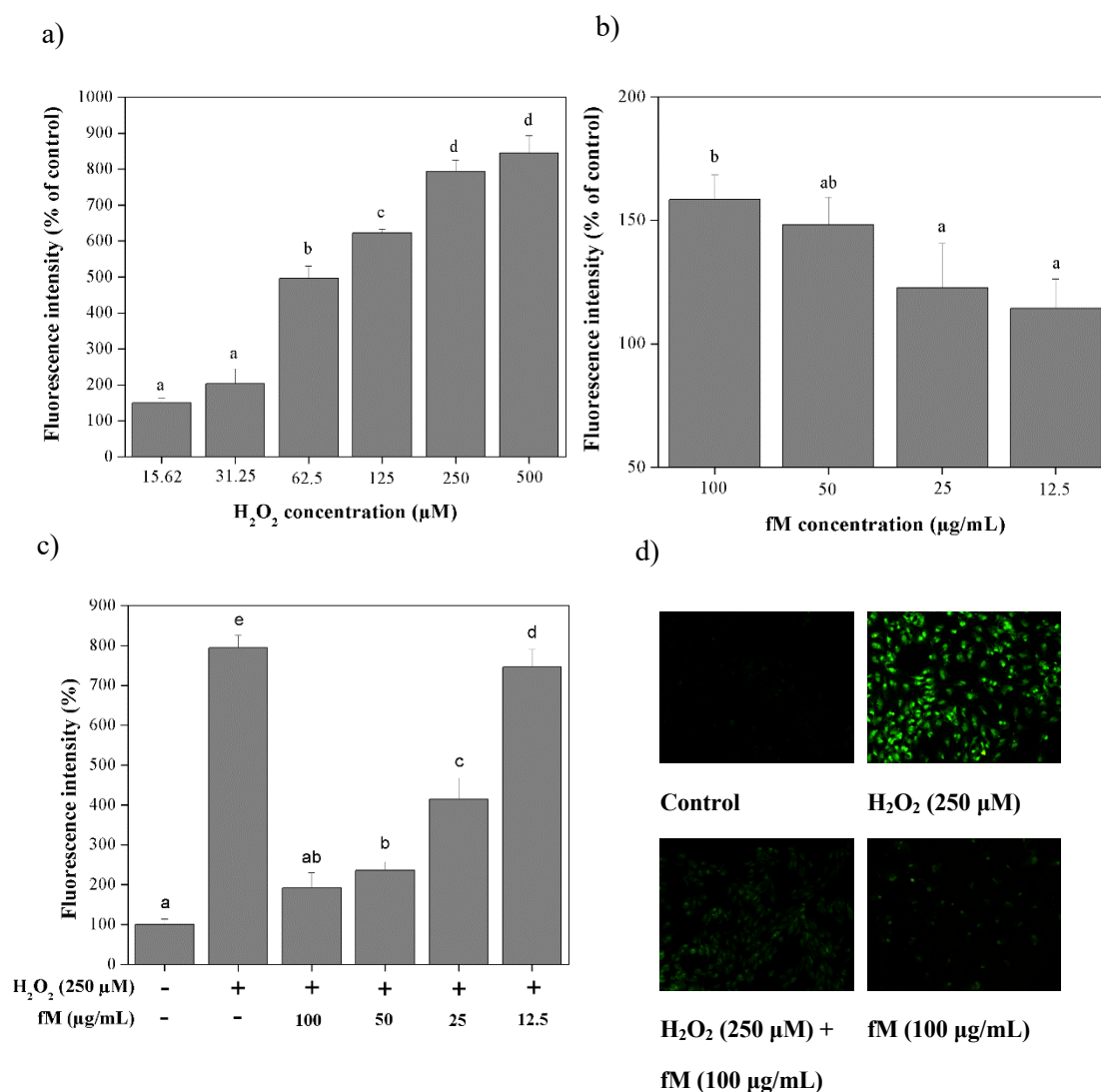
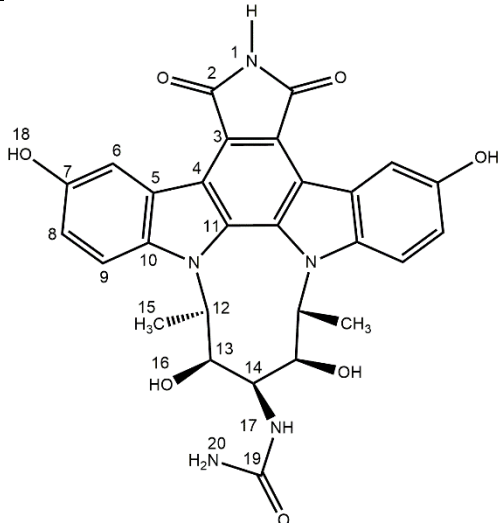
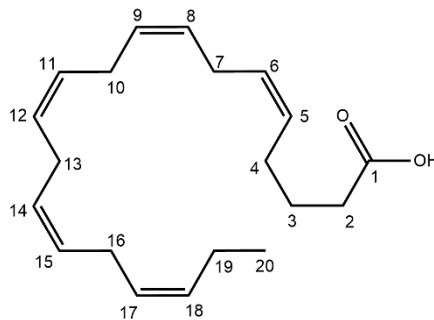
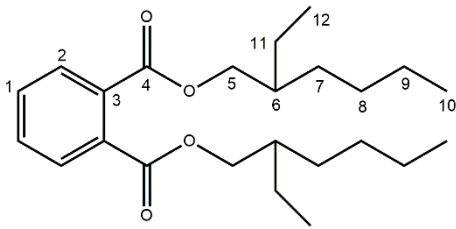


Figure 4. Retinoprotective effect of fraction M (fM) against H_2O_2 -induced intracellular ROS production in ARPE-19 cells. a) Intracellular ROS production in cells exposed to different concentrations of H_2O_2 . b) Intracellular ROS production in cells treated with different concentration of fM during 24 h. c) Intracellular ROS production in cells treated with and without 250 μM H_2O_2 and fM at different concentration per 24 h, (-) stimulus not used, (+) stimulus used. d) Microscopic visualization of the effect of fM on H_2O_2 -induced intracellular ROS production. Images were selected as representative data from

three independent experiments (at 20x). *Control*: not stimulated cells. Each value represents the mean \pm SD of three independent experiments ($P \leq 0.05$); Tukey's least significant difference test.

Table 2. ^{13}C - and ^1H -NMR analyses of fraction M dissolved in CDCl_3 .

Indolocarbazole alkaloid derivative			Eicosapentaenoic acid			Diethyl phthalate		
								
No.	δ_{C}	δ_{H}	No.	δ_{C}	δ_{H}	No.	δ_{C}	δ_{H}
2	172.51		1	174.47		1		7.53 (<i>dd</i> , $J=5.6, 3.3$ Hz, 2H)
3	134.00		2	33.45	2.27 (<i>m</i> , 2H)	2		7.71 (<i>dd</i> , $J=5.6, 3.3$ Hz, 2H)
5	123.44		3	24.32		5		4.22 (<i>m</i> , 4H)
6	110.89	7.32 (<i>d</i> , $J=2.6$ Hz, 2H)	4	28.78	2.02 (<i>m</i> , 2H)	6, 7, 8, 9, 11		1.25 (<i>s</i> , 18H)
7	153.98		5, 6, 8, 9, 11, 12, 14, 15, 17, 18	129 - 127	5.35 (<i>m</i> , 10 H)	10, 12		0.88 (<i>m</i> , 12H)
8	116.66	7.13 (<i>dd</i> , $J=8.7, 2.6$ Hz, 2H)	7, 10, 13, 16, 19	26.39	2.80 (<i>m</i> , 12 H)			
9	109.95	7.52 (<i>d</i> , $J=8.7$ Hz, 2H)	20	13.43	0.90 (<i>t</i> , 3H)			
10	129.11							
11	132.10							
12	65.45	3.65 (<i>m</i> , 2H)						
13	71.10	3.71 (<i>m</i> , 2H)						
14	56.27	3.47 (<i>t</i> , $J=4.0$ Hz, 1H)						
15	14.89	1.14 (<i>d</i> , $J=6.28$ Hz, 6H)						
18		9.77 (<i>s</i> , 2H)						
19	162.84							

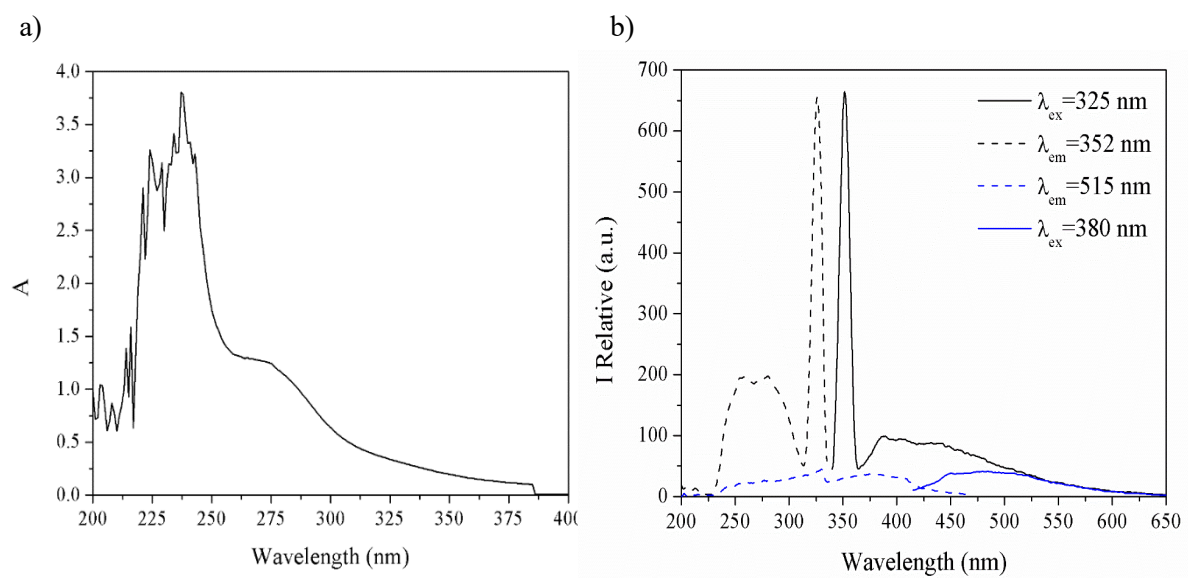
δ : chemical shift, J : coupling constant, *d*: doublet, *dd*: a doublet of doublets, *t*: triplet, *m*: multiplet, *s*: singlet.

Supplemental table 1. Mobile phase of the open column.

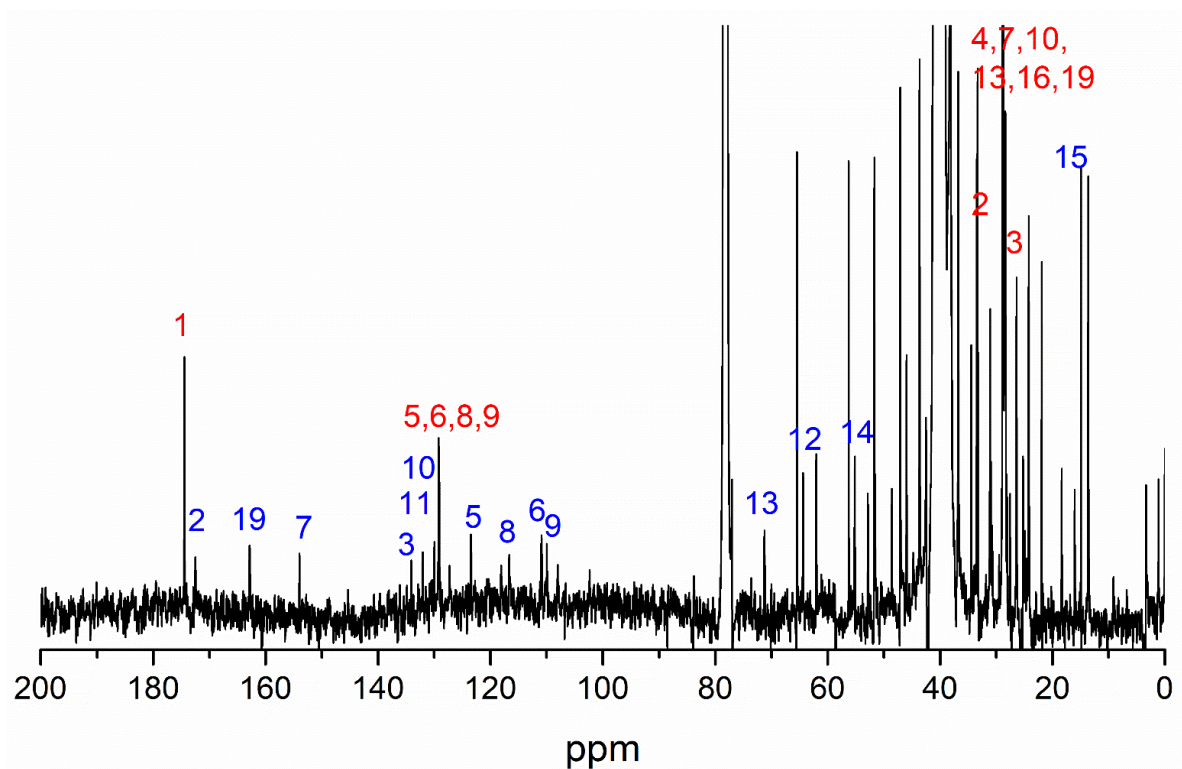
Volume (L)	Solvents	Relation (%)
0.5	Hx:AcOEt	100:0
2.0	Hx:AcOEt	95:5
1.0	Hx:AcOEt	90:10
1.5	Hx:AcOEt	85:15
0.5	Hx:AcOEt	80:20
0.5	Hx:AcOEt	70:30
0.5	AcOEt	100
0.5	Methanol	100

Supplemental table 2. Weight obtained of the each fraction isolated from shrimp (*L. stylirostris*) per g of chloroformed extract.

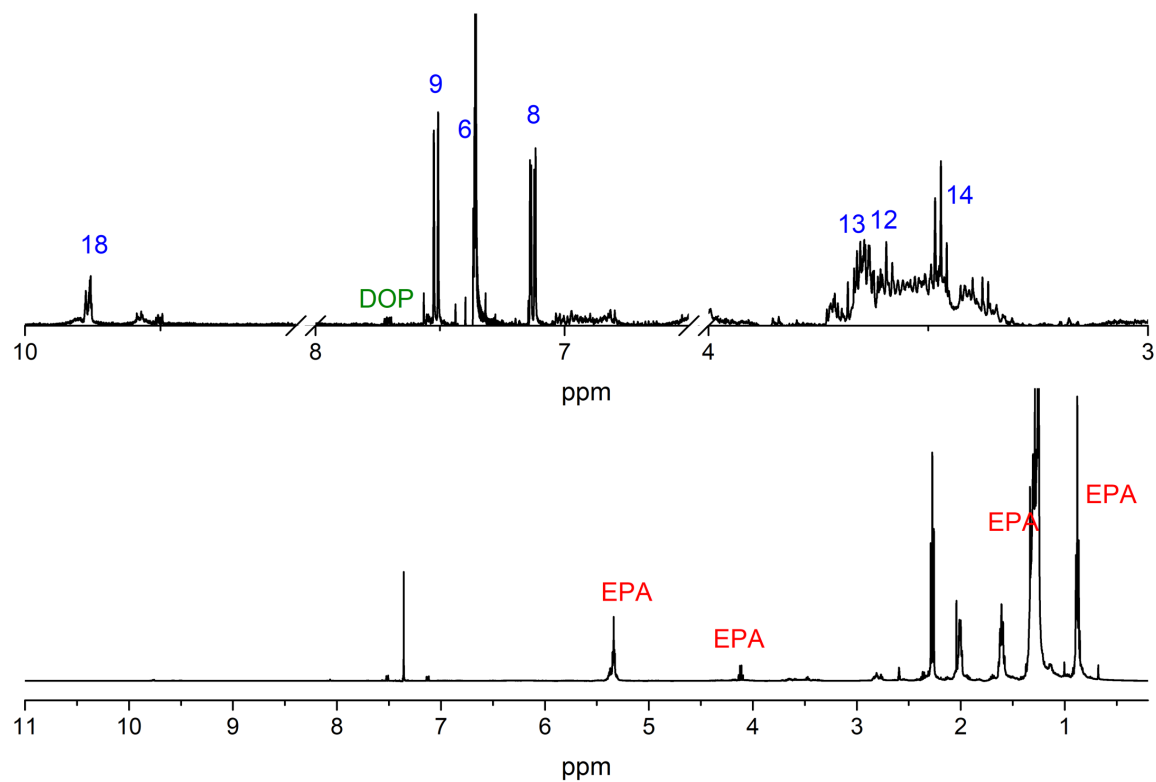
Fraction	Weight (mg)
A	2.1
B	17.8
C	18.3
D	9.6
E	2.7
F	6.1
G	7.2
H	5.1
I	182.9
J	395.8
K	37.8
L	61.3
M	70.9
N	26.9
O	17.8
P	25.4
Q	3.2
R	58.2



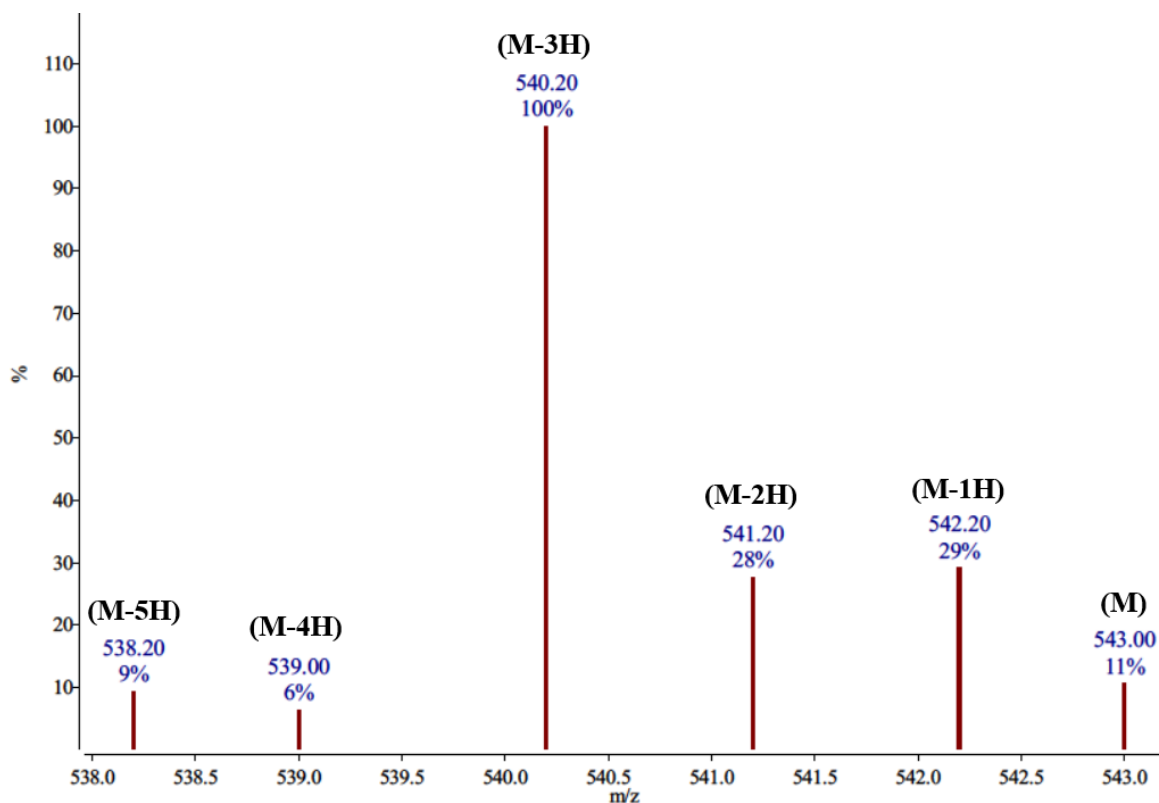
Supplemental figure 1. UV-Vis (a) and fluorescence (b) spectra of fM diluted in methanol.



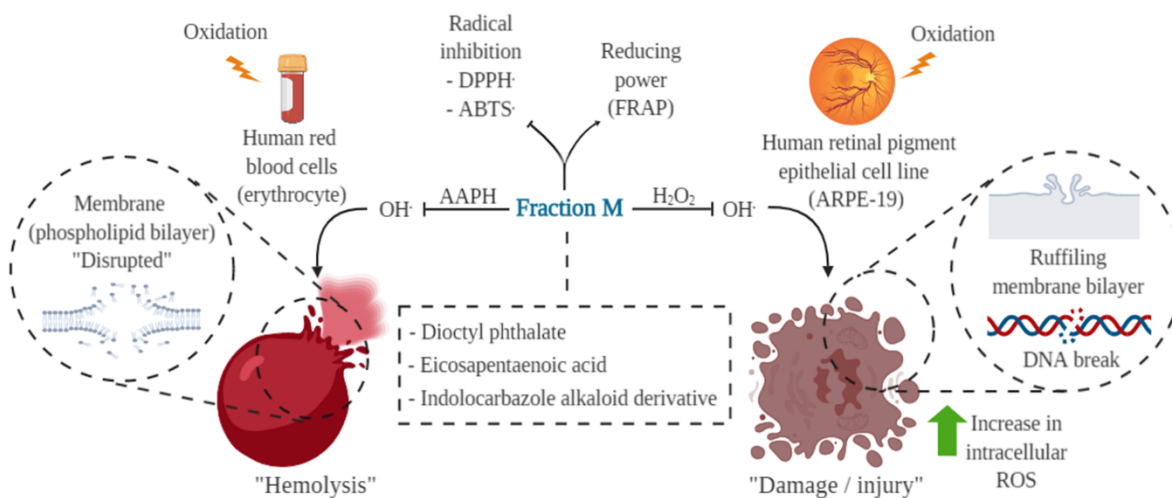
Supplemental figure 2. ¹³C-NMR of fM: EPA color red and IAD color blue.



Supplemental figure 3. ¹H-NMR of fM: EPA color red, DOP color green and IAD color blue.



Supplemental figure 4. Mode negative ESI /MS of IAD, pointing the mass / charge of IAD and their isotopes (M-H).



Graphical abstract. Bioactivities general diagram of fM isolated from wild shrimp (*Litopenaeus stylirostris*) muscle.

CAPÍTULO II

**Isolation and Identification of A New Antiproliferative Indolocarbazole Alkaloid
Derivative Extracted from Farmed Shrimp (*Litopenaeus Vannamei*) Muscle**

Artículo enviado a: JMBFS – journal of microbiology biotechnology and food science

Año: 2020

ISOLATION AND IDENTIFICATION OF A NEW ANTIPROLIFERATIVE INDOLOCARBAZOLE ALKALOID DERIVATIVE EXTRACTED FROM FARMED SHRIMP (*Litopenaeus vannamei*) MUSCLE

Joel Said García-Romo¹, Martín Samuel Hernández-Zazueta¹, Alma Carolina Galvez-Iriqui¹, Maribel Plascencia-Jatomea¹, María Guadalupe Burboa-Zazueta², Edgar Sandoval-Petris², Rosario Maribel Robles-Sánchez¹, Josué Elías Juárez-Onofre³, Javier Hernández-Martínez⁴, Hisila Del Carmen Santacruz-Ortega⁵, Carmen María López-Saiz¹, Armando Burgos-Hernández^{1*}

Address: Dr. Armando Burgos-Hernández

¹Departamento de Investigación y Posgrado en Alimentos, Universidad de Sonora, 83000 Sonora, Mexico. Tel.: + 526-622-592-208; Fax: + 526-622-592-209.

²Departamento de Investigaciones Científicas y Tecnológicas, Universidad de Sonora, 83000 Sonora, Mexico.

³Departamento de Física, Universidad de Sonora, 83000 Sonora, Mexico.

⁴Unidad de Servicios de Apoyo en Resolución Analítica, Universidad Veracruzana, 91190 Veracruz, Mexico

⁵Departamento de Investigación en Polímeros y Materiales, Universidad de Sonora, 83000 Sonora, Mexico.

*Corresponding author: armando.burgos@unison.mx

ABSTRACT

Farmed shrimp *Litopenaeus vannamei*, one of the most popular seafood worldwide, has been reported as a source of antiproliferative extracts still to be fully characterized. The aim of this study was to isolate and identify these antiproliferative compounds. From a chloroform-soluble extract from shrimp muscle, hexane- and methanol-soluble fractions were obtained and tested for antiproliferative activity (MTT), a bioassay that guided the fractionation and isolation of bioactive fractions using open column chromatography. MeOH-soluble fraction resulted bioactive and was subjected to further fractionation from which one subfraction outstand for being highly active against prostate cancer cell line. Antiproliferative effects were evaluated

using colorimetric assays and cell morphology observations. Further chromatographic procedures resulted in sub-fractions from which one was effective in causing damage to DNA and F-actin polymerization, suggesting cellular collapse and apoptosis. According to the structural chemical characterization carried out, dioctyl phthalate, eicosapentaenoic acid, and an indolocarbazole alkaloid type of compound were identified. This last compound, which resulted majorly responsible for the bioactivity, was not found reported in the available databases; however, further investigation is needed for a full chemical characterization and structural confirmation.

Keywords: shrimp, *Litopenaeus vannamei*, antiproliferative, bioactive compounds, marine source.

INTRODUCTION

Academic and pharmaceutical institutions have developed a number of chemotherapeutic compounds but their efficacy and adverse effects are limitations for their use (**Buzdar *et al.*, 2005; DeVita & Chu, 2008; Martin *et al.*, 2014**). Another problem in cancer chemotherapy is drug resistance (**Austreid, Lonning, & Eikesdal, 2014**). Therefore, the search for more effective and safer bioactive molecules gains importance (**Livstone, 2019**).

The search for novel natural bioactive products is not an easy task; there are many challenges throughout the process of obtaining new effective and efficient drugs. Despite that, various organizations have decided to reduce mortality and morbidity rates through investigation on biologically active compounds from nature (**De Kok, Van Breda, & Manson, 2008; Thomson, LeWinn, Newton, Alberts, & Martinez, 2003**), and the search for these new molecules in the marine environment is each time more frequently considered. Nowadays, a number of studies have reported the existence of potential anticancer compounds (**Lordan, Ross, & Stanton, 2011; Stankevics, Aiub, Maria, Lobo-Hajdu, & Felzenszwalb, 2008**), which include bacterial, fungal, but also higher animals including commonly consumed seafood; among them are shrimp species.

Shrimp, one of the most popular seafood in the world, has been reported to contain potential anticancer compounds in its lipid fraction (**López-Saiz *et al.*, 2016; López-Saiz, Suárez-Jiménez, Plascencia-Jatomea, & Burgos-Hernández, 2013; Wilson-Sanchez *et al.*, 2010**). Examples include carotenoids, which have been associated to apoptosis induction and oxidative stress promotion in cancer cells lines (**Sila *et al.*, 2013; Sowmya, Arathi, Vijay, Baskaran, & Lakshminarayana, 2017**). Also, hemocyanin has reported as a cancerous cell-growth inhibitor and apoptosis inductor (**Zheng *et al.*, 2016**), and to exert antitumorigenicity in *in vivo* studies (**S. Liu *et al.*, 2017**).

From our laboratory, a triglyceride esterified containing polyunsaturated fatty acids was reported to have the capability of inhibiting proliferation of a murine lymphoma cell line (López-Saiz *et al.*, 2014); however, other biologically active fractions obtained during this study were also reported. Based on the above, the aim of the present study was to characterize these antiproliferative fractions previously reported in farmed shrimp *Litopenaeus vannamei* and to study the possible ways by which these molecules might act.

MATERIALS AND METHODS

Testing species

Farmed shrimp (*Litopenaeus vannamei*) was obtained from a local market in Hermosillo, Sonora, Mexico and transported in ice to the University of Sonora Laboratory. Edible portions of shrimp (muscle) were separated and immediately processed for extraction according to reported procedure López-Saiz *et al.*, (2014).

Crude extraction and solvent partition

Shrimp muscle extraction and solvent partitioning procedures were conducted according to reported procedure López-Saiz *et al.*, (2014), from which hexane- and methanol-soluble fractions were obtained and dried under N₂ stream for further biological activity testing.

Column chromatography

Methanol-soluble fraction was reconstituted again in methanol and was subjected to fractionation using open column chromatography to obtain same fractions reported by López-Saiz *et al.*, (2014). All of the fractions were tested to confirm their biological activity.

Semi-preparative thin layer chromatography (TLC) and partial purification

The fraction with the highest biological activity were further fractionated using preparative silica gel-TLC, using hexane-ethyl acetate (95:5) as a developing solvent system (W. Liu *et al.*, 2019). All of the sub-fractions were evaluated for biological activity. For further purification of the most active compounds, undesired substances were eliminated by solvent partitioning.

Cell lines

Five cancerous- [A-549 (lung carcinoma), HCT116 (colon carcinoma), HeLa (epithelioid cervix carcinoma), MDA-MB-231 (breast adenocarcinoma), and 22Rv1 (prostate carcinoma)] and 1 non-cancerous [ARPE-19 (retinal pigmented epithelium)] human epithelial cell lines were used. Cells were cultured in Dulbecco's modified Eagle's medium (DMEM) and RPMI-1640 Medium

(Sigma Aldrich, St. Louis, MO, USA), supplemented with 10 and 15 % heat-inactivated fetal bovine serum (FBS) (Corning, NY, USA) and grown at 37 °C in an atmosphere of 5 % CO₂.

3-(4, 5-Dimethylthiazol-2-yl)-2, 5-Diphenyltetrazolium Bromide (MTT) assay

Antiproliferative activity on cell lines was evaluated using the MTT assay (Roche, cell proliferation kit I, Roche, Cat. No. 11-465-007-001), according to manufacturer's instructions. Briefly, 1×10^4 and 2×10^4 cells/well were suspended in 100 μ L on DMEM or RPMI at 10 – 15 % of SFB, according to ATCC specifications (**Boyd & Paull, 1995**); they were seeded on each well of a flat-bottom 96-well plate and incubated for 24 h. Then, cell cultures were incubated in 100 μ L of medium containing different concentrations of each of the samples dissolved in DMSO, diluted in supplemented medium at 10 – 15 % of FBS, and incubated for another 48 h. Control cell cultures were incubated with medium (final concentrations of DMSO 0.06 % – 0.5 % v/v) only. After 4 h of cell culture, 10 μ L of MTT stock solution (5 mg/mL) were added to each well. Formazan crystals formed were dissolved with 100 μ L sodium dodecyl sulfate (SDS) and the absorbance in each well was read overnight using an ELISA plate reader (Benchmark Microplate Reader; Bio-Rad, Hercules, CA, USA) at test wavelength of 570 nm and a reference wavelength of 650 nm. Cisplatin (CIS) (15663-27-1, Sigma-Aldrich) and docetaxel (DOC) (01885, Sigma-Aldrich) were used as positive antiproliferation controls. Dioctyl phthalate (DOP) (D201154, Sigma-Aldrich) and eicosapentaenoic acid (EPA) (E-2011, Sigma-Aldrich) were used as confirmatory standards for selected bioactive fractions. In order to evaluate the growth behavior of the most sensitive cell line to a specific fraction, a cellular growth kinetic was made from 0 to 72 h. Three independent assays were made and all testing concentrations were assayed in triplicate (**K. Liu, Xiao, Wang, Chen, & Hu, 2017**).

Phalloidin–tetramethylrhodamine B isothiocyanate and 4', 6-Diamidino-2-phenylindole, dilactate fluorescence cell staining

In order to observe the effect of shrimp fractions on internal morphological/structural aspects of cell lines, staining procedures were performed (**Van Vuuren, Botes, Jurgens, Joubert, & Van Den Bout, 2019**) with modifications. Testing cells were seeded onto 96-well microplates for 24 h and treated with sub-fractions at their GI₅₀. With the aim of seeking the incubation time at which morphological changes cell can be observed, cells were fixed with 3.7 % formaldehyde in PBS and were permeabilized with 0.2 % Triton X-100 in PBS for 15 min, after 4, 12, 24, and 48 h. Then, in order to visualize cell structures, cells were stained with both phalloidin–tetramethylrhodamine B isothiocyanate (phalloidin) (Sigma-Aldrich, MFCD00278840) and 4', 6-Diamidino-2-phenylindole, dilactate (DAPI) (Sigma-Aldrich, D9564) for F-actin and nuclear material through DNA, respectively. Microplates were mounted on an inverted epifluorescence microscope (Leica DMi8) to performed observations.

Ultraviolet–visible (UV-Vis) and fluorescence spectroscopies

Bioactive subfraction was solubilized in chromatographic-grade methanol and analyzed on an Agilent diode array spectrophotometer (model 8453, Shanghai, China) for the UV-Vis, and in a Perkin Elmer LS-50B Luminescence Spectrometer (Buckinghamshire, England) in case of fluorescence spectroscopy. In both determinations, a wavelength-range from 200 to 700 nm (at 25 °C), and 1 cm quartz cuvette were used.

Proton-nuclear magnetic resonance (¹H- NMR)

Measurements were performed in a Bruker NMR spectrometry equipment operated at 400 MHz (Billerica, MA, USA). Fractions were dissolved in CDCl₃ using tetramethylsilane (500 µL; Sigma-Aldrich, Saint Louis, MI, USA) as an internal standard. The resulting mixture was placed into a 5 mm diameter ultra-precision NMR sample tubes at 23°C. Chemical shifts were recorded in ppm, using TMS proton signal as an internal standard.

Electrospray ionization tandem mass spectrometry (ESI/MS)

The ESI/MS were performed on 6130 Quadrupole LC/MS of Agilent Technologies (Santa Clara USA). The instrument was operated in the negative [M-H]⁻ and positive [M+H]⁺ ion mode. The sample was performed in methanol acetonitrile 50:50, at 300 °C.

Statistical analysis

Data were analyzed using an analysis of variance (ANOVA) with Tukey multiple comparisons test (Tukey's post hoc test), at a 95 % confidence interval, and the level of significance of $P \leq 0.05$, (SPSS). In order to calculate GI₅₀ values (medium growth inhibition) for biologically active fractions, a probit analysis was performed using the Number Cruncher Statistical Software (NCSS), version 2001, NCSS Statistical Software, USA. All data are the mean value with their standard deviation (mean ± S.D.). Data computation was made following procedures reported by the National Cancer Institute (NCI) / National Institutes of Health (NIH). Developmental Therapeutics Program (DTP), Human Tumor Cell Line Screen Process (<http://dtp.nci.nih.gov/branches/btb/ivclsp.html>) and as described by **Monks *et al.*, 1991**.

RESULTS AND DISCUSSION

Extraction and fractions obtained

Chloroform-soluble extract (yield of 5.58 g/kg of shrimp muscle) was obtained, from which two partitions were achieved: a hexane- and a methanol-soluble partitions. Methanol-soluble partition resulted bioactive and it was fractionated using open column chromatography, from which were obtained 15 packages of fractions, denominating them fraction M (methanol partition) 1 - 15, whose yield (in mg per g of methanol partition) of each fractions are the following: 1, 7.9; 2, 23.5; 3, 24.1; 4, 15.4; 5, 8.4; 6, 11.9; 7, 12.9; 8, 10.9; 9, 188.7; 10, 401.5;

11, 43.6; 12, 67.0; 13, 76.7; 14, 32.7; 15, 23.6. In order to localize the compounds with the highest antiproliferative activity among these 15 fractions, they were tested against different human cancer cell line; then a sub-division (highest level of purity) of the most bioactive fraction (M.11), calls sub-fraction M.11.A, M.11.B, M.11.C, and M.11.D, where the % obtained was 30, 10, 60 and 10, respectively; once the present compounds were identified, a partial purification of bioactive sub-fraction, was carried out.

Bioactivity-guided isolation of antiproliferative compounds

The potential that sample has to prevent the proliferation of cancerous cells is known as antiproliferative activity; detection of this bioactivity in all of the fractions obtained was performed using the MTT assay and the selection of the most bioactive fractions was based on their half-maximal growth inhibition (GI_{50}) values, the lower this value the higher the bioactivity. As shown in **Table 1**, only methanol partition could reduce (GI_{50} values of 177 ± 8 $\mu\text{g/mL}$) the proliferation of 22Rv1 cell line, without affecting a non-cancerous cell line (ARPE-19). Methanol partition was then fractionated resulting in 15 fractions, from which M.11, M.12, and M.15 showed antiproliferative activity on human cell line 22Rv1 (prostate cancer), with GI_{50} values of 70.6 ± 5.8 , 71.0 ± 4.5 , and 70.3 ± 5.6 $\mu\text{g/mL}$, respectively (**Table 2**). However, as shown also in **Table 2**, fraction M.11 was significantly ($P \leq 0.05$) more active against HeLa, MDA-MB-231, and A549 cell lines than the other 2 fractions, therefore it was selected for further fractionation.

Table 1. Half-maximal growth inhibition (GI_{50}) for crude extract and partitions obtained from farmed shrimp (*Litopenaeus vannamei*) muscle on human epithelial cell lines after 48 h.

	($\mu\text{g/mL}$)	
	<i>Cancerous cell</i>	<i>Non-cancerous cell</i>
	22Rv1	ARPE-19
Chloroform crude extract	> 200 b	> 200 a
Hexane partition	> 200 b	> 200 a
Methanol partition	177 ± 8 a	> 200 a

Values represent means \pm S.D. from 3 determinations. Different letters within the same column are significantly different ($P \leq 0.05$); Tukey's least significant difference test. Control cell cultures were incubated with DMSO (0.5 %) and represent 100 % proliferation. These values were statistically estimated from a dose response curve using concentrations of 200 $\mu\text{g/mL}$ downwards.

Table 2. Half-maximal growth inhibition (GI₅₀) for fractions obtained from column chromatography fractionation of the methanol-partition, on human cancer epithelial cell lines after 48 h.

	(µg/mL)				
	<i>Adenocarcinomas</i>		<i>Carcinomas</i>		
	HeLa	MDA-MB-231	A549	22Rv1	HCT116
M.1	> 200 e	> 200 e	172 ± 16 d	135 ± 17 cd	> 200 e
M.2	> 200 e	> 200 e	86 ± 10 b	195 ± 11 f	> 200 e
M.3	> 200 e	> 200 e	> 200 e	> 200 f	> 200 e
M.4	> 200 e	> 200 e	> 200 e	> 200 f	> 200 e
M.5	> 200 e	> 200 e	> 200 e	142 ± 7 d	> 200 e
M.6	> 200 e	148 ± 10 cd	> 200 e	117 ± 7 c	> 200 e
M.7	> 200 e	> 200 e	> 200 e	> 200 f	> 200 e
M.8	> 200 e	> 200 e	> 200 e	> 200 f	> 200 e
M.9	> 200 e	> 200 e	167 ± 11 d	173 ± 11 e	189 ± 9 e
M.10	161 ± 9 d	> 200 e	131 ± 8 c	84.0 ± 6.2 b	130 ± 19 d
M.11	144 ± 13 c	101 ± 10 b	83.5 ± 12.2 b	70.6 ± 5.8 b	92.7 ± 16 c
M.12	148 ± 8 c	132 ± 6 c	174 ± 13 d	71.0 ± 4.5 b	112 ± 16 cd
M.13	> 200 e	> 200 e	> 200 e	> 200 f	> 200 e
M.14	> 200 e	> 200 e	> 200 e	> 200 f	> 200 e
M.15	> 200 e	138 ± 8 cd	> 200 e	70.3 ± 5.6 b	107 ± 15 cd
CIS	47.1 ± 3.8 b	152 ± 5 d	33.6 ± 2.6 a	21.6 ± 2.4 a	61.2 ± 5.1 b
DOC	10.9 ± 3.6 a	21.0 ± 3.5 a	18.5 ± 2.6 a	24.1 ± 6.6 a	12.8 ± 2.4 a

Values represent means ± S.D. from 3 determinations. Different letters within the same column are significantly different ($P \leq 0.05$); Tukey's least significant difference test. Control cell cultures were incubated with DMSO (0.5 %) and represent 100 % proliferation. These values were statistically estimated from a dose response curve using concentrations of 200 µg/mL downwards. Cisplatin (CIS) and docetaxel (DOC) were used as a positive control for cell growth inhibition. Adenocarcinomas and carcinomas refers to the cell disease.

In order to reach a higher level of isolation of the bioactive compounds, fraction M.11 was carried out by TLC in 4 groups of compounds with different polarities, which were coded sub-fractions M.11.A, M.11.B, M.11.C, and M.11.D. As shown in **Table 3**, sub-fraction M.11.B, was the most bioactive against the 22RV1 cell line, with a GI₅₀ = 46.6 ± 2.2 µg/ml; shows that the fraction procedure increased the antiproliferative activity, since the GI₅₀ value decreased from 70.6 ± 5.8 (in M.11) to 46.6 ± 2.2 µg/ml (in M.11.B), making it more effective against prostate cancerous cell line.

Table 3. Half-maximal growth inhibition (GI₅₀) for sub-fractions obtained from thin layer chromatography fractionation of fraction M.11, on human epithelial cell lines at 48 h.

	(μg/mL)		Biosselective index
	<i>Cancerous cell</i>	<i>Non-cancerous cell</i>	
	22Rv1	ARPE-19	
M.11.A	134 ± 11 c	> 200 c	> 1.48
M.11.B	46.6 ± 2.2 b	> 200 c	> 4.29
▪ M.11.B. 1	26.6 ± 8.0 a	180 ± 3 b	6.77
M.11.C	> 200 d	> 200 c	---
M.11.D	> 200 d	> 200 c	---
DOP	> 200 d	> 200 c	---
EPA	58.3 ± 10 b	> 200 c	> 3.42
CIS	21.6 ± 2.4 a	184 ± 15 b	8.52
DOC	24.1 ± 6.6 a	155 ± 4 a	6.44

Values represent means ± S.D. from 3 determinations. Different letters within the same column are significantly different ($P \leq 0.05$); Tukey's least significant difference test. Control cell cultures were incubated with DMSO (0.5 %) and represent 100 % proliferation. Dioctyl phthalate (DOP) and eicosapentaenoic acid (EPA) were used as standard controls. Cisplatin (CIS) and docetaxel (DOC) were used as a positive antiproliferative control. (---) means "was not determined".

Characterization of sub-fraction M.11.B

For chemical/structural characterization of fraction M.11.B, UV-Vis, fluorescence, $^1\text{H-NMR}$, and ESI/MS were used. UV-Vis analysis showed that compounds present in M.11.B have maximum absorption at wavelength of 205, 223, and 274 nm, these transitions are attributed to $\pi \rightarrow \pi^*$, which are associated to the presence of aromatic compounds (**Fig. 3 A**). In addition, two bands with low absorbance at 313 and 350 nm and attributed to $n \rightarrow \pi^*$ transition were also observed. This kind of transitions are related to aromatics rings that have attached atoms with available electrons (e.g. O and N). The fluorescence study (**Fig. 3 B**) showed an emission band centered at $\lambda = 311$ nm when the sample was excited at $\lambda = 250$ or 274 nm, suggesting the presence of a single compound responsible for this emission. These results confirm the presence of aromatics rings present in the extract.

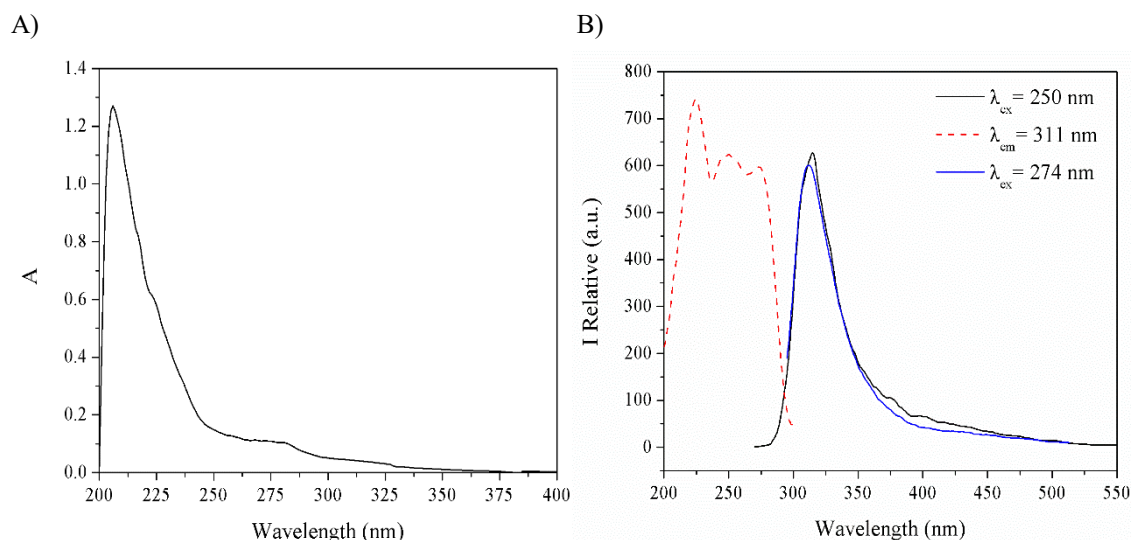


Figure 3. UV-Vis (A) and fluorescence (B) spectra of sub-fraction M.11.B diluted in methanol.

Results from ^1H -NMR showed that M.11.B consists of more than one compound (**Table 4**). A characteristic pattern of 1, 4 di-substituted aromatic ring [$\delta = 7.71$ ppm (*dd*, $J = 5.7, 3.3$ Hz)], coupling pattern of the protons of the aromatic ring [7.53 ppm (*dd*, $J = 5.7, 3.3$ Hz)], signals obtained at δ of 4.22 ppm (associated to O-CH_2), at δ high field of 1.25 ppm (CH_2) and signals at δ 0.88 ppm (CH_3 groups) suggest the presence of dioctyl phthalate (DOP), which has been reported by others (**Cruz-Ramírez *et al.*, 2015**; **López-Saiz *et al.*, 2014**; **García-Romo *et al.*, 2018**).

On the other hand, signals (ppm) on 5.33 (*m*), 2.83 (*m*), 2.35 (*t*, $J = 7.5$ Hz, 3H), 2.03 (*m*) suggested the presence of eicosapentaenoic acid (EPA), and they are in accordance with those reported in the literature (**Tyl, Brecker, & Wagner, 2008**). At this stage, results suggested the presence of DOP and EPA in M.11.B; however, others signals were also detected.

Likewise, signals that appeared at $\delta = 9.77$ (*s*) ppm; corresponding to alcohol groups, $\delta = 7.54$ (*d*), 7.36 (*d*) and 7.13 (*dd*) ppm; corresponding to protons belonging to aromatic rings with a substitution, signals at $\delta = 3.8 - 3.4$ (*m*) ppm; belong to aliphatic protons, and that at $\delta = 1.15$ (*d*) ppm; associated to methyl protons, were also observed. The signals in the ^1H -NMR spectrum of the proposed molecule presenting the activity show signals in the aromatic region as in the aliphatic region. The complex coupling pattern of the signals that appear in the aromatic region indicate that there is a trisubstituted type aromatic ring of type 1, 2, 4. The signals in the region 3-4 ppm indicate that the protons are attached electronegative elements such as oxygen or nitrogen.

Table 4. ¹H-NMR spectra of sub-fraction M.11.B in CDCl₃ at 400 Hz.

Diethyl phthalate (DOP)		Eicosapentaenoic acid (EPA)		Indolocarbazole alkaloids derivative (IAD)	
No.	δ_H	No.	δ_H	No.	δ_H
2	7.71 (dd, J= 5.7, 3.3 Hz, 2H)	5, 6, 8, 9,	5.35 (m, 10H)	18	9.77 (s, 2H)
1	7.53 (dd, J= 5.7, 3.3 Hz, 2H)	11, 12, 14,		9	7.54 (d, J=8.7 Hz, 2H)
5	4.22 (m, 4H)	15, 17, 18		6	7.36 (d, J=2.1 Hz, 2H)
6, 7,	1.25 (s, 18H)	4, 7, 10,	2.83 (m, 12H)	8	7.13 (dd, J=8.8, 2.6 Hz, 2H)
8,		13, 16, 19		12, 13, 14	3.8 – 3.4 (m, 5H)
9, 11					
10, 12	0.88 (m, 12H)	2	2.35 (t, J= 7.5 Hz, 3H)	15	1.15 (d, J= 6.28 Hz, 6H)
		4	2.03 (m, 2H)		

In addition, results from ESI-MS, in negative mode (**Fig. 4**), indicated a molecular weight of 540.06 m/z, which is not consisting neither with DOP or EPA, which indicates that the signal observed possibly corresponds to an indolocarbazole alkaloid derivative (IAD). Considering the number of signals observed in the NMR spectrum and the observed molecular weight found, it indicates that the molecule is symmetric. The shape of the signals in the aromatic region coincides with those in Arcyriaflavin C (**Kotha, Saifuddin, & Aswar, 2016; Nakatani *et al.*, 2003; Steglich, Steffan, Kopanski, & Eckhardt, 1980**). Based on the information obtained by the different spectroscopic data the molecules suggested as components of M.11.B (**Fig. 5**). **Table 4** shows the chemical shifts as well as the integrals of the signals observed in the NMR spectrum.

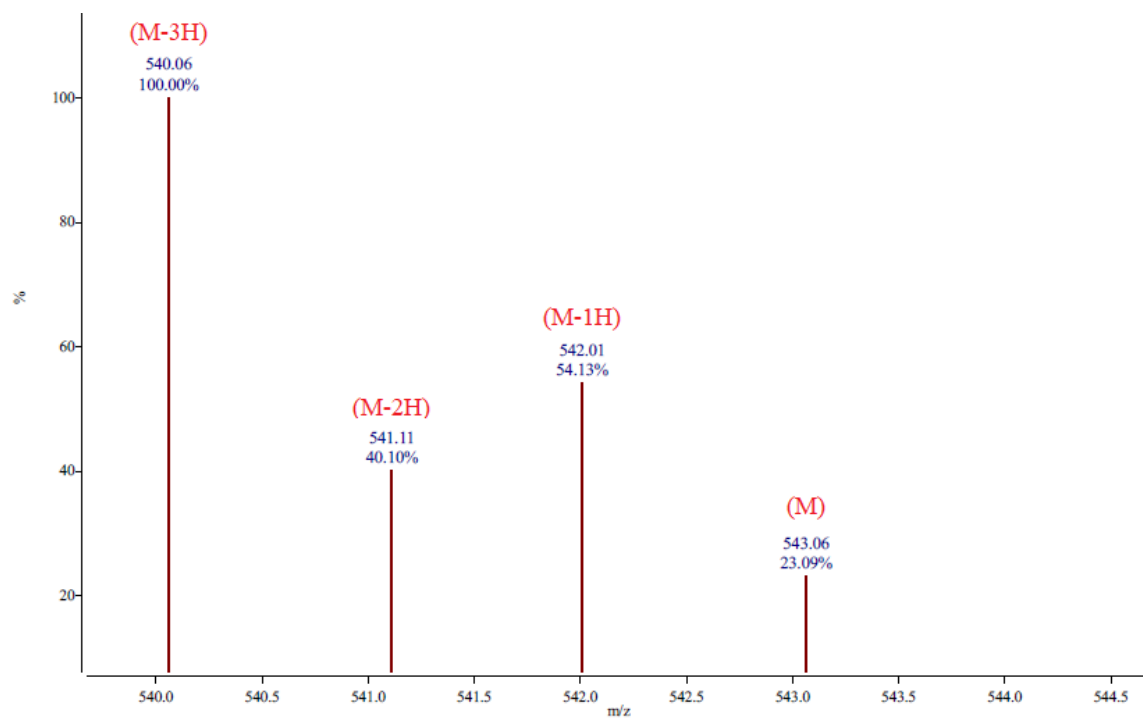


Figure 4. Mode negative ESI /MS of sub-fraction M.11.B, pointing the mass / charge of IAD and their isotopes (M-H).

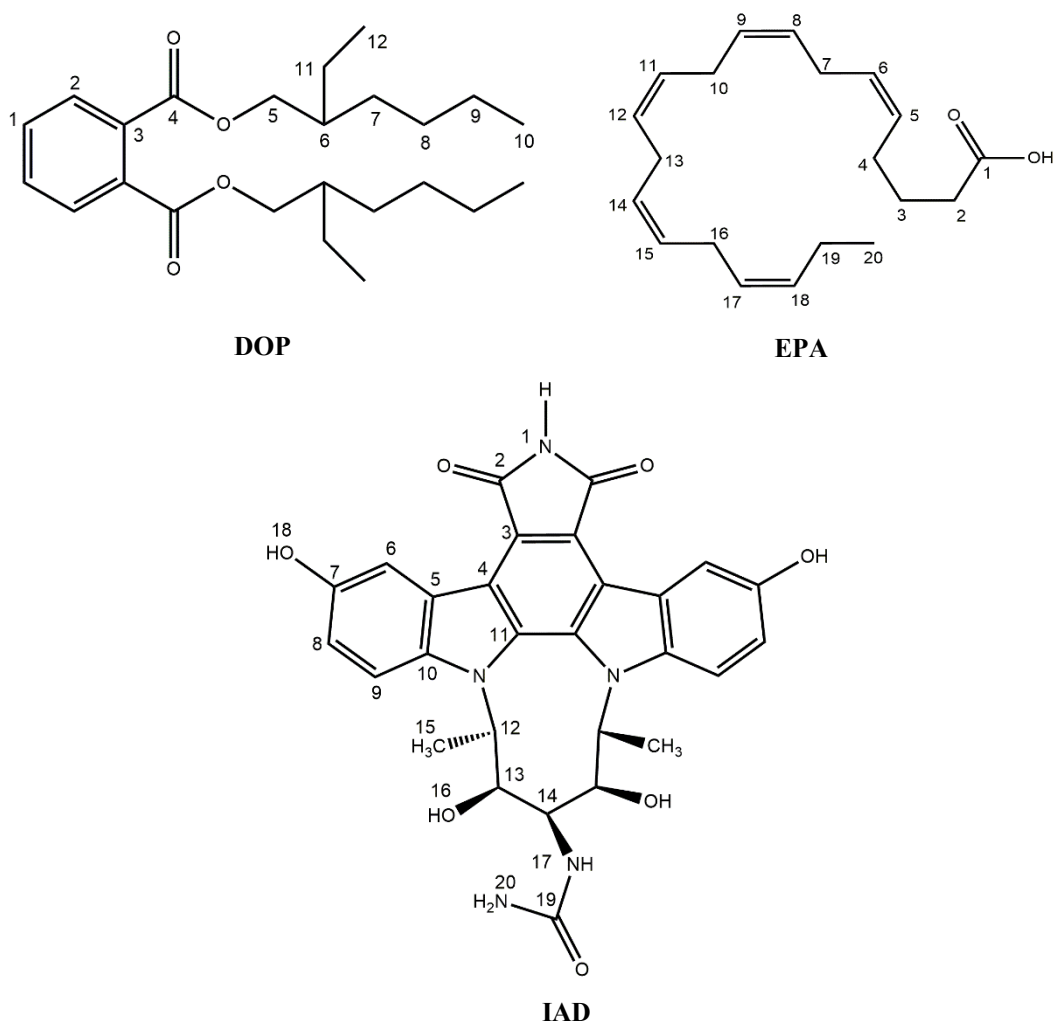


Figure 5. Compounds present in sub-fraction M.11.B based on structural chemical characterization

The molecule proposed as representative of antiproliferative activity is 1-((5*S*,7*r*,9*R*)-2,6,8,12-tetrahydroxy-5,9-dimethyl-14,16-dioxo-6,7,8,9,15,16-hexahydro-5*H*,14*H*-4*b*,9*a*,15 triazadibenzo [b, h] cyclonona [jkl] cyclopenta [e] -as-indacen-7-yl) urea (IUPAC nomenclature), with chemical formula $C_{28}H_{25}N_5O_7$ and with mass of 543 Da, this molecule has the characteristics of a new indolocarbazole alkaloid derivative (IAD). The molecule contains atoms of nitrogen related to alkaloid compounds, presenting heterocyclic aromatic organic rings characteristic of the indoles, these are widely distributed in the natural environment and can be produced by a wide variety of bacteria; being structures derived from the indoles, the indocarbazoles.

On the other hand, chemical structures derived from them and biologically active are the arcyriaflavin, whose molecule is structural base (substituted or not) of the compound isolated in the sample of shrimp; arcyriaflavin is a compound that is structurally related to staurosporine. The staurosporine, are chemical structures similar to our molecule present in M.11.B, example of these with anticancer activity are: 7-oxo-3, 8, 9-trihidroxiestaurosporina (more similarity with our molecule) and 7-oxo -8, 9-dihydroxy-4'-N demethystastaporine which were isolated from the ascidia marine *Cystodytes solitus* and both showed cytotoxicity to cell lines A549, HT-29 and MDA-MB-231 (Reyes *et al.*, 2008), as well as isolated in higher organisms (Jimenez *et al.*, 2012). Therefore, indolocarbazole are a class of compounds that are currently being studied due to their potential as anticancer drugs, as well as to the extensive and possible number of derivatives from them, since then a wide range of structures and derivatives have been found or developed throughout the world, as well as their important uses and applications (Sánchez, Méndez, & Salas, 2006; Wang, Zhang, Li, Ding, & Ma, 2018); and as we know there is an extensive list of indole alkaloids type of molecules that have been isolated from different marine organisms whit bioactivity potential (Netz & Opatz, 2015).

Antiproliferative activity of sub-fraction M.11.B.1 and bioselectivity

Chemical / structural characterization carried out on fraction M.11.B allowed the identification of 2 of at least three compounds present in this fraction; therefore, they were commercially obtain and tested for bioactivity confirmation (Table 3). Resulting for DOP (GI₅₀ greater than 200 µg/ml) against 22Rv1 cell line suggested that DOP does not contribute to M.11.B antiproliferative activity. On the other hand, a GI₅₀ = 58.3 ± 10 µg/ml value obtained for EPA indicated contribution of this compound to M.11.B bioactivity. Other studies have reported similar GI₅₀ values for EPA (Chiu & Wan, 1999; Lai, Ross, Fearon, Anderson, & Carter, 1996; Li, Hou, Yeh, & Yeh, 2017; Turan, Kaya, & Erdem, 2011). However, by being this GI₅₀ value higher than that obtained for M.11.B, the presence of a third more active compound is suggested. As an additional test, M.11.B was partially purified by removing DOP as much as possible with a wash with ethyl ether (10:1 DMSO v/v), and the resulted purified fraction (M.11.B.1) was tested again for bioactivity.

Sub-fraction M.11.B.1 showed the highest antiproliferative activity (Table 3), showing a GI₅₀ = 26.6 ± 8 µg/mL; according to American National Cancer Institute (NCI) criteria, GI₅₀ limit value to consider a crude extract promising for further purification is lower than 30 µg/mL (Upper limit) (Abdel-Hameed, Bazaid, Shohayeb, El-Sayed & El-Wakil, 2012; Suffness & Pezzuto, 1990).

Bioselectivity index (BI) is the term is used to refer to an agent that exhibits a difference growth

inhibitory effects between normal and cancerous cell lines. An agent is labeled as "bioselective" if it shows a ratio of at least 3 times its value between its GI₅₀ of normal and cancerous cells (Ciavatta *et al.*, 2017). In this case, the sub-fraction M.11.B.1 was bioselective against 22Rv1 cell line (Table 3); the BI was 6.77, and it has been established that the higher the BI, a greater chance has the agent of being effective on cancerous cells without harming non-cancerous cells.

Growth kinetics allows us to determine the number of cells affected by M.11.B.1; once the dose-response relationship is obtained, the number of affected (dead/ inhibited) cells by a certain concentration (at a determined time of incubation under stimulus) can be determined. This was obtained for 22Rv1 cell line in 10 % FBS (Fig. 1). The effective concentration (EC) is the proportion of a substance in a medium that causes a certain effect in a given model (cells); the number of prostate cancer cells obtained after 48 h of incubation were 32500, meaning that 22500 cells proliferated in 48 h since 10000 cells were seeded. Therefore, the EC to affect 50 % (EC₅₀) of cell growth (11250 cells) is $26.6 \pm 8 \mu\text{g/mL}$, considering this as antiproliferation.

To obtain inhibition values equal or lower than 10000 cells on *in vitro* proliferation systems, we would be talking about cytostatic and cytotoxic terms, like total growth inhibition (TGI), which refers to 0 % of proliferations cells (22500) and lethal concentration medium (LC₅₀) that refers to -50 % of viable cells (<10000, which refers to the number of cells seeded), respectively (Boyd & Paull, 1995), whose required concentrations to this values are greater than 200 $\mu\text{g/mL}$.

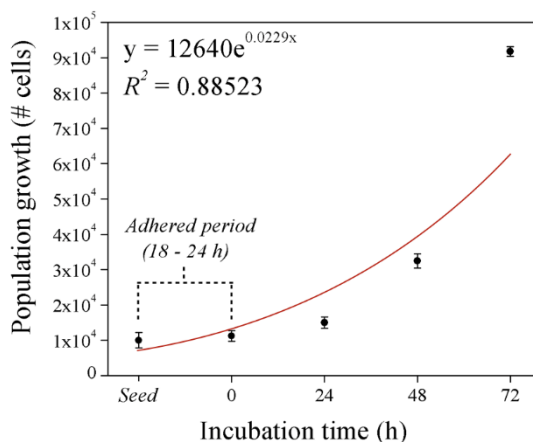


Figure 1. Growth kinetics of 22Rv1 cell line (human prostate epithelial carcinoma). Values represent means \pm S.D. from 3 determinations. Cells were plated in medium RPMI-1640 with 10 % FBS. These means optimal growth, when the cultures were incubated with DMSO (0.5 %) and represent 100 % proliferation on assays.

According to the ATCC, the 22Rv1 (ATCC® CRL-2505™) cell line, is a human epithelial prostate and tumorigenic carcinoma that has an androgen receptor and which growth is stimulated by epidermal growth factor (EGF), but is not inhibited by transforming growth factor

beta-1 (TGF beta- 1). Moreover, the compounds could be conducting an antiproliferative activity by means of this receptor, this if the extrinsic pathway were taken into account; however, another way of action would be the intrinsic or mitochondrial pathway where it is related to oxidative stress (**Kroemer *et al.*, 2009**). To make it clear, according to the GI₅₀ obtained for the rest of the fractions by the Probit test, they are not worthy to be further investigated for bioactivity since their GI₅₀ do not meet the NCI criteria for the development of drugs (**Boyd & Paull, 1995; Chakravarti & Klopman, 2008**).

Cell morphology changes induced by sub-fraction M.11.B.1

The purpose of this part of the present study was to observe the effects that M.11.B.1 has on cell structure and how these possibly might be related to cell death. Cell morphology changes induced by M.11.B.1 were discussed based on observations made after staining cells F-actin and nuclear material, using fluorescence microscopy; results are shown the in **Fig. 2**. Cells treated with 26.6 ± 8 µg/mL M.11.B.1 showed, after 4 h of exposure, cellular structures morphologically similar to those of control, which were cultured only in the presence of DMSO (<0.5 %). DNA staining with DAPI allowed the observation of cellular damages such as chromatin condensation and nuclear shrinkage (also called pyknosis); moreover, in most cells, DNA diffusion (karyolysis) was observed and, in others cells, karyorrhexis was observed as well, being both phenomena associated to DNA fragmentation. These morphological issues are characteristic of cells that undergoing dead pathways.

Different from control cells, in those treated with M.11.B.1 a decrease in the cell volume (shrinkage) was observed. Large plasma membrane protrusion (blebs) in 22Rv1 cells resulted from F-actin polymerization, which is associated to cell collapse (**Coleman *et al.*, 2001; Taylor, Cullen, & Martin, 2008; Wickman, Julian, & Olson, 2012**). Likewise, microtubule spike and beaded apoptopodia, and apoptotic bodies, which have been associated to cell fragmentation (**Poon *et al.*, 2014; Rubartelli, Poggi, & Zocchi, 1997; Witasz *et al.*, 2007**), were also observed. Results suggest that only a certain percentage of cells were in apoptotic processes, since plasma membrane rupture (which is associated to cellular and nuclear lysis as well as to necrosis pathways) could not be distinguished in cells. However, more studies are recommended to determine the proportions of cells that undergo either pathway.

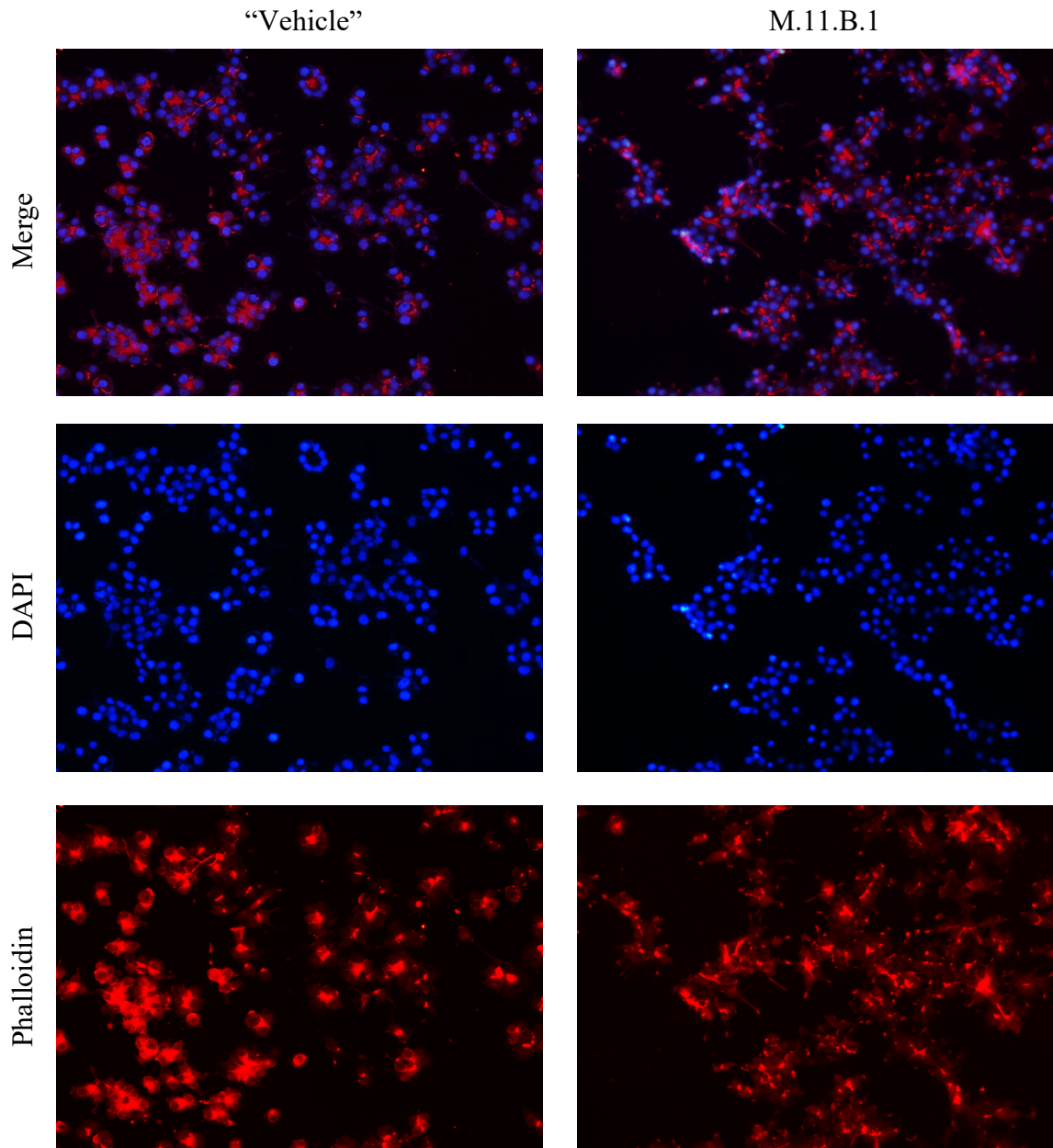


Figure 2. Effect of sub-fraction M.11.B.1 on 22Rv1 cell line (human prostate epithelial carcinoma) morphology changes after 4 h of incubation. Cell line 22Rv1 treated with solvent (DMSO to 0.5 %) only was considered the negative control (“Vehicle”). Fraction M.11.B.1 at GI_{50} ($26.6 \pm 8 \mu\text{g/mL}$) was used as the treatment. Actin cytoskeleton (red) and DNA (blue) were visualized by phalloidin–tetramethylrhodamine B isothiocyanate and DAPI staining, respectively. The cells were observed at 20x.

These results are evidences that the compound present in M.11.B.1 responsible for decreasing cancerous cell population and possibly of inducing apoptosis on prostate carcinoma *in vitro*, is

another one in addition to carotenoids, a triglyceride esterified containing PUFAs or even free PUFAs (as already reported). A general diagram of the bioassay guided isolation and the identification of the IAD extracted from *L. vannamei* with *in vitro* anticancer potential is shown in **Fig. 6**.

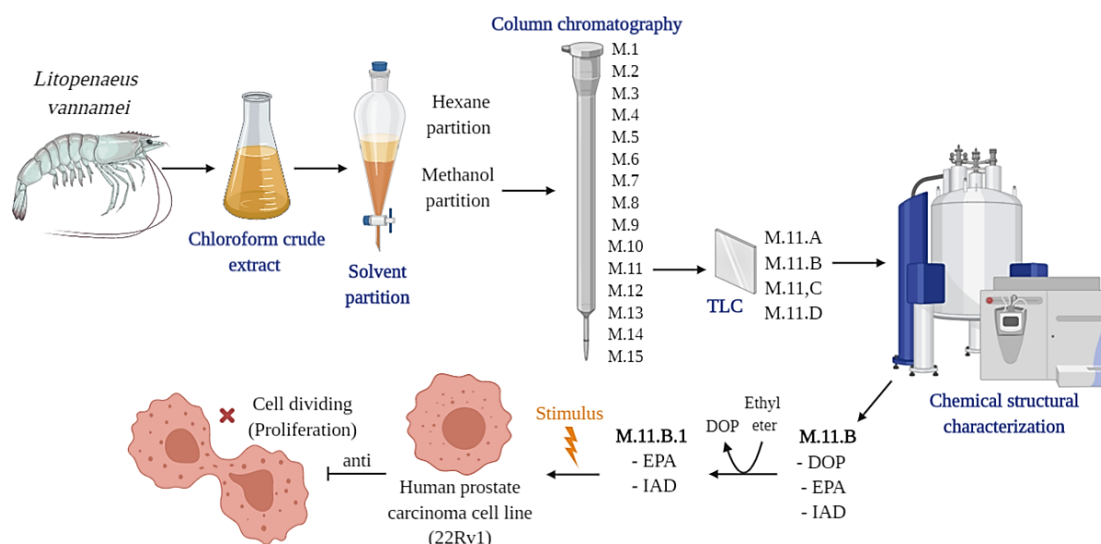


Figure 6. General diagram of the bio-assay guided isolation from farmed shrimp (*Litopenaeus vannamei*) muscle.

CONCLUSIONS

The present study demonstrated that the antiproliferative effect of M.11.B.1 on a prostate cancerous cell line is, in addition to EPA, majorly caused by another compound yet to be fully characterized (IAD). Also, this compound possibly has the capability of inducing cellular collapse associated to apoptosis. However, further investigation is needed to confirm the apoptotic activity of components of M.11.B.1.

Acknowledgments

Authors wish to thank *Consejo Nacional de Ciencia y Tecnología* (CONACYT) Mexico for financing the project No. 241133 and for granting research scholarships and for funding this project.

REFERENCE

- Abdel-Hameed, E. S. S., Bazaid, S. A., Shohayeb, M. M., El-Sayed, M. M., & El-Wakil, E. A. (2012). Phytochemical studies and evaluation of antioxidant, anticancer and antimicrobial properties of *Conocarpus erectus* L. growing in Taif, Saudi Arabia. *European Journal of Medicinal Plants*, 2(2), 93.

- Austreid, E., Lonning, P. E., & Eikesdal, H. P. (2014). The emergence of targeted drugs in breast cancer to prevent resistance to endocrine treatment and chemotherapy. *Expert Opinion on Pharmacotherapy*. <https://doi.org/10.1517/14656566.2014.885952>
- Boyd, M. R., & Paull, K. D. (1995). Some practical considerations and applications of the national cancer institute *in vitro* anticancer drug discovery screen. *Drug Development Research*, 34(2), 91–109. <https://doi.org/10.1002/ddr.430340203>
- Buzdar, A. U., Ibrahim, N. K., Francis, D., Booser, D. J., Thomas, E. S., Theriault, R. L., ... Hortobagyi, G. N. (2005). Significantly higher pathologic complete remission rate after neoadjuvant therapy with trastuzumab, paclitaxel, and epirubicin chemotherapy: results of a randomized trial in human epidermal growth factor receptor 2-positive operable breast cancer. *Journal of Clinical Oncology*, 23(16), 3676–3685. <https://doi.org/10.1200/JCO.2005.07.032>
- Chakravarti, S. K., & Klopman, G. (2008). A structural analysis of the differential cytotoxicity of chemicals in the NCI-60 cancer cell lines. *Bioorganic and Medicinal Chemistry*, 16(7), 4052–4063. <https://doi.org/10.1016/j.bmc.2008.01.024>
- Chiu, L. C. M., & Wan, J. M. F. (1999). Induction of apoptosis in HL-60 cells by eicosapentaenoic acid (EPA) is associated with downregulation of bcl-2 expression. *Cancer Letters*, 145(1–2), 17–27. [https://doi.org/10.1016/S0304-3835\(99\)00224-4](https://doi.org/10.1016/S0304-3835(99)00224-4)
- Ciavatta, M. L., Lefranc, F., Carbone, M., Mollo, E., Gavagnin, M., Betancourt, T., ... Kiss, R. (2017, July 1). Marine mollusk-derived agents with antiproliferative activity as promising anticancer agents to overcome chemotherapy resistance. *Medicinal Research Reviews*. John Wiley & Sons, Ltd. <https://doi.org/10.1002/med.21423>
- Coleman, M. L., Sahai, E. A., Yeo, M., Bosch, M., Dewar, A., & Olson, M. F. (2001). Membrane blebbing during apoptosis results from caspase-mediated activation of ROCK I. *Nature Cell Biology*, 3(4), 339–345. <https://doi.org/10.1038/35070009>
- Cruz-Ramírez, S. G., López-Saiz, C. M., Plascencia-Jatomea, M., Machi-Lara, L., Rocha-Alonzo, F., Márquez-Ríos, E., & Burgos-Hernández, A. (2015). Isolation and identification of an antimutagenic phthalate derivative compound from octopus (*Paraoctopus limaculatus*). *Tropical Journal of Pharmaceutical Research*, 14(7), 1257–1264. <https://doi.org/10.4314/tjpr.v14i7.19>
- De Kok, T. M., Van Breda, S. G., & Manson, M. M. (2008). Mechanisms of combined action of different chemopreventive dietary compounds: A review. *European Journal of Nutrition*. D. Steinkopff-Verlag. <https://doi.org/10.1007/s00394-008-2006-y>
- DeVita, V. T., & Chu, E. (2008). A history of cancer chemotherapy. *Cancer Research*. American Association for Cancer Research. <https://doi.org/10.1158/0008-5472.CAN-07-6611>
- García-Romo, J. S., Susana Yepiz-Gomez, M., Plascencia-Jatomea, M., del Carmen Santacruz-

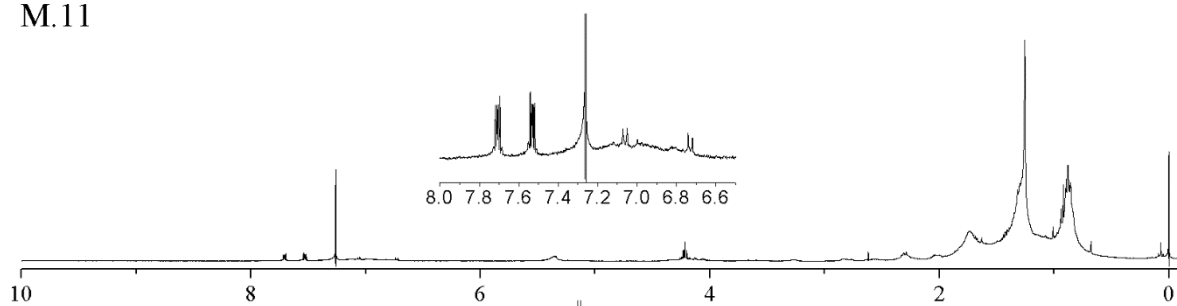
- Ortega, H., Burgos-Hernandez, A., de Leon, J. R., ... Borboa-Flores, J. (2018). Compounds with *in vitro* antibacterial activity from hydrosol of *lippia palmeri* and morphometric changes on *Listeria monocytogenes*. *biotecnia*, 20(3), 35–42. <https://doi.org/10.18633/biotecnia.v20i3.713>
- Jimenez, P. C., Wilke, D. V., Ferreira, E. G., Takeara, R., De Moraes, M. O., Silveira, E. R., ... Costa-Lotufo, L. V. (2012). Structure elucidation and anticancer activity of 7-oxostaurosporine derivatives from the Brazilian endemic tunicate *Eudistoma vannamei*. *Marine Drugs*, 10(5), 1092–1102. <https://doi.org/10.3390/md10051092>
- Kotha, S., Saifuddin, M., & Aswar, V. R. (2016). A diversity-oriented approach to indolocarbazoles: via Fischer indolization and olefin metathesis: Total synthesis of tjipanazole D and i. *Organic and Biomolecular Chemistry*, 14(41), 9868–9873. <https://doi.org/10.1039/c6ob01679k>
- Kroemer, G., Galluzzi, L., Vandenabeele, P., Abrams, J., Alnemri, E. S., Baehrecke, E. H., ... Melino, G. (2009). Classification of cell death: Recommendations of the nomenclature committee on cell death 2009. *Cell Death and Differentiation*. Nature Publishing Group. <https://doi.org/10.1038/cdd.2008.150>
- Lai, P. B. S., Ross, J. A., Fearon, K. C. H., Anderson, J. D., & Carter, D. C. (1996). Cell cycle arrest and induction of apoptosis in pancreatic cancer cells exposed to eicosapentaenoic acid *in vivo*. *British Journal of Cancer*, 74(9), 1375–1383. <https://doi.org/10.1038/bjc.1996.552>
- Li, C. C., Hou, Y. C., Yeh, C. L., & Yeh, S. L. (2017). Retraction: Effects of eicosapentaenoic acid and docosahexaenoic acid on prostate cancer cell migration and invasion induced by tumor-associated macrophages. *PloS One*. <https://doi.org/10.1371/journal.pone.0173325>
- Liu, K., Xiao, X., Wang, J., Chen, C.-Y. Y. O., & Hu, H. (2017). Polyphenolic composition and antioxidant, antiproliferative, and antimicrobial activities of mushroom *Inonotus sanghuang*. *LWT - Food Science and Technology*, 82, 154–161. <https://doi.org/10.1016/j.lwt.2017.04.041>
- Liu, S., Zheng, L., Aweya, J. J., Zheng, Z., Zhong, M., Chen, J., ... Zhang, Y. (2017). *Litopenaeus vannamei* hemocyanin exhibits antitumor activity in S180 mouse model *in vivo*. *PLoS ONE*, 12(8), e0183783. <https://doi.org/10.1371/journal.pone.0183783>
- Liu, W., Wang, L., Wang, B., Xu, Y., Zhu, G., Lan, M., ... Sun, K. (2019). Diketopiperazine and diphenylether derivatives from marine algae-derived *Aspergillus versicolor* OUCMDZ-2738 by epigenetic activation. *Marine Drugs*, 17(1), 6. <https://doi.org/10.3390/md17010006>
- Livstone, E. M. (2019). Colorectal cancer (colon cancer) - Merck Manual, Professional Version. <https://doi.org/10.3322/caac.21387>
- López-Saiz, C. M., Hernández, J., Cinco-Moroyoqui, F. J., Velázquez, C., Ocaño-Higuera, V.

- M., Plascencia-Jatomea, M., ... Burgos-Hernández, A. (2016). Antimutagenic compounds of white shrimp (*Litopenaeus vannamei*): Isolation and structural elucidation. *Evidence-Based Complementary and Alternative Medicine*, 2016, 1–7. <https://doi.org/10.1155/2016/8148215>
- López-Saiz, C. M., Suárez-Jiménez, G. M., Plascencia-Jatomea, M., & Burgos-Hernández, A. (2013). Shrimp lipids: A source of cancer chemopreventive compounds. *Marine Drugs*. Multidisciplinary Digital Publishing Institute. <https://doi.org/10.3390/md11103926>
- López-Saiz, C. M., Velázquez, C., Hernández, J., Cinco-Moroyoqui, F. J., Plascencia-Jatomea, M., Robles-Sánchez, M., ... Burgos-Hernández, A. (2014). Isolation and structural elucidation of antiproliferative compounds of lipidic fractions from white shrimp muscle (*Litopenaeus vannamei*). *International Journal of Molecular Sciences*, 15(12), 23555–23570. <https://doi.org/10.3390/ijms151223555>
- Lordan, S., Ross, R. P., & Stanton, C. (2011). Marine bioactives as functional food ingredients: Potential to reduce the incidence of chronic diseases. *Marine Drugs*. Molecular Diversity Preservation International. <https://doi.org/10.3390/md9061056>
- Martin, M., Brase, J. C., Calvo, L., Krappmann, K., Ruiz-Borrego, M., Fisch, K., ... Rodriguez-Lescure, A. (2014). Clinical validation of the EndoPredict test in node-positive, chemotherapy-treated ER+/HER2- breast cancer patients: Results from the GEICAM 9906 trial. *Breast Cancer Research*, 16(2), R38. <https://doi.org/10.1186/bcr3642>
- Monks, A., Scudiero, D., Skehan, P., Shoemaker, R., Paull, K., Vistica, D., ... Boyd, M. (1991). Feasibility of a high-flux anticancer drug screen using a diverse panel of cultured human tumor cell lines. *Journal of the National Cancer Institute*, 83(11), 757–766. <https://doi.org/10.1093/jnci/83.11.757>
- Nakatani, S., Naoe, A., Yamamoto, Y., Yamauchi, T., Yamaguchi, N., & Ishibashi, M. (2003). Isolation of bisindole alkaloids that inhibit the cell cycle from Myxomycetes *Arcyria ferruginea* and *Tubifera casparyi*. *Bioorganic and Medicinal Chemistry Letters*, 13(17), 2879–2881. [https://doi.org/10.1016/S0960-894X\(03\)00592-4](https://doi.org/10.1016/S0960-894X(03)00592-4)
- Netz, N., & Opatz, T. (2015). Marine indole alkaloids. *Marine Drugs*, 13(8), 4814–4914. <https://doi.org/10.3390/md13084814>
- Poon, I. K. H., Chiu, Y. H., Armstrong, A. J., Kinchen, J. M., Juncadella, I. J., Bayliss, D. A., & Ravichandran, K. S. (2014). Unexpected link between an antibiotic, pannexin channels and apoptosis. *Nature*, 507(7492), 329–334. <https://doi.org/10.1038/nature13147>
- Reyes, F., Fernández, R., Rodríguez, A., Bueno, S., De Eguilior, C., Francesch, A., & Cuevas, C. (2008). Cytotoxic staurosporines from the marine ascidian *Cystodytes solitus*. *Journal of Natural Products*, 71(6), 1046–1048. <https://doi.org/10.1021/np700748h>
- Rubartelli, A., Poggi, A., & Zocchi, M. R. (1997). The selective engulfment of apoptotic bodies by dendritic cells is mediated by the $\alpha\beta3$ integrin and requires intracellular and

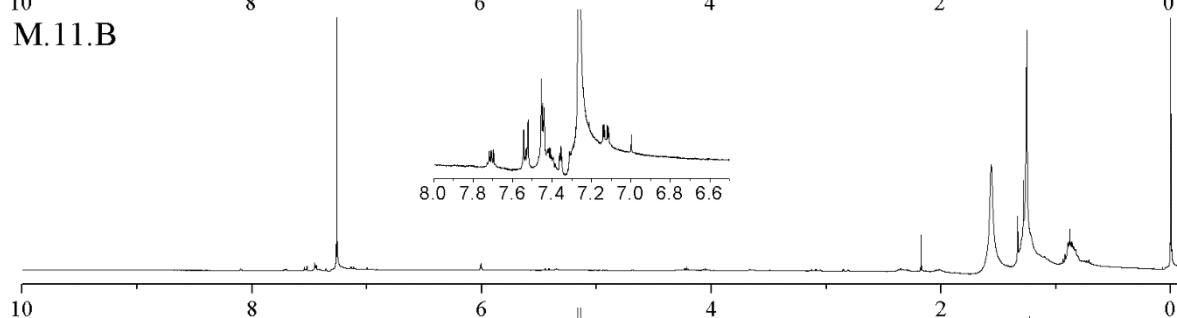
- extracellular calcium. *European Journal of Immunology*, 27(8), 1893–1900. <https://doi.org/10.1002/eji.1830270812>
- Sánchez, C., Méndez, C., & Salas, J. A. (2006). Indolocarbazole natural products: Occurrence, biosynthesis, and biological activity. *Natural Product Reports*. <https://doi.org/10.1039/b601930g>
- Sila, A., Ayed-Ajmi, Y., Sayari, N., Nasri, M., Martinez-Alvarez, O., & Bougatef, A. (2013). Antioxidant and Anti-proliferative activities of astaxanthin extracted from the shell waste of deep-water pink shrimp (*Parapenaeus longirostris*). *The Natural Products Journal*, 3(2), 82–89. <https://doi.org/10.2174/2210315511303020002>
- Sowmya, P. R. R., Arathi, B. P., Vijay, K., Baskaran, V., & Lakshminarayana, R. (2017). Astaxanthin from shrimp efficiently modulates oxidative stress and allied cell death progression in MCF-7 cells treated synergistically with β -carotene and lutein from greens. *Food and Chemical Toxicology*, 106, 58–69. <https://doi.org/10.1016/j.fct.2017.05.024>
- Stankevicius, L., Aiub, C., Maria, L. C. C. d. S., Lobo-Hajdu, G., & Felzenszwalb, I. (2008). Genotoxic and antigenotoxic evaluation of extracts from *Arenosciera brasiliensis*, a Brazilian marine sponge. *Toxicology in Vitro*, 22(8), 1869–1877. <https://doi.org/10.1016/j.tiv.2008.09.003>
- Steglich, W., Steffan, B., Kopanski, L., & Eckhardt, G. (1980). Indole Pigments from the Fruiting Bodies of the Slime Mold *Arcyria denudata*. *Angewandte Chemie International Edition in English*, 19(6), 459–460. <https://doi.org/10.1002/anie.198004591>
- Suffness, M., & Pezzuto, J. M. (1990). Assays related to cancer drug discovery. *Methods in Plant Biochemistry: Assays for Bioactivity*. Academic Press. Retrieved from <https://ci.nii.ac.jp/naid/10027518623/>
- Taylor, R. C., Cullen, S. P., & Martin, S. J. (2008). Apoptosis: Controlled demolition at the cellular level. *Nature Reviews Molecular Cell Biology*. Nature Publishing Group. <https://doi.org/10.1038/nrm2312>
- Thomson, C. A., LeWinn, K., Newton, T. R., Alberts, D. S., & Martinez, M. E. (2003). Nutrition and diet in the development of gastrointestinal cancer. *Current Oncology Reports*. Current Medicine Group. <https://doi.org/10.1007/s11912-003-0110-y>
- Turan, H., Kaya, Y., & Erdem, M. E. (2011). Proximate composition, cholesterol, and fatty acid content of brown shrimp (*Crangon crangon* L. 1758) from Sinop region, Black Sea. *Journal of Aquatic Food Product Technology*, 20(1), 100–107. <https://doi.org/10.1080/10498850.2010.526753>
- Tyl, C. E., Brecker, L., & Wagner, K. H. (2008). ¹H NMR spectroscopy as tool to follow changes in the fatty acids of fish oils. *European Journal of Lipid Science and Technology*, 110(2), 141–148. <https://doi.org/10.1002/ejlt.200700150>

- Van Vuuren, R. J., Botes, M., Jurgens, T., Joubert, A. M., & Van Den Bout, I. (2019). Novel sulphamoylated 2-methoxy estradiol derivatives inhibit breast cancer migration by disrupting microtubule turnover and organization 06 Biological Sciences 0601 Biochemistry and Cell Biology. *Cancer Cell International*, 19(1), 1. <https://doi.org/10.1186/s12935-018-0719-4>
- Wang, J. N., Zhang, H. J., Li, J. Q., Ding, W. J., & Ma, Z. J. (2018). Bioactive Indolocarbazoles from the Marine-Derived *Streptomyces* sp. DT-A61. *Journal of Natural Products*, 81(4), 949–956. <https://doi.org/10.1021/acs.jnatprod.7b01058>
- Wickman, G., Julian, L., & Olson, M. F. (2012). How apoptotic cells aid in the removal of their own cold dead bodies. *Cell Death and Differentiation*. Nature Publishing Group. <https://doi.org/10.1038/cdd.2012.25>
- Wilson-Sanchez, G., Moreno-Félix, C., Velazquez, C., Plascencia-Jatomea, M., Acosta, A., Machi-Lara, L., ... Burgos-Hernandez, A. (2010). Antimutagenicity and antiproliferative studies of lipidic extracts from white shrimp (*Litopenaeus vannamei*). *Marine Drugs*, 8(11), 2795–2809. <https://doi.org/10.3390/md8112795>
- Witas, E., Uthaisang, W., Elenström-Magnusson, C., Hanayama, R., Tanaka, M., Nagata, S., ... Fadeel, B. (2007). Bridge over troubled water: Milk fat globule epidermal growth factor 8 promotes human monocyte-derived macrophage clearance of non-blebbing phosphatidylserine-positive target cells [2]. *Cell Death and Differentiation*. Nature Publishing Group. <https://doi.org/10.1038/sj.cdd.4402096>
- Zheng, L., Zhao, X., Zhang, P., Chen, C., Liu, S., Huang, R., ... Zhang, Y. (2016). Hemocyanin from shrimp *litopenaeus vannamei* has antiproliferative effect against hela cell *in vitro*. *PloS One*, 11(3), e0151801. <https://doi.org/10.1371/journal.pone.0151801>

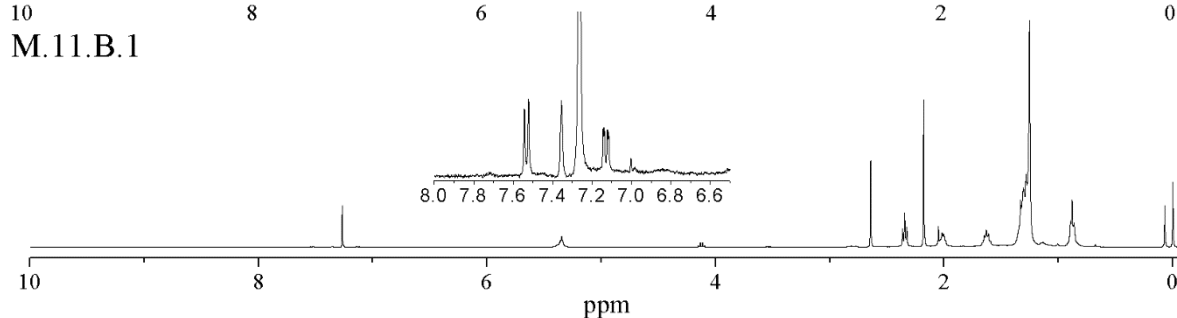
M.11



M.11.B



M.11.B.1



Supplemental figure. ¹H-NMR spectra of the bioactive fractions of farmed shrimp (*L. vannamei*) muscle in CDCl₃ at 400 Hz. * It can be observed how the concentration of DOP decreases (representative signal $\delta = 7.71 - 7.53$ ppm), showed greater DOP contraction in M.11 > M.11.B; also, the DOP signals in M.11.B.1 they are not visible, being that this sub-fraction could be found mainly complete free of DOP (higher level of purity = higher antiproliferative activity).

CAPÍTULO III

An Indolocarbazole Alkaloid Derivative Isolated from *Litopenaeus Stylirostris* Mediates Anti-Proliferative / Pro-Apoptotic Responses and Induce ROS Production on Human Epithelial Prostate Carcinoma Cells

Artículo enviado a: Lebensmittel-Wissenschaft & Technologie (LWT) - Food Science and Technology

Año: 2020

An indolocarbazole alkaloid derivative isolated from *Litopenaeus stylirostris* mediates anti-proliferative / pro-apoptotic responses and induce ROS production on human epithelial prostate carcinoma cells

Joel Said García-Romo¹, Edgar Sandoval-Petris², Martín Samuel Hernández-Zazueta¹, Juan Manuel Martínez-Soto³, Maribel Plascencia-Jatomea¹, María Guadalupe Burboa-Zazueta², Rosario Maribel Robles-Sánchez¹, Josué Juárez⁴, Javier Hernández-Martínez⁵, Maria del Carmen Candia-Plata³, Hisila del Carmen Santacruz-Ortega⁶, Armando Burgos-Hernández^{1*}.

¹ Departamento de Investigación y Posgrado en Alimentos, Universidad de Sonora, 83000 Sonora, Mexico.

² Departamento de Investigaciones Científicas y Tecnológicas, Universidad de Sonora, 83000 Sonora, Mexico.

³ Departamento de Medicina y Ciencias de la Salud, Universidad de Sonora, 83000 Sonora, Mexico.

⁴ Departamento de Física, Universidad de Sonora, 83000 Sonora, Mexico.

⁵ Unidad de Servicios de Apoyo en Resolución Analítica, Universidad Veracruzana, 91190 Veracruz, Mexico

⁶ Departamento de Investigación en Polímeros y Materiales, Universidad de Sonora, 83000 Sonora, Mexico.

* Corresponding Author. Tel.: + 526-622-592-208; Fax: + 526-622-592-209.

E-Mail: armando.burgos@unison.mx

Abstract

The anti-oxidant activities of a lipid fraction, containing a novel indolocarbazole alkaloid derivative isolated from *Litopenaeus stylirostris*, was previously reported; however, the way by which this compound present in this fraction might act in a cancer cell, is still unknown. The aim of this study was to determine the pro-apoptotic activity of this compound. The anti-proliferative activity was assessed colorimetrically assayed; cell morphology observations were carried out using fluorescence cell dyes, as well as pro-apoptosis and intracellular oxidative stress induction. Results suggest that, the fraction obtained have anti-proliferative potential mainly responses against human prostate carcinoma cell line, and that is effectively the same fraction had previously reported as an anti-oxidant and above the presence of the new novel indolocarbazole alkaloid derivative is reported; even so, similar influence evidence (to previous reports) to damage of DNA and F-actin polymerization, signifying cellular death, pathway apoptosis from 4 h after treatment induced; this is confirmed by estimating early apoptosis, being at 12 h when the highest percentage of early apoptosis is present; likewise, results showing that the bioactive fraction could significantly increase the production of reactive oxygen species. This proves, that IAD can be proposed as an agent of chemoprotective interest.

Keywords: Anti-proliferative, pro-apoptosis, ROS, *Litopenaeus stylirostris*, marine source.

1. Introduction

Scientific efforts around the world have focused on the search of chemoprotective molecules that could be used to effectively reduce the incidence of cancer, as well as on the understanding of how these compounds might have the ability of attacking cancerous cells without representing a danger to adjacent still-healthy ones.

Recently, in our laboratory, the antioxidant capacity of several fractions chromatographically isolated from a lipid extract obtain from wild shrimp (*Litopenaeus stylirostris*) muscle was studied, reporting that one of these fractions, with a high cytoprotective potential on human erythrocytes and on a human cell line of retinal pigmented epithelium, contains a novel indolocarbazole alkaloid derivative (IAD) which presumably is one of the molecules responsible for this activity (Garcia-Romo et al., 2020).

Indocarbazoles are a group of widely distributed compounds in nature, displaying different types of bioactivities (Netz & Opatz, 2015), some of them having anti-cancer (Nakatani et al., 2003; Wang, Zhang, Li, Ding, & Ma, 2018). Arcyriaflavin, an indolocarbazole type of compounds previously reported as an biologically active, has a chemical structure closely related IAD (Hirakawa, Nasu, Aoyagi, Takebayashi, & Narahara, 2017; Horton, Longley, McConnell, & Ballas, 1994; Hoshino et al., 2015; Steglich, Steffan, Kopanski, & Eckhardt, 1980). Staurosporine, is another indolocarbazole type of biological interest due to its activity (Reyes et al., 2008; Zong et al., 1999) and found in higher organisms (such as the tunicate *Eudistoma vannamei*) (Jimenez et al., 2012), given its structure shows structural features intimately associated to some also observed in IAD.

Where in general, one of the main activities of staurosporine is the inhibition of protein kinases by the binding of ATP to the kinase (Karaman et al., 2008); in addition, research leads to the ability to induce apoptosis by activating caspase-3 (Chae et al., 2000), and also induces cell cycle arrest in G₁ or in G₂ phase (Darzynkiewicz, Ardelt, Skierski, Traganos, & Darzynkiewicz, 1992), and according to all this information, other structures similar to those already reported could also have a pro-apoptotic effect.

Oxidative stress is involved in a series of pathological processes including cancer (Kietzmann, 2010), and one of the factors that can increase oxidative stress are reactive oxygen species (ROS). ROS are products of normal metabolism, as well as caused by exposure to many kinds of xenobiotics; depending on their concentration, ROS can be harmful to cells (Circu & Aw, 2010). Interestingly, there is evidence supporting that cancerous cells have higher ROS levels than non-cancerous cells and they seem to be more sensitive to ROS stimuli by exogenous agents (Trachootham, Alexandre, & Huang, 2009). Therefore, the exposure of cancerous cells to a certain concentration of an oxidative stress-inducing xenobiotic, it would increase their ROS content causing cellular damage, while in the case of a non-cancerous cell, this would not result affected. In addition, excessive ROS may induce cell death, including apoptosis (A. D. Kim et al., 2013; Larocque et al., 2014); various studies have shown that ROS-induced apoptosis during cell death is mediated by the activation of different metabolic pathways (p38 MAPK and JNK) (Hsieh et al., 2014; J. Y. Kim et al., 2011; Ramiro-Cortés, Guemez-Gamboa, & Morán, 2011).

Based on the above, the aim of the present study was to determine the pro-apoptotic activities of the antioxidant IAD previously reported.

2. Materials and methods

2.1. Isolation of indolocarbazole alkaloid derivative present in the bioactive fraction

The isolation of 18 fractions (A-R) and the indolocarbazole alkaloid derivative was performed as previously described by Garcia-Romo et al., (2020).

2.2. Cell lines

Six human epithelial cell lines were used, ARPE-19 (retinal pigmented epithelium), A-549 (lung carcinoma), HCT116 (colon carcinoma), HeLa (epithelioid cervix adenocarcinoma), MDA-MB-231 (breast adenocarcinoma), and 22Rv1 (prostate carcinoma). Cells were cultured in Dulbecco's modified Eagle's medium (DMEM) and RPMI-1640 Medium (Both medium was Sigma Aldrich, St. Louis, MO, USA), supplemented with 10 and 15 % heat-inactivated fetal bovine serum (FBS) (Corning, NY, USA) and grown at 37 °C in an atmosphere of 5 % CO₂ (VWR 2325 Water-Jacketed CO₂ Incubator, Pa, USA).

2.3. *MTT assay*

Antiproliferative activity of isolated fractions was evaluated using the MTT assay (Roche, cell proliferation kit I, Roche, Cat. No. 11-465-007-001), according to manufacturer's instructions. Absorbance was recorded using an ELISA microtitration plate reader (Benchmark Microplate Reader; Bio-Rad, Hercules, CA, USA). Cisplatin (CIS) (15663-27-1, Sigma-Aldrich) and docetaxel (DOC) (01885, Sigma-Aldrich) were used as positive antiproliferation controls. Dioctyl phthalate (DOP) (D201154, Sigma-Aldrich) and eicosapentaenoic acid (EPA) (E-2011, Sigma-Aldrich) were used as confirmatory standards for selected bioactive fractions. In addition, concentrations of 200 µg/mL downwards were used to obtain their GI₅₀ (half-maximal growth inhibition).

2.4. *Phalloidin and DAPI staining*

In order to observe the effect on internal morphological/structural aspects of cell line, staining procedures were performed (Van Vuuren, Botes, Jurgens, Joubert, & Van Den Bout, 2019). Testing cells were seeded onto 96-well microtitration plates for 24 h and treated with

bioactive fraction at their GI_{50} . With the aim of seeking the incubation time (2, 4, 8, consecutively h) at which morphological changes cell can be observed, cells were stained with phalloidin–tetramethylrhodamine B isothiocyanate (phalloidin) (Sigma-Aldrich, MFCD00278840) and 4', 6-Diamidino-2-phenylindole, dilactate (DAPI) (Sigma-Aldrich, D9564) in order to observe F-actin and nuclear material through DNA, respectively. Microtitration plates were mounted on an inverted epifluorescence microscope (Leica DMi8, Leica Microsystems GmbH, Wetzlar, Germany) to performed observations (equipped with fluorescence filters [546/10 RHOD excitation filter and emission 585/40, 350/50 DAPI excitation filter and 460/40 emission, and 480/40 excitation FITC filter and 527/30 emission], a cooled monochromatic DFC 450C camera [Leica Microsystems, Wetzlar, Germany] and fluorescence overlay software [LAS AF version 3.1.0, Leica Microsystems CMS GmbH, Mannheim, Germany]).

2.5. Annexin V / propidium iodide staining

In order to evaluate the apoptotic activity of bioactive fraction that resulted anti-proliferative (at their GI_{50}) over the most sensitive cell line, annexin V and propidium iodide (PI) staining was carried out (eBioscience™ Annexin V Apoptosis Detection Kit FITC, Cat. No. 88-8005-74), according to manufacturer's instructions. Cells were analyzed by flow cytometry using a flow cytometer (BD FACSVerse™ Flow Cytometer - BD Biosciences NY, USA), counting 10,000 events per experiment. The percentage of induction of apoptosis at different induction time (0, 4, 12, 24 and 48) was analyzed and once the time in which the bioactive fraction induces the maximum percentage of early apoptosis was selected, it was compared against positive controls (cisplatin, Docetaxel and H_2O_2).

2.6. DCFH-DA assay

In order to determine the intracellular ROS generation levels, an oxidation-sensitive fluorescent probe of 2',7'-dichlorodihydrofluorescein diacetate (DCFH-DA) was used as described by (Halliwell & Whiteman, 2004). Testing cells were seeded onto 96-well microtitration plates for 24 h and treated with bioactive fraction at their GI_{50} per 4 h (because at that time morphological changes were observed alluding to apoptosis); later, cells were incubated in the presence of 10 μ M DCFH-DA at 37 °C for 30 min, then washed 2 times with PBS. The intracellular fluorescence was determined by excitation at 498 nm and emission 530 nm using a microtitration plate reader (FLUOstar Omega, BMG Labtech Inc., Ortenberg, Germany); also, for qualitatively measuring the effect of bioactive fraction an inverted fluorescence microscope (Leica DMI8, Leica Microsystems GmbH, Wetzlar, Germany) was used to performed observations of cellular structures (with same characteristics as those described above).

2.8. Statistical analysis

Data were analyzed using an analysis of variance (ANOVA) with Tukey multiple comparisons test (Tukey's post hoc test), at a 95 % confidence interval, and the level of significance of $P \leq 0.05$, (SPSS). In order to calculate GI_{50} values (Half-maximal growth inhibition) for biologically active fractions, a probit analysis was performed using the Number Cruncher Statistical Software (NCSS, LLC, Kaysville, Utah, USA) version 2001, NCSS Statistical Software, USA. All data were presented as the mean value with their indicated standard deviation (mean \pm S.D.) from three independent experiments. Data calculations were

made according to the method described by the National Cancer Institute (NCI) / National Institutes of Health (NIH); Developmental Therapeutics Program (DTP), Human Tumor Cell Line Screen Process (<http://dtp.nci.nih.gov/branches/btb/ivclsp.html>) and as described previously (Monks et al., 1991).

3. Results and discussion

3.2. *Anti-proliferative activity of fraction M*

The anti-proliferative activity of the fractions is associated to the ability they have to prevent the growth of cancerous cell lines; the resulting reduction of cell population is denominated anti-proliferation and was obtained based on the MTT assay. The assay is based on the amount of metabolically active cells that remains after a certain time of have received a stimulus and compared to cells which were not subjected (control) to such treatment. Results are shown in **Table 1**.

In the present study, the fraction M resulted bioactive on several human cancerous cell lines; this means that it was capable of inhibiting cellular proliferation in a more efficient way in some cells than in others. When tested on 22Rv1 cell line, fraction M, achieved a GI_{50} value of $44.7 \pm 3.6 \mu\text{g/mL}$, which is comparable to the GI_{50} values of 35.0 ± 6.6 and $28.1 \pm 6.5 \mu\text{g/mL}$, corresponding to positive controls CIS and DOC, respectively; CIS is based on platinum which reacts with cells binding DNA inducing apoptosis (programmed cell death); CIS is recognized as a cytotoxic agent. On the other hand, DOC stimulates the assembly of tubulin into stable microtubules inhibiting its polymerization, which leads to a marked decrease in free tubulin; *in vitro*, it alters the tubular network of cells that is essential for the vital functions of mitosis and

cellular interface; this provides of an idea of the effectiveness of the compounds present in this fraction.

One way to determine which of the constituents of the fraction is responsible for most of the activity, is the evaluation of the control standards. In this study, EPA and DOC, showed less activity (comparing GI_{50} values) than that of fraction M, therefore, the compound responsible for most of the bioactivity is the one that remains among those three compounds, that is, IAD (**Table 2**). Also in this study, in order to determine the selectivity of the antiproliferative action of fraction M, this was tested on the non-cancerous cell line ARPE-19. Results shown in **Table 2**, suggest that fraction M had a bioselective index of 4.22, less than positive controls (5.24 to CIS and 5.52 to DOC), but equally high.

3.4. Cell morphology changes induced by fraction M

The processes for cell death can be classified by reactions or biochemical pathways and by the morphological appearance of the cells and, to be able to observe the phenomena concerning the types of cell damage present after a treatment, cells are exposed to fixation and staining with cellular markers (Kroemer et al., 2009). In this study the phalloidin and DAPI cell staining were used to observe these phenomena and the result are shown in the **Figure 2**. Cells treated with fraction M showed morphological changes compared to control cells, which were cells from the same cell line cultured with DMSO (0.5 %) and they represent 100 % proliferation.

The cell morphology changes induced by fraction M, were observed, after staining F-actin and nuclear material, using fluorescence microscopy. Cells (22Rv1 cell line) treated with

fM at GI_{50} ($44.7 \pm 3.6 \mu\text{g/mL}$) showed morphological changes after being incubated for 4 h. A reduction of the cell volume (cell contraction), the F-actin polymerization in cells resulting in a large plasma membrane protrusion, called blebs, and migration activity, which is associated to cell collapse, was observed after staining with phalloidin. Microtubule spike and beaded apoptopodia (apoptotic bodies) which have been associated to cell fragmentation (Poon et al., 2014; Rubartelli, Poggi, & Zocchi, 1997; Witaspl et al., 2007), were also observed. Chromatin condensation and nuclear shrinkage were observed after DNA staining using DAPI dye; this kind of DNA structural change is characteristic of cells that undergoes apoptosis (Coleman et al., 2001; Taylor, Cullen, & Martin, 2008; Wickman, Julian, & Olson, 2012).

3.5. Fraction M induced apoptosis in human prostate cancer cells

Once the anti-proliferative activity of fraction M was determined, whether cell death is mediated by apoptosis was investigated. The externalization of phosphatidylserine to the outer leaflet of the plasma membrane is associated with apoptosis. Phosphatidylserine, which is usually located on the inner leaflet of cytoplasmic membrane, is translocated to the outer leaflet in the early phase of apoptosis (Huigslout, Tijdens, Mulder, & Van de Water, 2001). Thus, to evaluate the apoptosis induction on prostate cancer cell (22Rv1) due to treatment with fraction M, the externalization of phosphatidylserine was determined through staining cell with Annexin (V-FITC) and propidium iodide (PI), followed by flow cytometric analysis.

Results suggested that 22Rv1 cells treated with fraction M died undergoing apoptosis, since early events of this process were detected (**Table 3**). The ratio of early apoptosis cells was higher in treated cells compared to control untreated cells; this is evidenced by a shift of cell population toward quadrant Annexin V positive and PI negative (FITC-A⁺/PE-A⁻), especially

after 12 h. Positive controls (apoptosis inducers), produced a higher percentage of early apoptotic cells after 12 h and those values were not significantly ($P \leq 0.05$) different from those induced by fraction M (**Figure 3**).

3.5. Fraction M increases intracellular ROS levels in human prostate cancer cells.

In this study, trials were conducted to evaluate the levels of intracellular ROS generated in human prostate cancer cells (22Rv1) after treatment with fraction M (at their GI_{50}); this was measured using the fluorescent indicator DCFH-DA and recorded with a microtitration plate reader and a fluorescence microscope. Readings in cells were taken after 4 h of being stimulated with the fraction M.

ROS generation was significantly ($P \leq 0.05$) induced by treatment with fraction M as suggested by the increase in fluorescence intensity; compared to untreated cells, more than 50 % of ROS was generated in treated cells after 4 h of being stimulated (**Figure 4a**). In addition, in order to determine the participation of ROS in cell death induced by positive controls (cisplatin and docetaxel), the fluorescence intensity of the fraction M was compared to the controls, noting that there was no significant ($P \leq 0.05$) difference; however, the control hydrogen peroxide (500 μ M per 30 min) generated a response significantly ($P \leq 0.05$) different to that obtained for fraction M (a greater effect), this is because H_2O_2 leads to different oxidizing derivatives, such as hydroxyl radicals, the most harmful physiological radicals for the cell (Kwee, 2014). All of this might suggest that the production of intracellular ROS plays an important role in the signaling pathway that triggers apoptosis during cell death.

Likewise, a qualitative detection of ROS was examined by fluorescence microscope; whereas 22Rv1 cells were treated with fraction M, clearly it shows the intracellular fluorescence

compared with the untreated cell (negative control negative control doesn't show the same observable fluorescence intensity) (**Figure 4b**). The incubation time used for the treatment (stimulus) was 4 h, since is the time after which the first morphological changes in the cells could be observed, as well as for the induction of early apoptosis. In addition, in this way the no reduction in cell viability is ensured, as well as the fact that the measurement is given by the fluorescence intensity, which is associated to oxidative stress through the production of intracellular ROS. In addition, hydrogen peroxide (500 μ M per 30 min) was used as another positive control, since it is known as an oxidative stress initiator at low concentrations.

ROS are by-products of cellular metabolism and they might have a dual effect during cancer progression, since certain levels of ROS are essential for cell proliferation and DNA mutation, as well as the fact that excessive redox stress often leads to depletion of the intracellular antioxidant system which leads to cellular apoptosis (Okon & Zou, 2015). Therefore, when prostate cancer cells are stimulated with fraction M, the concentration of ROS increases, leading to cell death via apoptosis and, as fraction M acts as an anti-oxidant agent in non-cancerous cells (Garcia-Romo et al., 2020), it also may act as a pro-oxidant agent in cancerous cells.

Conclusion

The new indolocarbazole alkaloid derivative (IAD) isolated from wild shrimp (*Litopenaeus stylirostris*) muscle has anti-proliferative activity through the activation of pro-apoptosis mechanisms, specifically by activating a pathway of oxidative stress associated to intracellular ROS production. As far as we know, this is the first time that this molecule has

been reported as an apoptosis inducer, however, further investigation is necessary for a full characterization of IAD apoptotic mechanisms.

Acknowledgment

Authors wish to thank Consejo Nacional de Ciencia y Tecnología (CONACYT) Mexico for financing the project No. 241133, for granting research scholarships, and for funding this project.

Reference

- Chae, H. J., Kang, J. S., Byun, J. O., Han, K. S., Kim, D. U., Oh, S. M., ... Kim, H. R. (2000). Molecular mechanism of staurosporine-induced apoptosis in osteoblasts. *Pharmacological Research*, 42, 373–381. <https://doi.org/10.1006/phrs.2000.0700>
- Circu, M. L., & Aw, T. Y. (2010, March 15). Reactive oxygen species, cellular redox systems, and apoptosis. *Free Radical Biology and Medicine*. <https://doi.org/10.1016/j.freeradbiomed.2009.12.022>
- Coleman, M. L., Sahai, E. A., Yeo, M., Bosch, M., Dewar, A., & Olson, M. F. (2001). Membrane blebbing during apoptosis results from caspase-mediated activation of ROCK I. *Nature Cell Biology*, 3, 339–345. <https://doi.org/10.1038/35070009>
- Darzynkiewicz, Z., Ardelt, B., Skierski, J. S., Traganos, F., & Darzynkiewicz, Z. (1992). Different Effects of Staurosporine, an Inhibitor of Protein Kinases, on the Cell Cycle and Chromatin Structure of Normal and Leukemic Lymphocytes. *Cancer Research*, 52, 470–473.
- Garcia-Romo, J. S. (2020). Antioxidant, antihemolysis, and retinoprotective potentials of bioactive lipidic compounds from wild shrimp (*Litopenaeus stylirostris*) muscle. In Press. *CyTA - Journal of Food*. <https://doi.org/10.1080/19476337.2020.1719210>
- Halliwell, B., & Whiteman, M. (2004, May 1). Measuring reactive species and oxidative damage in vivo and in cell culture: How should you do it and what do the results mean? *British Journal of Pharmacology*. John Wiley & Sons, Ltd (10.1111). <https://doi.org/10.1038/sj.bjp.0705776>
- Hirakawa, T., Nasu, K., Aoyagi, Y., Takebayashi, K., & Narahara, H. (2017). Arcyriaflavin a, a cyclin D1-cyclin-dependent kinase4 inhibitor, induces apoptosis and inhibits

- proliferation of human endometriotic stromal cells: A potential therapeutic agent in endometriosis. *Reproductive Biology and Endocrinology*, 15(1). <https://doi.org/10.1186/s12958-017-0272-3>
- Horton, P. A., Longley, R. E., McConnell, O. J., & Ballas, L. M. (1994). Staurosporine aglycone (K252-c) and arcyriaflavin A from the marine ascidian, *Eudistoma* sp. *Experientia*, 50, 843–845. <https://doi.org/10.1007/BF01956468>
- Hoshino, S., Zhang, L., Awakawa, T., Wakimoto, T., Onaka, H., & Abe, I. (2015). Arcyriaflavin E, a new cytotoxic indolocarbazole alkaloid isolated by combined-culture of mycolic acid-containing bacteria and *Streptomyces cinnamoneus* NBRC 13823. *Journal of Antibiotics*, 68, 342–344. <https://doi.org/10.1038/ja.2014.147>
- Hsieh, C. J., Kuo, P. L., Hsu, Y. C., Huang, Y. F., Tsai, E. M., & Hsu, Y. L. (2014). Arctigenin, a dietary phytoestrogen, induces apoptosis of estrogen receptor-negative breast cancer cells through the ROS/p38 MAPK pathway and epigenetic regulation. *Free Radical Biology and Medicine*, 67, 159–170. <https://doi.org/10.1016/j.freeradbiomed.2013.10.004>
- Huigsloot, M., Tijdens, I. B., Mulder, G. J., & Van de Water, B. (2001). Differential regulation of phosphatidylserine externalization and DNA fragmentation by caspases in anticancer drug-induced apoptosis of rat mammary adenocarcinoma MTLn3 cells. *Biochemical Pharmacology*, 62, 1087–1097. [https://doi.org/10.1016/S0006-2952\(01\)00755-9](https://doi.org/10.1016/S0006-2952(01)00755-9)
- Jimenez, P. C., Wilke, D. V., Ferreira, E. G., Takeara, R., De Moraes, M. O., Silveira, E. R., ... Costa-Lotufo, L. V. (2012). Structure elucidation and anticancer activity of 7-oxostaurosporine derivatives from the Brazilian endemic tunicate *Eudistoma vancouveri*. *Marine Drugs*, 10, 1092–1102. <https://doi.org/10.3390/md10051092>
- Karaman, M. W., Herrgard, S., Treiber, D. K., Gallant, P., Atteridge, C. E., Campbell, B. T., ... Zarrinkar, P. P. (2008). A quantitative analysis of kinase inhibitor selectivity. *Nature Biotechnology*, 26, 127–132. <https://doi.org/10.1038/nbt1358>
- Kietzmann, T. (2010, August 15). Intracellular redox compartments: Mechanisms and significances. *Antioxidants and Redox Signaling*. Mary Ann Liebert, Inc. 140 Huguenot Street, 3rd Floor New Rochelle, NY 10801 USA. <https://doi.org/10.1089/ars.2009.3001>
- Kim, A. D., Kang, K. A., Kim, H. S., Kim, D. H., Choi, Y. H., Lee, S. J., ... Hyun, J. W. (2013). A ginseng metabolite, compound K, induces autophagy and apoptosis via generation of reactive oxygen species and activation of JNK in human colon cancer cells. *Cell Death and Disease*, 4. <https://doi.org/10.1038/cddis.2013.273>
- Kim, J. Y., Yu, S. J., Oh, H. J., Lee, J. Y., Kim, Y., & Sohn, J. (2011). Panaxydol induces apoptosis through an increased intracellular calcium level, activation of JNK and p38 MAPK and NADPH oxidase-dependent generation of reactive oxygen species. *Apoptosis*,

16, 347–358. <https://doi.org/10.1007/s10495-010-0567-8>

- Kroemer, G., Galluzzi, L., Vandenabeele, P., Abrams, J., Alnemri, E. S., Baehrecke, E. H., ... Melino, G. (2009, January 10). Classification of cell death: Recommendations of the Nomenclature Committee on Cell Death 2009. *Cell Death and Differentiation*. Nature Publishing Group. <https://doi.org/10.1038/cdd.2008.150>
- Kwee, J. K. (2014). A paradoxical chemoresistance and tumor suppressive role of antioxidant in solid cancer cells: A strange case of Dr. Jekyll and Mr. Hyde. *BioMed Research International*. Hindawi Publishing Corporation. <https://doi.org/10.1155/2014/209845>
- Larocque, K., Ovadje, P., Djurdjevic, S., Mehdi, M., Green, J., & Pandey, S. (2014). Novel analogue of colchicine induces selective pro-death autophagy and necrosis in human cancer cells. *PLoS ONE*, 9(1), 1–10. <https://doi.org/10.1371/journal.pone.0087064>
- Monks, A., Scudiero, D., Skehan, P., Shoemaker, R., Paull, K., Vistica, D., ... Boyd, M. (1991). Feasibility of a high-flux anticancer drug screen using a diverse panel of cultured human tumor cell lines. *Journal of the National Cancer Institute*, 83, 757–766. <https://doi.org/10.1093/jnci/83.11.757>
- Nakatani, S., Naoe, A., Yamamoto, Y., Yamauchi, T., Yamaguchi, N., & Ishibashi, M. (2003). Isolation of bisindole alkaloids that inhibit the cell cycle from *Myxomycetes Arcyria ferruginea* and *Tubifera casparyi*. *Bioorganic and Medicinal Chemistry Letters*, 13, 2879–2881. [https://doi.org/10.1016/S0960-894X\(03\)00592-4](https://doi.org/10.1016/S0960-894X(03)00592-4)
- Netz, N., & Opatz, T. (2015). Marine indole alkaloids. *Marine Drugs*, 13, 4814–4914. <https://doi.org/10.3390/md13084814>
- Okon, I. S., & Zou, M. H. (2015, October 27). Mitochondrial ROS and cancer drug resistance: Implications for therapy. *Pharmacological Research*. Academic Press. <https://doi.org/10.1016/j.phrs.2015.06.013>
- Poon, I. K. H., Chiu, Y. H., Armstrong, A. J., Kinchen, J. M., Juncadella, I. J., Bayliss, D. A., & Ravichandran, K. S. (2014). Unexpected link between an antibiotic, pannexin channels and apoptosis. *Nature*, 507, 329–334. <https://doi.org/10.1038/nature13147>
- Ramiro-Cortés, Y., Guemez-Gamboa, A., & Morán, J. (2011). Reactive oxygen species participate in the p38-mediated apoptosis induced by potassium deprivation and staurosporine in cerebellar granule neurons. *International Journal of Biochemistry and Cell Biology*, 43, 1373–1382. <https://doi.org/10.1016/j.biocel.2011.06.001>
- Reyes, F., Fernández, R., Rodríguez, A., Bueno, S., De Eguilior, C., Francesch, A., & Cuevas, C. (2008). Cytotoxic staurosporines from the marine ascidian *Cystodytes solitus*. *Journal of Natural Products*, 71(6), 1046–1048. <https://doi.org/10.1021/np700748h>

- Rubartelli, A., Poggi, A., & Zocchi, M. R. (1997). The selective engulfment of apoptotic bodies by dendritic cells is mediated by the $\alpha\text{v}\beta 3$ integrin and requires intracellular and extracellular calcium. *European Journal of Immunology*, 27, 1893–1900. <https://doi.org/10.1002/eji.1830270812>
- Steglich, W., Steffan, B., Kopanski, L., & Eckhardt, G. (1980). Indole Pigments from the Fruiting Bodies of the Slime Mold *Arcyria denudata*. *Angewandte Chemie International Edition in English*, 19, 459–460. <https://doi.org/10.1002/anie.198004591>
- Taylor, R. C., Cullen, S. P., & Martin, S. J. (2008, March 1). Apoptosis: Controlled demolition at the cellular level. *Nature Reviews Molecular Cell Biology*. Nature Publishing Group. <https://doi.org/10.1038/nrm2312>
- Trachootham, D., Alexandre, J., & Huang, P. (2009). Targeting cancer cells by ROS-mediated mechanisms: A radical therapeutic approach? *Nature Reviews Drug Discovery*. <https://doi.org/10.1038/nrd2803>
- Van Vuuren, R. J., Botes, M., Jurgens, T., Joubert, A. M., & Van Den Bout, I. (2019). Novel sulphamoylated 2-methoxy estradiol derivatives inhibit breast cancer migration by disrupting microtubule turnover and organization 06 Biological Sciences 0601 Biochemistry and Cell Biology. *Cancer Cell International*, 19(1), 1. <https://doi.org/10.1186/s12935-018-0719-4>
- Wang, J. N., Zhang, H. J., Li, J. Q., Ding, W. J., & Ma, Z. J. (2018). Bioactive Indolocarbazoles from the Marine-Derived *Streptomyces* sp. DT-A61. *Journal of Natural Products*, 81, 949–956. <https://doi.org/10.1021/acs.jnatprod.7b01058>
- Wickman, G., Julian, L., & Olson, M. F. (2012, May 16). How apoptotic cells aid in the removal of their own cold dead bodies. *Cell Death and Differentiation*. Nature Publishing Group. <https://doi.org/10.1038/cdd.2012.25>
- Witas, E., Uthaisang, W., Elenström-Magnusson, C., Hanayama, R., Tanaka, M., Nagata, S., ... Fadeel, B. (2007, January 26). Bridge over troubled water: Milk fat globule epidermal growth factor 8 promotes human monocyte-derived macrophage clearance of non-blebbing phosphatidylserine-positive target cells [2]. *Cell Death and Differentiation*. Nature Publishing Group. <https://doi.org/10.1038/sj.cdd.4402096>
- Zong, Z. P., Fujikawa-Yamamoto, K., Li, A. L., Yamaguchi, N., Chang, Y. G., Murakami, M., ... Ishikawa, Y. (1999). Both low and high concentrations of staurosporine induce G1 arrest through down-regulation of cyclin E and cdk2 expression. *Cell Structure and Function*, 24 457–463. <https://doi.org/10.1247/csf.24.457>

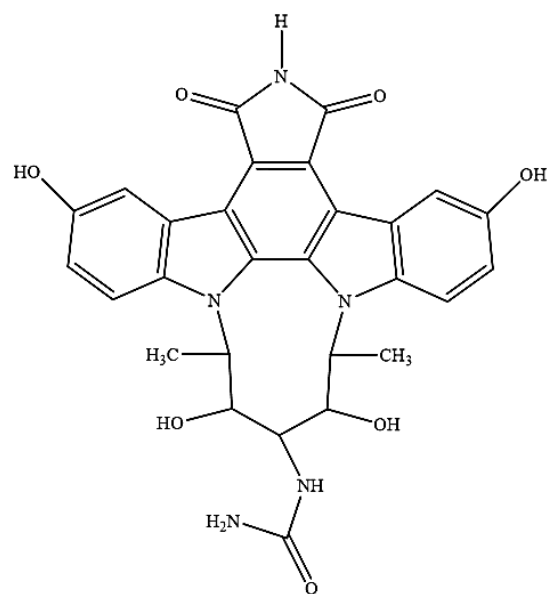


Figure 1. Novel antiproliferative indolocarbazole alkaloid derivative (García-Romo et al., 2020).

Table 1. Half-maximal growth inhibition (GI₅₀) of the anti-proliferative effect of all fractions obtained from wild shrimp (*Litopenaeus stylirostris*) muscle on human epithelial cell lines after 48 h of incubation.

	(µg/mL)				
	<i>Adenocarcinomas</i>		<i>Carcinomas</i>		
	HeLa	MDA-MB-231	A549	22Rv1	HCT116
A	> 200 ^a	> 200 ^a	> 200 ^a	> 200 ^a	> 200 ^a
B	> 200 ^a	> 200 ^a	> 200 ^a	> 200 ^a	> 200 ^a
C	> 200 ^a	> 200 ^a	> 200 ^a	> 200 ^a	> 200 ^a
D	> 200 ^a	> 200 ^a	> 200 ^a	> 200 ^a	> 200 ^a
E	> 200 ^a	> 200 ^a	> 200 ^a	> 200 ^a	> 200 ^a
F	> 200 ^a	89.8 ± 4.4 ^c	> 200 ^a	> 200 ^a	> 200 ^a
G	> 200 ^a	92.0 ± 4.3 ^c	> 200 ^a	> 200 ^a	> 200 ^a
H	> 200 ^a	> 200 ^a	> 200 ^a	118.8 ± 12.3 ^{bc}	112.1 ± 16.9 ^b
I	> 200 ^a	89.3 ± 7.1 ^c	> 200 ^a	> 200 ^a	117.0 ± 10.6 ^b
J	> 200 ^a	> 200 ^a	> 200 ^a	> 200 ^a	> 200 ^a
K	> 200 ^a	> 200 ^a	> 200 ^a	> 200 ^a	> 200 ^a
L	> 200 ^a	> 200 ^a	> 200 ^a	135.5 ± 6.6 ^b	> 200 ^a
M	112.6 ± 5.2 ^c	58.2 ± 2.6 ^d	69.7 ± 6.9 ^c	44.7 ± 3.6 ^d	117.1 ± 7.5 ^b
N	> 200 ^a	78.0 ± 7.7 ^c	> 200 ^a	> 200 ^a	> 200 ^a
O	> 200 ^a	> 200 ^a	> 200 ^a	> 200 ^a	> 200 ^a
P	> 200 ^a	143.5 ± 14.1 ^b	> 200 ^a	119.4 ± 12.3 ^b	105.2 ± 12.7 ^b
Q	133.3 ± 7.8 ^b	58.6 ± 2.1 ^d	91.7 ± 4.6 ^b	95.9 ± 9.3 ^c	> 200 ^a
R	> 200 ^a	> 200 ^a	> 200 ^a	> 200 ^a	> 200 ^a
CIS	53.2 ± 8.0 ^d	54.1 ± 6.5 ^d	38.8 ± 4.9 ^d	35.0 ± 6.6 ^{de}	74.0 ± 12.3 ^c
DOC	10.9 ± 3.6 ^c	21.0 ± 1.5 ^c	18.5 ± 2.6 ^c	28.1 ± 6.5 ^c	12.8 ± 2.5 ^d

Values represent means ± S.D. from three determinations. Values with different letters within the same column are significantly different ($P \leq 0.05$); Tukey's least significant difference test. Control cell cultures were incubated with DMSO (0.5 %) and represent 100 % proliferation. Cisplatin (CIS) and docetaxel (DOC) were used as a positive control.

Table 2. Half-maximal growth inhibition (GI₅₀) and bioselective index of the most bioactive fraction (fM) and its standards of composition on human epithelial cell lines at 48 h of incubation.

	(µg/mL)		<i>Bioselective index</i>
	<i>ARPE-19</i>	<i>22Rv1</i>	
Fraction	188.9 ± 3.6 ^a	44.7 ± 3.6 ^{bc}	4.22
M			
DOP	> 200 ^a	> 200 ^a	-
EPA	> 200 ^a	58.3 ± 10.0 ^b	3.42
CIS	183.3 ± 15.5 ^a	35.0 ± 6.6 ^c	5.24
DOC	155.3 ± 3.8 ^b	28.1 ± 6.6 ^c	5.52

Values represent means ± S.D. from three determinations. Values with different letters within the same column are significantly different ($P \leq 0.05$); Tukey's least significant difference test. Control cell cultures were incubated with DMSO (0.5 %) and represent 100 % proliferation. Dioctyl phthalate (DOP) and eicosapentaenoic acid (EPA) were used as standard controls. Cisplatin (CIS) and docetaxel (DOC) were used as a positive antiproliferative control.

DAPI

Phalloidin

“Merge”

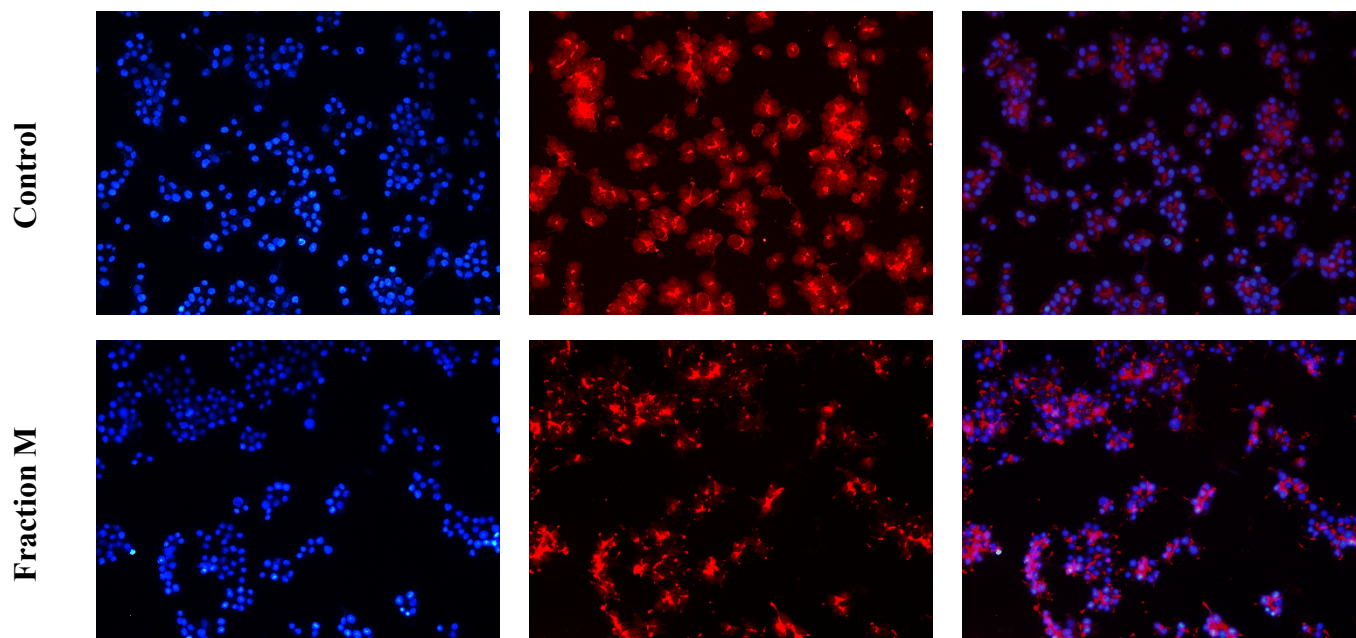


Figure 2. Effect of fraction M isolated from wild shrimp (*Litopenaeus. stylirostris*) muscle on the most sensitive cell line (22Rv1) and morphology changes after 4 h to incubation, time at which they began to show changes. Control means, 22Rv1 cell line treated only with vehicle (DMSO to 0.5 %). The GI_{50} ($44.7 \pm 3.6 \mu\text{g/mL}$) for fraction M was used. The actin cytoskeleton (red) and DNA (blue) were visualized by phalloidin–tetramethylrhodamine B isothiocyanate and DAPI staining, respectively. Cells were observed at 20x.

Table 3. Apoptosis induction capacity (%) of fraction M obtained from wild shrimp (*Litopenaeus stylirostris*) muscle against 22Rv1 cell line at different times of induction (h).

Time induction	(%)			
	Lives ^{Q4}	Early apoptosis ^{Q3}	Late apoptosis ^{Q2}	Dead's ^{Q1}
0	89.5 ± 0.6 a	2.8 ± 0.2 c	4.0 ± 0.5 d	4.1 ± 0.4 d
4	80.8 ± 0.9 b	9.4 ± 0.9 b	2.7 ± 0.3 d	7.1 ± 0.3 cd
12	40.9 ± 2.3 c	26.5 ± 1.7 a	21.8 ± 0.6 b	10.8 ± 0.4 c
24	30.8 ± 0.8 d	5.7 ± 2.5 bc	25.8 ± 1.0 a	37.7 ± 2.8 b
48	22.8 ± 0.5 e	2.6 ± 1.3 c	8.3 ± 1.8 c	66.3 ± 2.8 a

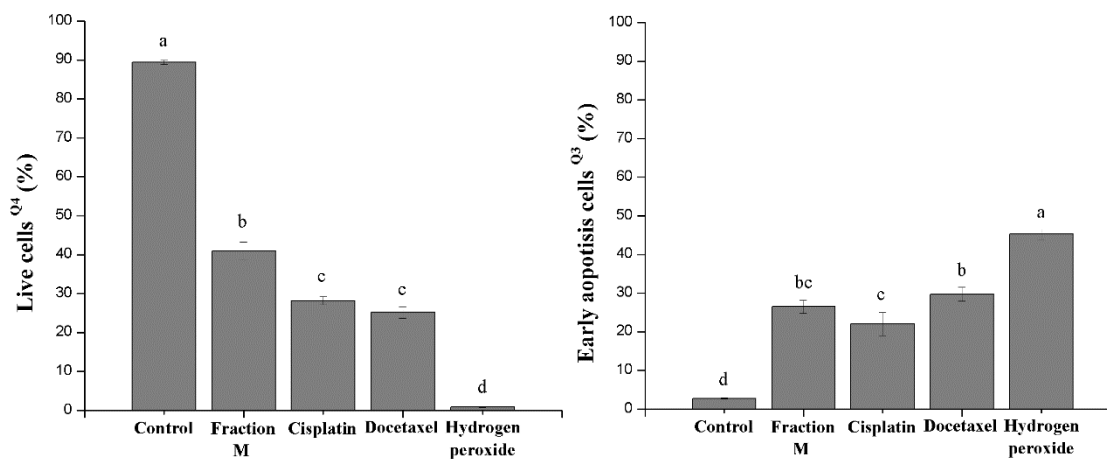
Fraction M was evaluated at GI₅₀ (44.7 ± 3.6 µg/mL). Values represent means ± S.D. from three determinations. Values with different letters within the same column are significantly different (P ≤ 0.05); Tukey's least significant difference test. Time 0 h represents DMSO at 0.5 % as control cells.

Q4 (Live cells): FITC–/PI–.

Q3 (Early apoptosis cells): FITC+/PI–.

Q2 (Late apoptosis cells): FITC+/PI+.

Q1 (Dead cells): FITC–/PI+.



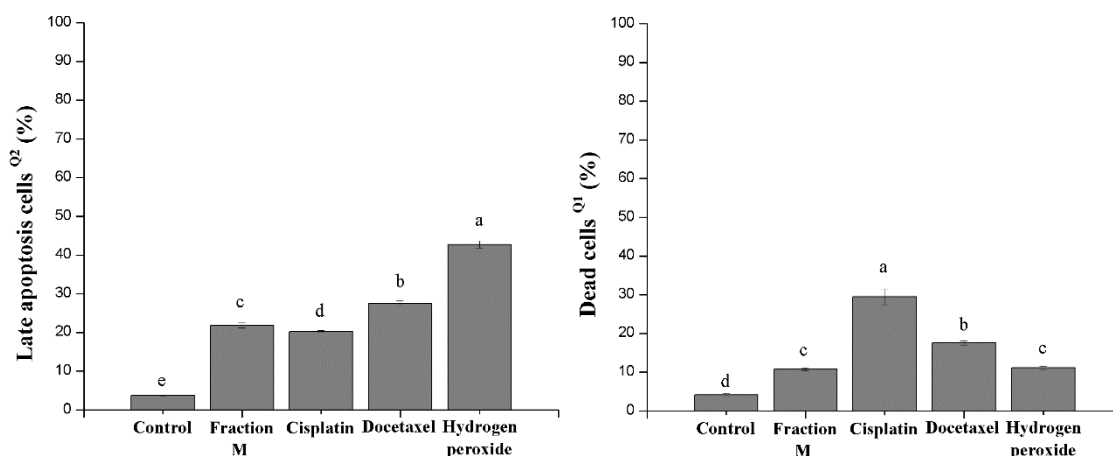


Figure 3. Apoptosis induction capacity of fraction M obtained from wild shrimp (*Litopenaeus stylirostris*) muscle against 22Rv1 cell line after 12 h compared whit controls. Compounds were evaluated at each GI₅₀ (μg/mL). In addition, hydrogen peroxide (500 μM per 30 min) was used as positive control. Values represent means ± S.D. from three determinations. Values with different letters within the same column are significantly different ($P \leq 0.05$); Tukey's least significant difference test. Control represent DMSO at 0.05 %.

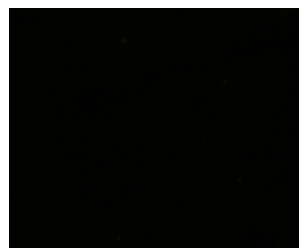
Q4 (Live cells): FITC–/PI–.

Q3 (Early apoptosis cells): FITC+/PI–.

Q2 (Late apoptosis cells): FITC+/PI+.

Q1 (Dead cells): FITC–/PI+.

Control



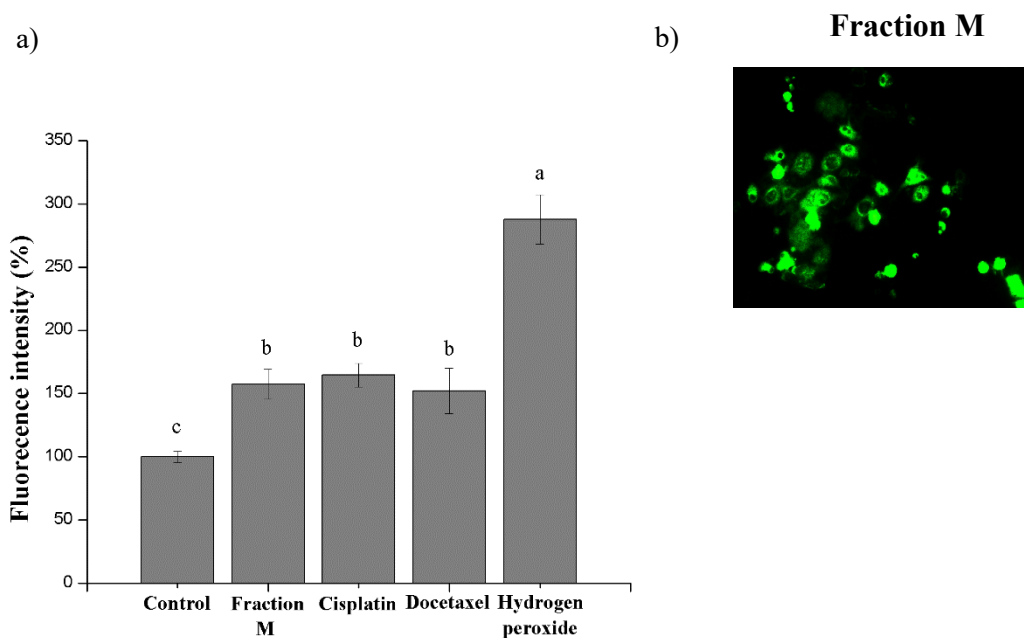
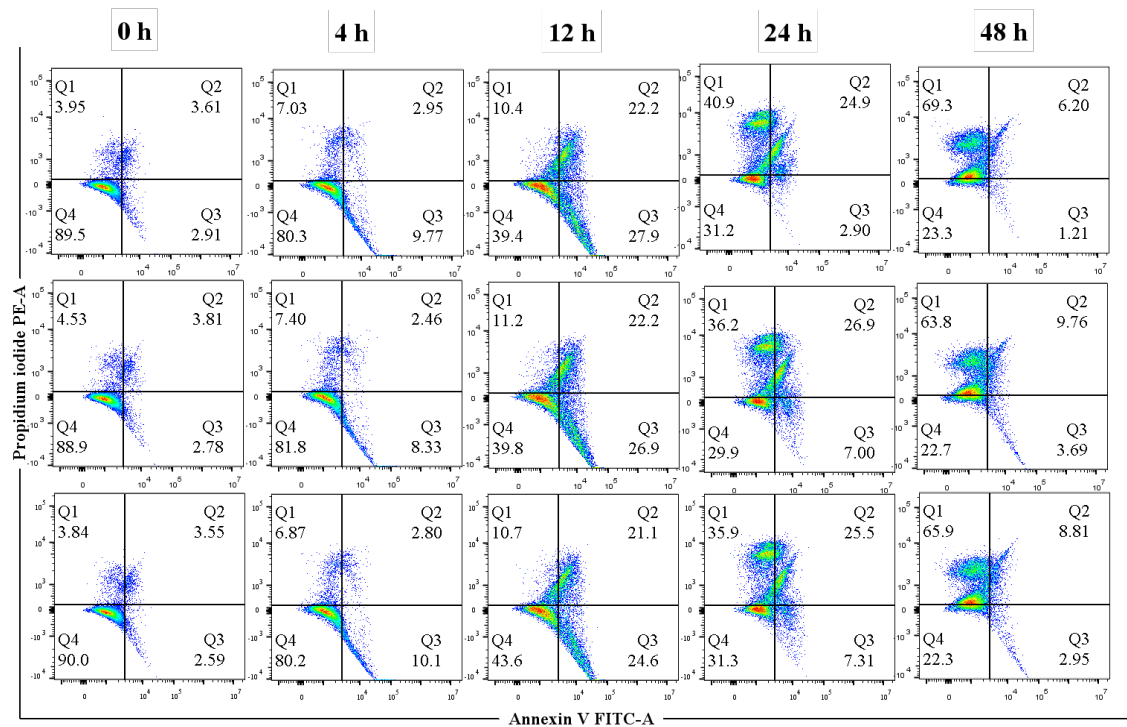
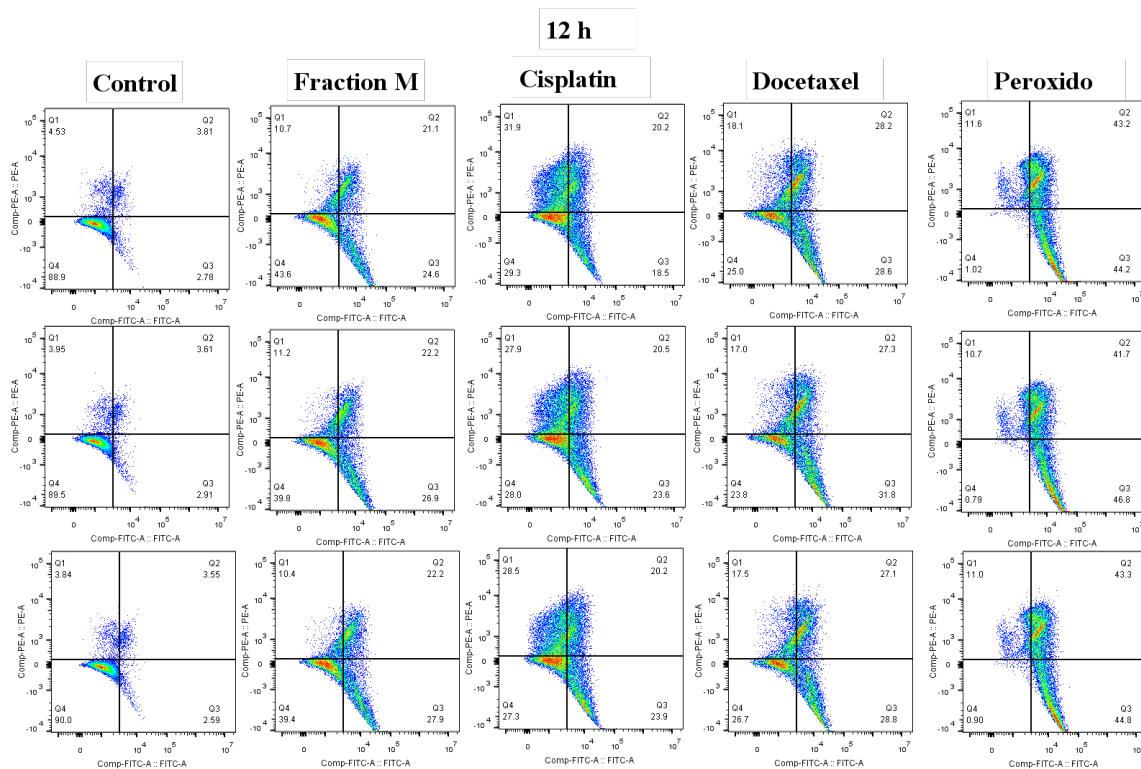


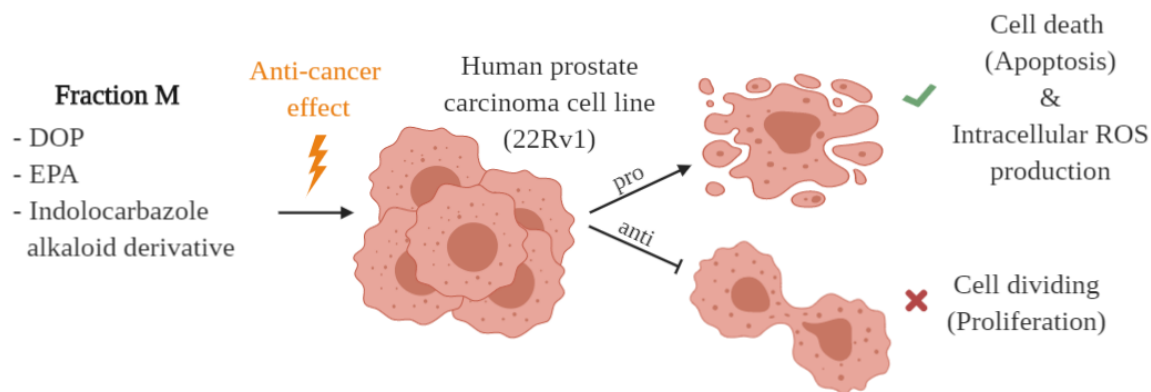
Figure 4. Intracellular ROS generation induction of fraction M (GI₅₀) obtained from wild shrimp (*Litopenaeus stylirostris*) muscle against 22Rv1 cell line at 4 h; a) Quantitative analysis was performed by measuring fluorescence intensity (%) by a fluorescence microtitration plate reader. Each value represents the mean \pm SD from three independent experiments ($P \leq 0.05$); b) Qualitative detection of ROS was examined by fluorescence microscope at 40x. For all assays, 22Rv1 cells were treated with GI₅₀ of fraction M; cisplatin and docetaxel were used as positive control after 4 h. In addition, hydrogen peroxide (500 μ M per 30 min) was used as another positive control; the cells were incubated with 10 μ M DCFH-DA later per 30 min.



Supplemental figure 1. Induction of apoptosis of fraction M (fM) at different incubation times.



Supplemental figure 2. Induction of apoptosis of fraction M (fM) after 12 h of incubation time compared to pro-apoptosis controls.



Graphical abstract

CAPÍTULO IV

Evaluation of Anti-Inflammatory-Related Activity of a Bioactive Fraction (Constituted By a Novel Indolocarbazole Alkaloid Derivative, a Polyunsaturated Fatty Acid and an Ester of Phthalic Acid Type) Isolated from *Litopenaeus Stylirostris*

Artículo por enviar

Evaluation of anti-inflammatory-related activity of a bioactive fraction (constituted by a novel indolocarbazole alkaloid derivative, a polyunsaturated fatty acid and an ester of phthalic acid type) isolated from *Litopenaeus stylirostris*

Joel Said García-Romo¹, Juan Manuel Martínez-Soto⁶, Martín Samuel Hernández-Zazueta¹, Edgar Sandoval-Petris², Maribel Plascencia-Jatomea¹, María Guadalupe Burboa-Zazueta², Rosario Maribel Robles-Sánchez¹, Josué Elías Juárez-Onofre³, Javier Hernández-Martínez⁴, Hisila del Carmen Santacruz-Ortega⁵, Armando Burgos-Hernández^{1*}.

¹ Departamento de Investigación y Posgrado en Alimentos, Universidad de Sonora, 83000 Sonora, México.

² Departamento de Investigaciones Científicas y Tecnológicas, Universidad de Sonora, 83000 Sonora, México.

³ Departamento de Física, Universidad de Sonora, 83000 Sonora, México.

⁴ Unidad de Servicios de Apoyo en Resolución Analítica, Universidad Veracruzana, 91190 Veracruz, México

⁵ Departamento de Investigación en Polímeros y Materiales, Universidad de Sonora, 83000 Sonora, México.

⁶ Departamento de Medicina y Ciencias de la Salud, Universidad de Sonora, 83000 Sonora, México.

* Corresponding Author. Tel.: + 526-622-592-208; Fax: + 526-622-592-209.

E-Mail: armando.burgos@unison.mx

Abstract

According to OMS, in 2018 (of the deaths caused by diseases), almost one out of six deaths is due to cancer and, many types of cancer might be prevented by avoiding exposure to risk factors; one of these factors is related to inflammatory processes. Currently, the search for new drugs that control the carcinogenic microenvironment is constant, and a source of new drugs resides in the marine ecosystem. Our research group previously evaluated cellular protective activity of a fraction isolated from *Litopenaeus stylirostris*, found to be composed of a novel indolocarbazole alkaloid derivative, a polyunsaturated fatty acid and an ester of phthalic acid type. However, complete biological characterization of this fraction and its components is not yet carried out. The aim of this work is to investigate if the fraction have a possible anti-inflammatory-related agent. RNS scavenging tests,

percentage of viability of a murine macrophage cell line, as well as the percentage of NO produced after LPS-stimulated cells, were performed with colorimetric techniques, while the percentage of ROS produced after LPS-stimulated cells (murine macrophages) was performed by fluorometric techniques; in addition, the determination of up- and down-regulation cytokine production was evaluated after LPS-stimulated cells (human peripheral blood mononuclear cells), using a fluorometric technique. Results suggests that: the compound that could be responsible for RNS and ROS scavenging is the indolocarbazole alkaloid derivative, while the compound most active in the inhibition of NO is polyunsaturated fatty acid; in addition, the fraction had the ability to up- and down-regulation cytokine production (increase in anti-inflammatory proteins and decrease in pro-inflammatory proteins). Based on the above, the isolated fraction of *L. stylirostris* contains components that could be anti-inflammatory agents.

Keywords: Anti-inflammatory activity, RNS, cytotoxicity, oxide nitric, ROS, interleukins.

1. Introduction

Cancer is the second cause of death in the world; in 2018, it caused 9.6 million deaths and almost one out of six deaths is due to this disease (“WHO | Cancer,” 2019) and an increase of 22.2 million of new cases per year is predicted to be achieved by year 2030 (Bray, Jemal, Grey, Ferlay, & Forman, 2012). Many types of cancer might be prevented by avoiding exposure to common risk factors such as microorganism infections, high fat consumption, smoking, hereditary factors, etc. (Alberts et al., 2010); however, inflammatory processes is another important factor to consider which provides conditions that may favor the development of several cancer related events such as cell transformation, promotion, survival, proliferation, invasion, angiogenesis, and metastasis. It is estimated that 25 % of all types of cancer and about 15 % of deaths due to this disease are related to inflammatory processes (Allavena, Garlanda, Borrello, Sica, & Mantovani, 2008; Coussens & Werb, 2002).

The marine ecosystem represent the majority of the planet's surface and comprise a continuous resource of compounds with many biological activities; due to different, and sometimes extreme conditions, the organisms within this environment may produce metabolites with structural characteristics that differentiate them from those of other natural sources, and showing great biotechnological potential (Braekman & Daloze, 1986; Stankevics, Aiub, Maria, Lobo-Hajdu, & Felzenszwalb, 2008). Because of the above, marine organisms have been considered as important sources of bioactive substances with great value for either prevention or treatment of several illnesses; these bioactivities may include anti-bacterial, anti-viral, anti-mutagenic, anti-proliferative, anti-inflammatory, anti-tumor, and anti-neoplastic, among others (Gerwick & Moore, 2012). Based on these arguments, several authors support the idea that secondary metabolites of marine organisms are much more likely

to produce cancer drugs than terrestrial sources (Fahmy, 2013).

Our research group, previously (Garcia-Romo et al., 2020) evaluated the cellular protective activity of a bioactive fraction (fM) obtained after a chromatographic separation of a chloroform-soluble extract from wild shrimp (*Litopenaeus stylirostris*) muscle. From this study, the fM was chemico-structurally characterized and it was found to be composed of a mixture of mostly 3 compounds, dioctyl phthalate (DOP), eicosapentaenoic acid (EPA), and a novel indolocarbazole alkaloid derivative (IAD). However, a complete biological characterization of this fraction is not yet carried out.

Based on the above, the objective of this work was to investigate the bioactive fraction previously reported by Garcia-Romo et al., 2020 as a possible source of anti-nitrosative and/or anti-inflammatory activity, and to determine which of its components is the responsible for such bioactivities.

2. Materials and methods

2.1. Isolation of the bioactive fraction (fM)

The isolation of fM and the lipids present in it (EPA, DOP, and IAD) was performed as previously described by Garcia-Romo et al., (2020).

2.2. Sodium nitroprusside (SNP) assay

In order to establish the capability of fM to capture nitric oxide (NO), which is associated to the inhibition of reactive nitrogen species (RNS) derived from nitric oxide, the sodium nitroprusside (SNP) assay was used according to (Awad, Abd-Alla, Mahmoud, & El-Toumy, 2014). At physiological pH, SNP spontaneously produces NO, which interacts with oxygen to generate nitrite (NO_2^-) (Schroeter et al., 2002). In a 96-well microplate, SNP (10 mM) and samples (including fM and controls) [100 – 800 $\mu\text{g/mL}$ in PBS (pH 7.4)] were combined and incubated at 25 °C during 150 min. Then, 100 μL of the supernatant of each well was mixed with the same volume of Griess reagent [0.1% N-(1-naphthyl)-ethylenediamine, 1 % sulfanilamide in 5 % phosphoric acid] in H_2O per 10 min in order to measure the nitrite produced from sodium nitroprusside. Finally, the mixture's absorbance was measured at 550 nm on a microtitration plate using an ELISA plate reader (Benchmark Microplate Reader; Bio-Rad, Hercules, CA, USA).

2.3. Test cells

Mouse macrophage cells line (RAW 264.7) was cultured in Dulbecco's modified Eagle medium (DMEM) (Sigma-Aldrich, St. Louis, MO, USA) supplemented with 10 % fetal bovine serum (FBS) (Corning, NY, USA). Monocytes and macrophages from human blood were cultured using RPMI 1640

medium (R7388, Sigma-Aldrich); booth cells were incubated at 37 °C in 5 % CO₂ (VWR 2325 Water-Jacketed CO₂ Incubator, Pa, USA) and the treatments were assayed at different concentrations (25, 50, 100, and 200 µg/mL) and LPS (1 µg/mL) for 24 h.

3.4. 3-(4, 5-Dimethylthiazol-2-yl)-2, 5-Diphenyltetrazolium Bromide (MTT) assay

The MTT assay was carried out according to the manufacturer (Roche, cell proliferation kit I, Roche, Cat. No. 11-465-007-001) instructions. Briefly, 5 x 10⁴ cells/well were suspended in 100 µL on culture medium and seeded in each well of a flat 96-well plate. After incubation time, cell cultures were incubated with 100 µL on medium containing different concentrations of each samples (25 to 200 µg/mL).

Control cell cultures were incubated with DMSO (0.5 %) and they represent 100 % viability. Dioctyl phthalate (DOP) (D201154, Sigma-Aldrich) and eicosapentaenoic acid (EPA) (E-2011, Sigma-Aldrich) were used as standard controls. Nω-Nitro-L-arginine methyl ester hydrochloride (L-NAME) (N5751, Sigma-Aldrich) and gallic acid (GA) (G7384, Sigma-Aldrich) were used as anti-inflammatory and anti-oxidant controls, respectively. Prior to the last 4 h of the cell culture, 10 µL of MTT stock solution (5 mg/mL) were added to each well. Formazan crystals formed were dissolved with 100 µL of a sodium dodecyl sulfate (SDS) solution and the plates were read overnight using an ELISA plate reader (Benchmark Microplate Reader; Bio-Rad, Hercules, CA, USA) at a test wavelength of 550 nm and a reference wavelength of 650 nm (Liu, Xiao, Wang, Chen, & Hu, 2017).

3.5. Nitric oxide (NO) measurement assay

RAW 264.7 cells line were incubated in a 96-well plate (5 x 10⁴/well) in 200 µL of medium (DMEM-FBS 10 %) and incubated during 24 h. After that, the medium was removed and the cells were treated by LPS (1 µg/mL), either in the presence or absence of the test samples at different concentrations (25 to 200 µg/mL), and incubated for 24 h. Each 100 µL of cultured supernatant was mixed with a 100 µL of Griess reagent [0.1% N-(1-naphthyl)-ethylendiamina, 1 % sulfanilamide in 5 % phosphoric acid] and incubated at darkness for 10 min. The total production of nitrite was calculated based on the sample absorbance at 550 nm using an ELISA plate reader (Benchmark Microplate Reader; Bio-Rad, Hercules, CA, USA) and a series of known concentrations of sodium nitrite which was used to construct a standard curve.

3.6. 2, 7-dichlorofluorescein diacetate (DCF-DA) assay

Measurements of intracellular ROS levels in RAW 264.7 cells were made using 2',7'-dichlorodihydrofluorescein diacetate (DCFH-DA) assay as described by (Halliwell & Whiteman, 2004), who reported this assay as reliable for studying intracellular ROS. Briefly, 5×10^4 cells/well were suspended in 100 μ L on culture medium and seeded in each well of a flat 96-well plate and incubated per 24 h. After incubation, cell cultures were incubated with medium containing different concentrations of each samples (25 to 200 μ g/mL). Later, cell samples were incubated in the presence of 10 μ M DCFH-DA at 37 °C for 30 min and washed two times with PBS (pH 7.4). The intracellular fluorescence was assayed by excitation at 498 nm and emission 530 nm to monitor intracellular ROS (FLUOstar Omega, BMG Labtech Inc., Ortenberg, Germany). Also, for qualitatively measuring of the effect of bioactive fraction on H₂O₂-induced intracellular ROS production, cells were labeled with DCFH-DA and microscopic visualization were done under an inverted fluorescence microscope (Leica DMI8, Leica Microsystems GmbH, Wetzlar, Germany) (equipped with fluorescence filters [546/10 RHOD excitation filter and emission 585/40, 350/50 DAPI excitation filter and 460/40 emission, and 480/40 excitation FITC filter and 527/30 emission], to carry out observations which were recorded with a cooled monochromatic DFC 450C camera [Leica Microsystems, Wetzlar, Germany] and fluorescence overlay software [LAS AF version 3.1.0, Leica Microsystems CMS GmbH, Mannheim, Germany]).

3.7. Mouse anti-human antibody assay

The regulation effect of the fM on the production of IL-4, IL-10, and IL-6 were determined by the mouse anti-human antibody assay. The cells [peripheral blood mononuclear cell (PBMCs)] were isolated by a gradient of density of human peripheral blood using Ficoll-Paque PLUS (GE Healthcare, Otelfingen, Switzerland). For the isolation of PBMCs, blood was diluted 1:2 with PBS, layered on top of the corresponding amount of Ficoll-Paque PLUS and centrifuged at 450 xg for 30 min at room temperature. After separation, the lymphocytes were transferred to a fresh tube and washed three times with PBS. Then the cells were re-suspended in culture medium and counted to prepare the assay. The cells were examined before and after activation, which was performed with lipopolysaccharide (LPS) over 24 h, along with fM. After the treatment, cells were incubated with fluorescent markers associated to inflammation regulatory processes: FITC anti-human IL-4 Clone: MP4 25D2, a monoclonal antibody reacts with human IL-4 (interlukin-4) (Cat. 500806, BioLegend, San Diego, CA, USA), PE anti-human IL-10 Clone: JES3-9D7, a monoclonal antibody reacts with human IL-10 (interlukin-10) (Cat. 501404, BioLegend, San Diego, CA, USA), FITC anti-human IL-6 Clone: MQ2-13A5, a monoclonal antibody reacts with human IL-6 (interlukin-6) (Cat. 501104, BioLegend, San Diego, CA, USA). After that,

10,000 events were analyzed with by flow cytometry using a flow cytometer (BD FACSVerse™ Flow Cytometer - BD Biosciences NY, USA).

3.8. Statistical analysis

All biological assays were performed in triplicate; in addition, three individual assays of each were performed. Data were analyzed by means of an analysis of variance (ANOVA) with Tukey multiple comparisons test (Tukey's post hoc test), at a 95 % confidence interval, and the level of significance of $P \leq 0.05$, (SPSS). All data were presented as the mean value with their indicated standard deviation (mean \pm S.D.).

4. Results and discussion

4.1. Inhibition of RNS production

This test was carried out using the SNP assay using the Griess reagent and the nitric oxide radical scavenging capability was determined for two reasons, 1) to evaluate antioxidant activity against reactive species of biological importance, such as reactive nitrogen species (RNS), and 2) to know if once the effects on nitric oxide (NO) level production (%) in LPS-stimulated Raw 264.7 cells have been tested, the NO radical scavenger will affect.

At the intracellular level there are antioxidant systems that provides the cell of protection against damage by reactive oxygen species (ROS) and, at certain conditions, these systems might be inadequate or faulty and the elevation of ROS produces cytotoxicity (Muravchick, 2006). Then, NO when combined with superoxide radicals (O_2^-), generates molecules such as peroxynitrite ($ONOO^-$) and, as ROS does, it may induce apoptosis. The $ONOO^-$ radical produces irreversible protein nitration, enzymatic inactivation, DNA damage, disruption of mitochondrial integrity and other components of the cell structure, and all of these effects are either by direct contact or by lipid peroxidation (Muravchick, 2006; Peng et al., 2019). The NO radical is of great importance for its physiological function, however is also considered an important toxic intermediary because of its status as a free radical (Moncada, Palmer, & Higgs, 1991).

Table 1 shows the effect of samples over the production (%) of RNS derived from NO, considering the decrease in RNS production as anti-nitrosative activity. Gallic acid (GA), at a maximum concentration of 800 μ g/mL, showed the major anti-nitrosative activity, allowing the generation of only 11.63 % of RNS. However, GA is a polyphenol (belonging to the group of hydrolysable tannins), that contains a phenolic ring substituted with several hydroxyl groups, which confers this molecule a great

antioxidant capacity through mechanisms of donation of protons and electrons (Badhani, Sharma, & Kakkar, 2015).

Diethyl phthalate (DOP) also showed anti-nitrosative activity (even at the lowest concentration tested), therefore, the chemical configurational monitoring by which this molecule could be stabilizing radicals should be studied. The fM sample (subject of study), showed activity only at the highest concentrations tested (400 and 800 µg/mL); this may be due to the amount of DOP contained in fM and, according to the chemical characterization carried out by Garcia-Romo et al., (2020), DOP is the minority compound contained in fM; however, the amount of DOP might be too small to produce a significant activity, therefore, the inhibition of RNS could be attributed to the indolocarbazole alkaloid derivative (IAD) (since the EPA standard did not show inhibition activity); therefore, at lower concentrations (100 - 200 µg/mL), the production of RNS did not decrease, which suggest that this factor might not intervene in subsequent anti-inflammation tests.

4.2. Inhibition of cell viability

This test was carried out using the MTT assay with the objective of determine the cytotoxicity effect of testing samples against the RAW 264.7 cell line, in order to discard that any reduction in NO is due to cell death, during the anti-inflammation test.

The MTT assay is a colorimetric assay used to evaluate the metabolic activity of a cell and NADPH-dependent cellular oxidoreductase enzymes may, under defined conditions, indicate the number of metabolically active cells that in turn reflects cell viability (Stockert, Horobin, Colombo, & Blázquez-Castro, 2018); therefore, the reduction of viability indicates a cytotoxic activity.

Table 2 shows that none of the samples decreased the viability when tested at their lowest concentrations (25 and 50 µg/mL). With regard to fM, only at concentrations greater than 100 µg/mL a significant ($P \leq 0.05$) decrease was observed. Based on this observation, fM lacks cytotoxicity against RAW 264.7 cell line at the lowest (25 and 50 µg/mL) concentrations tested, suggesting that cytotoxicity would not be a factor during subsequent anti-inflammation tests.

4.3. Inhibition of NO production

This test was carried out measuring NO production using the Griess reagent with the objective of investigating whether or not the anti-inflammatory activity of the samples is mediated by the inhibition of NO production; the nitrite concentration was used to determine NO production (%).

NO is a signaling molecule synthesized by a family of nitric oxide synthases (NOS) and, although NO has beneficial roles (host defense system against tumor cells, viral replication and other

factors), but excessive production of NO causes various inflammatory diseases (Kim, Seong, Jang, & Kim, 2011). Based on this, NO is an important regulator of inflammatory responses and a reduction in NO production is an indicator of anti-inflammatory activity (Korhonen, Lahti, Kankaanranta, & Moilanen, 2005; Moncada et al., 1991; Vane et al., 1994).

Table 3 shows that all samples decreased NO production, being DOP the compound showed the lowest percentage of NO inhibition, being significantly different from the rest ($P \leq 0.05$). On the other hand, EPA inhibited NO production as its concentration was increased; this is consistent with the literature since its anti-inflammatory capacity has been demonstrated, related to the displacement of arachidonic acid from the cell membrane (Bagga, Wang, Farias-Eisner, Glaspy, & Reddy, 2003), the capability to decrease the production of tumor necrosis factor alpha (TNF- α) (Babcock, Helton, Hong, & Espat, 2002; Babcock, Novak, et al., 2002), molecular level alterations that include decreased activation of nuclear factor kappa B and activator protein 1 (Novak, Babcock, Jho, Helton, & Espat, 2003), as well as by lowering NO production in LPS-stimulated macrophages through altered iNOS protein expression (Aldridge, Razzak, Babcock, Helton, & Espat, 2008). The fM also was able to inhibit NO production at the lowest concentration (25 and 50 $\mu\text{g/mL}$, which are not cytotoxic); however, this effect was not significant ($P \leq 0.05$) different from that observed with EPA standard; based on this observation, the anti-inflammatory activity of IAD by inhibiting NO production is suggested.

Both controls, L-NAME and gallic acid, effectively worked as an anti-inflammatory positive controls, decreasing NO production showing a dose-response type of relationship. This is consistent with the fact that L-NAME is a specific inhibitor of NO synthase enzyme activity (Wang, Lai, Chen, Yen, & Yang, 2000) and GA a well-known antioxidant (Locatelli, Filippin-Monteiro, Centa, & Creczinsky-Pasa, 2013). These results suggest that EPA may be a major bioactive compound that is responsible for the anti-inflammatory effects of fM; however, in order to confirm that IAD does not possess anti-inflammatory activity, pure IAD needs to be assayed.

4.4. Inhibition of intracellular ROS production

This test was carried out using the DCFH-DA assay in order to measure the inhibition of intracellular ROS production. High levels of ROS induce oxidative stress and subsequently inflammatory reactions, and may lead to a variety of biochemical and physiological lesions (Conforti et al., 2009). Likewise, once an inflammatory response is generated, the excessive production of ROS is also increased, which may cause significant damage to the cells (DNA damage and mutations) (Lonkar & Dedon, 2011); the pro-inflammation and the generation of ROS is a circle of reactions where each one

stimulates the other. ROS are crucial inflammatory mediators; therefore, anti-inflammatory activity involves a decrease in ROS production.

Table 4 shows that all of the samples tested decreased intracellular ROS production. The greatest decreases in ROS production were achieved when GA was used at its highest concentration; this is consistent with that reported in the literature since GA is a known potent agent against oxidative stress (Erol-Dayi, Arda, & Erdem, 2012). 3) fM showed the highest activity at the lowest concentration (25 $\mu\text{g/mL}$), but there were no significant differences compared to the two standards (DOP and EPA) ($P \leq 0.05$); so we cannot say that this compound acts only against ROS. In addition, the activity of fM can be qualitatively verified as shown in **Figure 2**, where fM at 25 $\mu\text{g/mL}$ decreased the fluorescence intensity observed under a microscope (compared to cells stimulated with LPS and without fM); however, to ensure that IAD does not possess the major anti-ROS activity, it is appropriate to evaluate it in its pure form after a chemical synthesis.

Inducible nitric oxide synthase (iNOS) synthesizes NO and it has a key role in various physiological and pathological conditions. However, it does not have regulatory effects on the immune system (Pando & Verma, 2000); but, when present in excess, NO leads to the accumulation of reactive oxygen species (ROS), cell death and interruption of homeostasis (Tegeder et al., 2001), and the inflammatory stimulus needs a signal transduction mediated by NF- κ B. Therefore, NF- κ B has the ability to regulate gene expression associated with immunity and inflammation, such as NO, PGE2, IL-1 β , IL-6 and MCP-1 (Davis, Martin, Turko, & Murad, 2001; Ghosh, May, & Kopp, 1998) and, after activation in response to a stimulus (LPS), it translocate in the nucleus and regulates the transcription of the target gene (Funk, 2001; Hwisa, Chandu, Katakam, & Nama, 2013); consequently, the search for agents capable of regulating these responses is a major focus of attention in research carried out with the decrease of inflammatory processes.

4.5. Determination of up- and down-regulation cytokine production

This test was carried out using the mouse anti-human antibody assay and the objective was to measure [average fluorescence intensity (a.u.)] the regulation of cytokine production. Macrophages play a key role in the immune system because they provide defense against exogenous agents; they also detect pathogenic substances through Pattern Recognition Receptors [PRR, including Toll-like receptors (TLR)], and subsequently regulate the inflammatory response using pro-inflammatory mediators (TNF- α , IL-6, MCP-1, IL-1 β , NO, PGE2 and LTB4) (Goodwin & Ceuppens, 1983). LPS is one of the most effective activators of macrophages; these once stimulated lead to the activation of NF- κ B that induces pro-inflammatory mediating expression, where it includes cytokine IL-6; therefore, down-regulating it

would decrease the inflammatory response (Furuya et al., 2015; Wan & Lenardo, 2010); this is closely related to an anti-inflammatory activity.

Table 5 shows the down-regulation of IL-6 in the presence of fM after activation with LPS, establishing significant ($P \leq 0.05$) differences with untreated cells; fM has the capacity to intervene in inflammatory processes, since IL-6 is a cytokine released by macrophages stimulated by norepinephrine (NA) as a part of the hypothalamic-pituitary-adrenal axis; this in turn releases corticosterone, modulating the systemic inflammatory response (Dalmas, Clément, & Guerre-Millo, 2011).

Regulatory responses of cell cycles, associated to inflammatory processes, are not limited to regulation of certain signals that promote pro-inflammation (such as IL-6), these may also include signals that promote anti-inflammation. Therefore, other activated macrophage phenotypes are induced by glucocorticoids, IL-4 and IL-10 produce anti-inflammatory cytokines (Dalmas et al., 2011). In the **Table 5**, the effect of fM on up-regulation of the anti-inflammatory cytokines (IL-4 and IL-10) is shown. Fraction M significantly ($P \leq 0.05$) induced IL-4 and IL-10 showing a dose-response type of relationship; this suggest that the fM not only has a regulating action by removing pro-inflammatory processes (IL-6), but it also promotes anti-inflammatory processes (IL-4 and IL-10), an anti-inflammatory activity mainly attributed to EPA.

Conclusion

Based on the results, fM has the ability to inhibit the formation of RNS at high concentrations ($>800 \mu\text{g/mL}$); in addition, at cellular level, fM was not cytotoxic at concentrations $<100 \mu\text{g/mL}$, so it can limit the production of NO to more than 60 % with this same concentration ($100 \mu\text{g/mL}$), also when using the lower concentration ($50 \mu\text{g/mL}$) can inhibit the production of ROS by up to 50 %. Additionally, the determination of the production of cytokines with up- and down-regulation was verified, showing a dose-response effect with at different concentrations. For that reason, the compounds present in fM act in some way as anti-inflammatory-related agents on *Litopeaneus stylirostris*.

Acknowledgment

Authors wish to thank Consejo Nacional de Ciencia y Tecnología (CONACYT) Mexico for financing the project No. 241133, for granting research scholarships, and for funding this project.

Reference

Alberts, B., Johnson, A., Lewis, J., Morgan, D., Raff, M., Roberts, K., ... Hunt, T. (2010). *Molecular*

Biology of the Cell. Artmed Editora.

- Aldridge, C., Razzak, A., Babcock, T. A., Helton, W. S., & Espat, N. J. (2008). Lipopolysaccharide-Stimulated RAW 264.7 Macrophage Inducible Nitric Oxide Synthase and Nitric Oxide Production Is Decreased by an Omega-3 Fatty Acid Lipid Emulsion. *Journal of Surgical Research*, 149(2), 296–302. <https://doi.org/10.1016/j.jss.2007.12.758>
- Allavena, P., Garlanda, C., Borrello, M. G., Sica, A., & Mantovani, A. (2008). Pathways connecting inflammation and cancer. *Current Opinion in Genetics and Development*. <https://doi.org/10.1016/j.gde.2008.01.003>
- Awad, H. M., Abd-Alla, H. I., Mahmoud, K. H., & El-Toumy, S. A. (2014). In vitro anti-nitrosative, antioxidant, and cytotoxicity activities of plant flavonoids: A comparative study. *Medicinal Chemistry Research*, 23(7), 3298–3307. <https://doi.org/10.1007/s00044-014-0915-2>
- Babcock, T. A., Helton, W. S., Hong, D., & Espat, N. J. (2002). Omega-3 fatty acid lipid emulsion reduces LPS-stimulated macrophage TNF- α production. *Surgical Infections*, 3(2), 145–149. <https://doi.org/10.1089/109629602760105817>
- Babcock, T. A., Novak, T., Ong, E., Jho, D. H., Helton, W. S., & Espat, N. J. (2002). Modulation of lipopolysaccharide-stimulated macrophage tumor necrosis factor- α production by ω -3 fatty acid is associated with differential cyclooxygenase-2 protein expression and is independent of interleukin-10. *Journal of Surgical Research*, 107(1), 135–139. <https://doi.org/10.1006/jsre.2002.6498>
- Badhani, B., Sharma, N., & Kakkar, R. (2015). Gallic acid: A versatile antioxidant with promising therapeutic and industrial applications. *RSC Advances*, 5(35), 27540–27557. <https://doi.org/10.1039/c5ra01911g>
- Bagga, D., Wang, L., Farias-Eisner, R., Glaspy, J. A., & Reddy, S. T. (2003). Differential effects of prostaglandin derived from ω -6 and ω -3 polyunsaturated fatty acids on COX-2 expression and IL-6 secretion. *Proceedings of the National Academy of Sciences of the United States of America*, 100(4), 1751–1756. <https://doi.org/10.1073/pnas.0334211100>
- Braekman, J. C., & Daloze, D. (1986). Chemical defence in sponges. *Pure and Applied Chemistry*, 58(3), 357–364. <https://doi.org/10.1351/pac198658030357>
- Bray, F., Jemal, A., Grey, N., Ferlay, J., & Forman, D. (2012). Global cancer transitions according to the Human Development Index (2008-2030): A population-based study. *The Lancet Oncology*, 13(8), 790–801. [https://doi.org/10.1016/S1470-2045\(12\)70211-5](https://doi.org/10.1016/S1470-2045(12)70211-5)
- Conforti, F., Sosa, S., Marrelli, M., Menichini, F., Statti, G. A., Uzunov, D., ... Menichini, F. (2009). The protective ability of Mediterranean dietary plants against the oxidative damage: The role of radical oxygen species in inflammation and the polyphenol, flavonoid and sterol contents. *Food*

- Chemistry*, 112(3), 587–594. <https://doi.org/10.1016/j.foodchem.2008.06.013>
- Coussens, L. M., & Werb, Z. (2002). Inflammation and cancer. [Nature. 2002 Dec 19-26] - PubMed result. *Nature*, 420(6917), 860–867. <https://doi.org/10.1038/nature01322>
- Dalmas, E., Clément, K., & Guerre-Millo, M. (2011, July). Defining macrophage phenotype and function in adipose tissue. *Trends in Immunology*. <https://doi.org/10.1016/j.it.2011.04.008>
- Davis, K. L., Martin, E., Turko, I. V., & Murad, F. (2001). Novel effects of nitric oxide. *Annual Review of Pharmacology and Toxicology*, 41(1), 203–236. <https://doi.org/10.1146/annurev.pharmtox.41.1.203>
- Erol-Dayi, Ö., Arda, N., & Erdem, G. (2012). Protective effects of olive oil phenolics and gallic acid on hydrogen peroxide-induced apoptosis. *European Journal of Nutrition*, 51(8), 955–960. <https://doi.org/10.1007/s00394-011-0273-5>
- Fahmy, R. (2013). In vitro antioxidant, analgesic and cytotoxic activities of *Sepia officinalis* ink and *Coelatura aegyptiaca* extracts. *African Journal of Pharmacy and Pharmacology*, 7(22), 1512–1522. <https://doi.org/10.5897/ajpp2013.3564>
- Funk, C. D. (2001, November 30). Prostaglandins and leukotrienes: Advances in eicosanoid biology. *Science*. <https://doi.org/10.1126/science.294.5548.1871>
- Furuya, S., Kono, H., Hara, M., Hirayama, K., Sun, C., & Fujii, H. (2015). Interleukin 17A plays a role in lipopolysaccharide/d-galactosamine-induced fulminant hepatic injury in mice. *Journal of Surgical Research*, 199(2), 487–493. <https://doi.org/10.1016/j.jss.2015.05.060>
- Gerwick, W. H., & Moore, B. S. (2012, January 27). Lessons from the past and charting the future of marine natural products drug discovery and chemical biology. *Chemistry and Biology*. Cell Press. <https://doi.org/10.1016/j.chembiol.2011.12.014>
- Ghosh, S., May, M. J., & Kopp, E. B. (1998). NF- κ B AND REL PROTEINS: Evolutionarily Conserved Mediators of Immune Responses. *Annual Review of Immunology*, 16(1), 225–260. <https://doi.org/10.1146/annurev.immunol.16.1.225>
- Goodwin, J. S., & Ceuppens, J. (1983). Regulation of the immune response by prostaglandins. *Journal of Clinical Immunology*, 3(4), 295–315. <https://doi.org/10.1007/BF00915791>
- Halliwell, B., & Whiteman, M. (2004, May 1). Measuring reactive species and oxidative damage in vivo and in cell culture: How should you do it and what do the results mean? *British Journal of Pharmacology*. John Wiley & Sons, Ltd (10.1111). <https://doi.org/10.1038/sj.bjp.0705776>
- Hwisa, N. T., Chandu, B. R., Katakam, P., & Nama, S. (2013). Pharmacognostical studies on the leaves of *Ficus altissima* blume. *Journal of Applied Pharmaceutical Science*, 3(4SUPPL.1), 165–171. <https://doi.org/10.7324/JAPS.2013.34.S10>

- Kim, S.-B., Seong, Y.-A., Jang, H.-J., & Kim, G.-D. (2011). The Anti-Inflammatory Effects of *Persicaria thunbergii* Extracts on Lipopolysaccharide-Stimulated RAW264.7 Cells. *Journal of Life Science*, 21(12), 1689–1697. <https://doi.org/10.5352/jls.2011.21.12.1689>
- Korhonen, R., Lahti, A., Kankaanranta, H., & Moilanen, E. (2005). Nitric oxide production and signaling in inflammation. *Current Drug Targets: Inflammation and Allergy*. Bentham Science Publishers. <https://doi.org/10.2174/1568010054526359>
- Liu, K., Xiao, X., Wang, J., Chen, C.-Y. Y. O., & Hu, H. (2017). Polyphenolic composition and antioxidant, antiproliferative, and antimicrobial activities of mushroom *Inonotus sanghuang*. *LWT - Food Science and Technology*, 82, 154–161. <https://doi.org/10.1016/j.lwt.2017.04.041>
- Locatelli, C., Filippin-Monteiro, F. B., Centa, A., & Creczinsky-Pasa, T. B. (2013). Antioxidant, antitumoral and anti-inflammatory activities of gallic acid. In *Handbook on Gallic Acid: Natural Occurrences, Antioxidant Properties and Health Implications* (pp. 215–230). Retrieved from https://www.researchgate.net/publication/236262423_Antioxidant_Antitumoral_and_Anti-Inflammatory_Activities_of_Gallic_Acid
- Lonkar, P., & Dedon, P. C. (2011, May 1). Reactive species and DNA damage in chronic inflammation: Reconciling chemical mechanisms and biological fates. *International Journal of Cancer*. <https://doi.org/10.1002/ijc.25815>
- Moncada, S., Palmer, R. M. J., & Higgs, E. A. (1991). Nitric oxide: Physiology, pathophysiology, and pharmacology. *Pharmacological Reviews*.
- Muravchick, S. and R. J. L. (2006). Clinical implications of mitochondrial dysfunction. *The Journal of the American Society of Anesthesiologists*, 105, 819–837.
- Novak, T. E., Babcock, T. A., Jho, D. H., Helton, W. S., & Espat, N. J. (2003). NF-kappa B inhibition by omega -3 fatty acids modulates LPS-stimulated macrophage TNF-alpha transcription. *American Journal of Physiology. Lung Cellular and Molecular Physiology*, 284(1), L84-9. <https://doi.org/10.1152/ajplung.00077.2002>
- Pando, M. P., & Verma, I. M. (2000). Signal-dependent and -independent degradation of free and NF- κ b-bound I κ B α . *Journal of Biological Chemistry*, 275(28), 21278–21286. <https://doi.org/10.1074/jbc.M002532200>
- Peng, W., Cai, G., Xia, Y., Chen, J., Wu, P., Wang, Z., ... Wei, D. (2019, March 2). Mitochondrial Dysfunction in Atherosclerosis. *DNA and Cell Biology*. <https://doi.org/10.1089/dna.2018.4552>
- Schroeter, H., Boyd, C., Spencer, J. P. E., Williams, R. J., Cadenas, E., & Rice-Evans, C. (2002). MAPK signaling in neurodegeneration: Influences of flavonoids and of nitric oxide. *Neurobiology of Aging*, 23(5), 861–880. [https://doi.org/10.1016/S0197-4580\(02\)00075-1](https://doi.org/10.1016/S0197-4580(02)00075-1)

- Stankevicius, L., Aiub, C., Maria, L. C. C. d. S., Lobo-Hajdu, G., & Felzenszwalb, I. (2008). Genotoxic and antigenotoxic evaluation of extracts from *Arenosclera brasiliensis*, a Brazilian marine sponge. *Toxicology in Vitro*, 22(8), 1869–1877. <https://doi.org/10.1016/j.tiv.2008.09.003>
- Stockert, J. C., Horobin, R. W., Colombo, L. L., & Blázquez-Castro, A. (2018, April 1). Tetrazolium salts and formazan products in Cell Biology: Viability assessment, fluorescence imaging, and labeling perspectives. *Acta Histochemica*. Elsevier GmbH. <https://doi.org/10.1016/j.acthis.2018.02.005>
- Tegeder, I., Niederberger, E., Israr, E., Gühring, H., Brune, K., Euchenhofer, C., ... Geisslinger, G. (2001). Inhibition of NF-kappaB and AP-1 activation by R- and S-flurbiprofen. *The FASEB Journal : Official Publication of the Federation of American Societies for Experimental Biology*, 15(1), 2–4. <https://doi.org/10.1096/fasebj.15.3.595>
- Vane, J. R., Mitchell, J. A., Appleton, I., Tomlinson, A., Bishop-Bailey, D., Croxtall, J., & Willoughby, D. A. (1994). Inducible isoforms of cyclooxygenase and nitric-oxide synthase in inflammation. *Proceedings of the National Academy of Sciences of the United States of America*, 91(6), 2046–2050. <https://doi.org/10.1073/pnas.91.6.2046>
- Wan, F., & Lenardo, M. J. (2010, January). The nuclear signaling of NF-κB: Current knowledge, new insights, and future perspectives. *Cell Research*. <https://doi.org/10.1038/cr.2009.137>
- Wang, C. C., Lai, J. E., Chen, L. G., Yen, K. Y., & Yang, L. L. (2000). Inducible nitric oxide synthase inhibitors of Chinese herbs. Part 2: Naturally occurring furanocoumarins. *Bioorganic and Medicinal Chemistry*, 8(12), 2701–2707. [https://doi.org/10.1016/S0968-0896\(00\)00200-5](https://doi.org/10.1016/S0968-0896(00)00200-5)
- WHO | Cancer. (2019). *WHO*.

Table 1. Effects of bioactive fraction (fM), DOP, EPA, L-NAME, and GA on Reactive Nitrogen Species (RNS) level production (%) derived from nitric oxide (NO) using sodium nitroprusside (SNP) assay.

	(µg/mL)			
	100	200	400	800
fM	100 ± 1.7 c	100 ± 8.1 c	90.3 ± 2.1 c	77.8 ± 8.0 c
DOP	70.9 ± 3.1 b	66.3 ± 1.5 b	64.1 ± 1.7 b	62.0 ± 0.5 b
EPA	100 ± 5.7 c	100 ± 4.5 c	100 ± 1.1 d	96.2 ± 6.8 d
L-NAME	100 ± 0.7 c	100 ± 6.1 c	91 ± 4.8 c	89 ± 3.3 cd
GA	33.7 ± 1.1 a	30.2 ± 3.6 a	24.3 ± 0.6 a	11.6 ± 1.8 a

Values represent means ± S.D. from three determinations. Different letters within the column are significantly different ($P \leq 0.05$); Tukey's least significant difference test. Dioctyl phthalate (DOP) and eicosapentaenoic acid (EPA) were used as standard controls. L-NAME and gallic acid were used as anti-inflammatory and anti-oxidant controls, respectively.

Table 2. Effects of bioactive fraction (fM), DOP, EPA, L-NAME, and GA on RAW 264.7 cell viability (%) at 24 h of incubation.

	(µg/mL)			
	25	50	100	200
BF	100 ± 6.1 a	100 ± 12.4 a	80.6 ± 1.6 b	59.9 ± 1.7 c
DOP	100 ± 4.3 a	100 ± 3.7 a	100 ± 11.9 b	100 ± 2.0 d
EPA	100 ± 20.7 a	100 ± 3.3 a	49.3 ± 1.0 a	38.0 ± 1.6 a
L-NAME	100 ± 6.1 a	100 ± 4.9 a	100 ± 15.0 b	100 ± 1.9 d
GA	100 ± 6.1 a	89.6 ± 15.7 a	71.3 ± 16.5 ab	49.1 ± 2.2 b

Values represent means ± S.D. from three determinations. Different letters within the column are significantly different ($P \leq 0.05$); Tukey's least significant difference test. Control cell cultures were incubated with DMSO (0.5 %) and represent 100 % viability. Dioctyl phthalate (DOP) and eicosapentaenoic acid (EPA) were used as standard controls. L-NAME and gallic acid were used as anti-inflammatory and anti-oxidant controls, respectively. LPS control at 1 µg/mL had a viability of 99.7 ± 8.0 %.

Table 3. Effects of bioactive fraction (fM), DOP, EPA, L-NAME, and GA on nitric oxide (NO) level production (%) in LPS-stimulated RAW 264.7 cells at 24 h of incubation.

Samples (µg/mL) + LPS (1 µg/mL)

	25	50	100	200
fM	63.0 ± 9.7 a	46.4 ± 4.1 ab	38.7 ± 5.5 ab	28.2 ± 1.7 ab
DOP	100 ± 10.6 b	100 ± 7.2 d	90.8 ± 4.9 d	86.7 ± 13.9 d
EPA	70.7 ± 5.7 a	43.2 ± 9.8 a	27.3 ± 3.5 a	27.0 ± 3.1 a
L-NAME	79.8 ± 2.8 a	75.3 ± 7.3 c	66.0 ± 5.8 c	45.4 ± 1.7 bc
GA	74.7 ± 3.6 a	65.1 ± 6.6 bc	52.6 ± 8.9 bc	46.3 ± 3.7 c

Values represent means ± S.D. from three determinations. Different letters within the column are significantly different ($P \leq 0.05$); Tukey's least significant difference test. All of the treatments were compared with control (cells + LPS at 1 µg/mL), which represent 100 % of NO production; in addition, the absorbance results are related to a NaNO₃ standard curve ($R^2 = 0.9986$), where showed a maximum production of NO of 0.5 µg/mL. Untreated negative control cell cultures were incubated only with DMSO (0.5 %) and represents the natural NO production of the cells (26.6 ± 4.7) by spontaneous stress. Dioctyl phthalate (DOP) and eicosapentaenoic acid (EPA) were used as standard controls. L-NAME and gallic acid were used as anti-inflammatory and anti-oxidant controls, respectively.

Table 4. Effects of bioactive fraction (fM), DOP, EPA, L-NAME, and GA on intracellular reactive oxygen species (ROS) level production (%) in LPS-stimulated RAW 264.7 cells at 24 h of incubation.

	Samples (µg/mL) + LPS (1 µg/mL)			
	25	50	100	200
fM	59.5 ± 7.9 a	55.0 ± 7.6 ab	48.5 ± 5.2 ab	37.1 ± 5.5 ab
DOP	68.6 ± 1.4 ab	62.0 ± 11.5 ab	58.6 ± 4.2 bc	42.2 ± 8.8 ab
EPA	75.8 ± 9.0 ab	50.2 ± 12.7 ab	45.4 ± 9.9 ab	38.5 ± 10.6 ab
L-NAME	81.0 ± 2.1 b	74.7 ± 10.6 b	68.9 ± 8.7 c	54.2 ± 8.5 b
GA	60.7 ± 9.3 a	41.8 ± 3.9 a	31.7 ± 5.2 a	30.6 ± 4.5 a

Values represent means ± S.D. from three determinations. Different letters within the column are significantly different ($P \leq 0.05$); Tukey's least significant difference test. All of the treatments were compared with controls (cells + LPS at 1 µg/mL), which represent 100 % of ROS production. Untreated negative control cell cultures were incubated only with DMSO (0.5 %), and represent the natural ROS production of the cells (23.2 ± 11.6) by spontaneous stress. Dioctyl phthalate (DOP) and eicosapentaenoic acid (EPA) were used as standard controls. L-NAME and gallic acid were used as anti-inflammatory and anti-oxidant controls, respectively.

Non-fM

fM

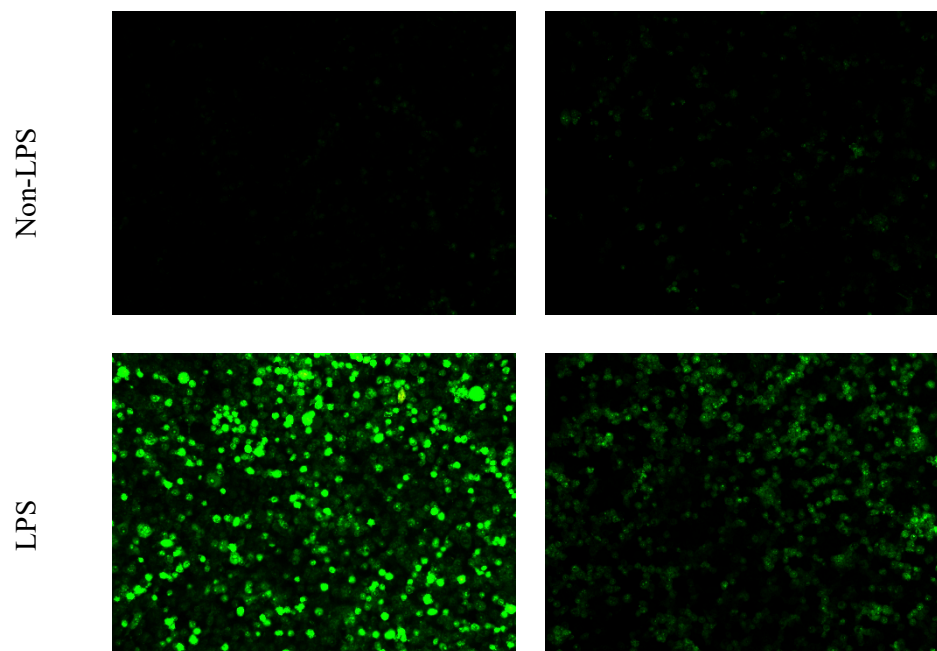


Figure 1. Effect of reactive oxygen species production on RAW264.7 cell line; the cells were pre-incubated with or without fM (25 µg/mL) and activated with or without lipopolysaccharide (LPS, 1 µg/mL) per 24 hr and staining with H₂DCFDA (10 µM) per 30 min incubation (37 °C). 2, 7-Dichlorofluorescein fluorescence was evaluated using fluorescence microscopy (20x).

Table 5. Effect of bioactive fraction (fM) on up-regulation of anti-inflammatory cytokines (IL-4 and IL-10) and down-regulation of pro-inflammatory cytokines (IL-6) of interleukins production activation by LPS-activated human monocytes cells.

Average fluorescence intensity (a.u.)			
	IL-4	IL-10	IL-6
Control	421.7 ± 6.7 b	192.3 ± 12.9 ab	181.0 ± 4.0 a
LPS	287.0 ± 3.5 a	114.3 ± 8.5 a	811.3 ± 2.1 d
fM (µg/mL)			
25	509.7 ± 12.7 c	226.3 ± 12.0 bc	243.3 ± 4.0 c
50	532.0 ± 8.9 c	315.0 ± 6.0 c	194.0 ± 1.0 b
100	626.7 ± 17.9 d	588.0 ± 72.1 d	188.0 ± 3.6 ab
200	978.3 ± 28.2 e	591.0 ± 31.2 d	185.3 ± 6.4 ab

Values represent means ± S.D. from three determinations. Different letters within the column are significantly different ($P \leq 0.05$); Tukey's least significant difference test. LPS control cells means cells + LPS at 1 µg/mL. Control untreated cell cultures were incubated only with DMSO (0.5 %). Treated cells were preincubated with fM (µg/mL) and activated with lipopolysaccharide (LPS, 1 µg/mL) per 24 hr.

CAPÍTULO V

**Cytotoxic Evaluation of EPA-Loaded PLGA-PVA Nanoparticles against Human
Prostate Carcinoma Cell Line *in Vitro***

Artículo por enviar

**Cytotoxic Evaluation of EPA-Loaded PLGA-PVA Nanoparticles against Human
Prostate Carcinoma Cell Line *in Vitro***

Joel Said García-Romo¹, Marisol Gastelum-Cabrera², Josué Elías Juárez Onofre², Alma Carolina Gálvez-Irqui¹, Edgar Sandoval-Petris³, María Guadalupe Burboa-Zazueta³, Maribel Plascencia-Jatomea¹, Rosario Maribel Robles-Sánchez¹, Armando Burgos-Hernández^{1*}.

¹ Departamento de Investigación y Posgrado en Alimentos, Universidad de Sonora, 83000 Sonora, Mexico.

² Departamento de Física, Universidad de Sonora, 83000 Sonora, Mexico.

³ Departamento de Investigaciones Científicas y Tecnológicas, Universidad de Sonora, 83000 Sonora, Mexico.

* Corresponding Author. Tel.: + 526-622-592-208; Fax: + 526-622-592-209.

E-Mail: armando.burgos@unison.mx

Abstract

In this work, an EPA-loaded PLGA was designed capable of possesses the ability to deliver a drug, increase its effectiveness and make it less toxic at high concentrations. It is known that eicosapentaenoic acid (EPA) (a polyunsaturated fatty acid clinically approved by the FDA) plays a role in preventing the promotion and progression stages of some types of cancer by pro-apoptosis action; this effect does not occur in normal (non-cancerous) cells; however, EPA has problems due to its low solubility in aqueous medium (like blood), also is high susceptible to physiological environments that should affect its bioactive action; this barrier can overcome using nanotechnological strategies using polymeric nanoparticles to encapsulate and bring protection to EPA. That is why was evaluated the binding of one (n-3) PUFAs to a biodegradable and non-toxic synthetic polymer (PLGA); the PLGA nanoparticles were prepared by the oil-in-water (O/W) single emulsion-solvent evaporation method, using PVA as stabilizer to later evaluated on a human cancerous and non-cancerous cell lines to show a cytotoxic effect. PLGA-EPA 10 % particles, showed an average diameter and zeta potential of ~ 143 nm and -17 mV, respectively; the encapsulation efficiency, loading capacity and yield of ~ 75 %, 7.6 % and 2.28 mg/mL, respectively; the PLGA and PLGA-EPA nanoparticle showed spherical shape and size structures corresponding to that analyzed by average diameter; finally, the PLGA-EPA 10 % system showed an improvement in cytotoxic activity on the cancerous cell (prostate carcinoma) in comparison to the pure EPA standard, as well as diminishing the cytotoxicity in the non-cancerous cell (ARPE-19).

Keywords: Nanoparticles, PLGA, EPA, anti-proliferative, cancer cell line.

1. Introduction

The eicosapentaenoic acid (EPA) belongs to the family of the n-3 polyunsaturated fatty acids (PUFAs), as well of other PUFAs, EPA have been promoted beneficial health effects such as cardiovascular and immunological health (Brouwer, 2008; Harris, Miller, Tighe, Davidson, & Schaefer, 2008; Kris-Etherton, Harris, & Appel, 2003; Ryan et al., 2010). EPA can be obtained from different sources, especially from marine organism such fish and shrimp (reference). In addition, EPA was clinically approved by the FDA (Gerwick & Moore, 2012). At present, the scientific society has been attributed other benefits to PUFAs, including EPA; they have been involved in preventing the promotion and progression stages of some types of cancer.

The anti-cancer effect has been attributed to pro-apoptosis action; promoting the generation of free radicals (reactive oxygen and nitrogen species mainly) and lipid peroxidation in tumor cells, however, apparently this effect does not occur in normal (non-cancerous) cells (Colquhoun & Schumacher, 2001; Tsuzuki et al., 2007). This suggests that EPA can be used as anti-cancer agent, since it can induce a pro-oxidant effect in cancerous and not in non-cancerous cells (this is very important because a similar effect between both cells would cause side effects against health.). This because of the cells found in tumors contain a low amounts of c-UFA and also have a minimum natural ability to generate free radicals; therefore, they are highly susceptible to cytotoxicity induced by free radicals compared to non-cancerous cells (Das, 1990). One explanation is that cancer cells focus their metabolism more on proliferation-related processes (mitosis), and de-focus processes related to cell homeostasis (such as enzymes related to the deactivation of reactive oxygen species) (reference). In addition, Motaung et al., (1999) published studies of the cytotoxic effects of EPA in prostate cancer cells.

As already mentioned, the EPA has been attributed pro-apoptotic activity by induction of ROS (this related to death intrinsic pathway); However, the articles related to this, usually use very high concentrations (this to achieve the effective dose) that also generates a cytotoxic effect against non-cancer cells, leading to bioselectivity problems (the term "bioselective" is used to refer to a compound which shows differential inhibitory effects between non-cancerous and cancerous cell lines (Ciavatta et al., 2017).

Despite the benefits mentioned, EPA as well as other n-3 polyunsaturated fatty acids have high susceptibility to oxidative deterioration (Arab-Tehrany et al., 2012; Romeu-Nadal, Castellote, & López-Sabater, 2004). Some of the factors that induce oxidative deterioration are oxygen, light, heating, UV irradiation, and in general free radicals, these accelerate the oxidation of lipids, decreasing stability and shelf-life (Johnson & Decker, 2015; Shahidi & Zhong, 2010). Lipid oxidation by free radicals not only occurs in the environment, these are constantly occurring in the human body at physiological conditions (Carocho, Morales, & Ferreira, 2018; Aruoma, 1998); this suggest that if EPA enters to the blood system, it can be oxidized by physiological radicals, and to afterward modify cell homeostasis causing adverse health effects, especially for the production of aldehydes which have been implicated in aging, mutagenesis and carcinogenesis (Lobo, Patil, Phatak, & Chandra, 2010; Kampa, Nifli, Notas, & Castanas, 2007). The toxicological effect is largely due to aldehydes as mentioned (malondialdehyde precisely) and 4-hydroxy-2-nonenal (4-HNE), this is due to its ability to cross-link to proteins and covalently bind to nucleic acids present in the genetic material (Nair, Cooper, Vietti, & Turner, 1986). Therefore the low oxidative stability of EPA requires effective antioxidant protection barrier to prevent oxidative deterioration (Jacobsen et al., 2001; Sisein, 2014).

In brief, due to the physicochemical characteristics of EPA, there are currently emerging technologies that arise from the same need for drug protection in the blood system such as nanotechnology. In the pharmaceutical food supplementation area, the (n-3) PUFAs are used with covered by softgel, a cover/capsule, which consist of a jelly-based cover that surrounds a liquid filler (Steele & Dietel, 1993); this cover/capsule solves problems related to oxidation due to environmental factors, in addition to provide greater bioavailability and absorption through the gastrointestinal tract (Gullapalli, 2010). In addition, there are different nanosystems with anti-cancer activity, these include injectable nanovectors and drug delivery, such as liposomes for breast cancer therapy (Malam, Loizidou, & Seifalian, 2009; Park, 2002) as a biodegradable nanoparticles (Hans & Lowman, 2002), PLGA nanoparticles (Indu Bala, Hariharan, & Kumar, 2004), among others (Wang et al., 2011).

In addition, there are studies in which can efficiently encapsulated bioactive compounds with enhanced physical and chemical stability, and high load, using a system by formation of solid shell nanoparticles with liquid (n-3) PUFAs core, this using a matrix of glyceryl stearic

acid ester called tristearin (Salminen, Helgason, Kristinsson, Kristbergsson, & Weiss, 2013); and that even a EPA nanoparticle systems have been created, as an *in vivo* tumor-selective drug delivery carrier, this using a matrix of glycol chitosan (Kim, Lee, Jeong, & Lee, 2011). It's for all this, that the aim of this study was to design an EPA-loaded PLGA to capable of possesses the ability to deliver a drug, increase its effectiveness and make it less toxic at high concentrations.

2. Materials and methods

2.1. Preparation of nanoparticles

The nanoparticles were prepared by oil-in-water (O/W) single emulsion-solvent evaporation method, using PVA as stabilizer, with slight modifications (Sahoo & Labhasetwar, 2005). Briefly, 10 mg of Poly D, L-lactide-co-glycolide (PLGA) [Lactide: glycolide 65:35, Mw 40,000-75,000 (CAT. P2066, Sigma-Aldrich)] was dissolved in 1 mL of organic solvent (40:60 dichloromethane: acetone) to form a primary solution which was further emulsified in an aqueous Poly (vinyl alcohol) (PVA) [M_w 9,000-10,000, 80 % hydrolyzed (CAT. 360627, Sigma-Aldrich)] solution at 1 % w/v (in a 7:3 ratio PVA: PLGA) to form an oil-in-water emulsion using a probe sonicator (Q125, 1/8" Probe, QSonica, 110 V, CT, USA) set at 60 % of energy output per 5 min over an ice bath. The emulsion was stirred overnight for the evaporation of the organic solvent. Excess of PVA was removed by ultracentrifugation at 13,500 rpm, 21 °C per 30 min (Allegra™ 64R Benchtop, Beckman Coulter Life Sciences, Ind, USA) followed by three washed with double distilled water.

The EPA (CAT. E-2011, Sigma-Aldrich) loaded PLGA nanoparticles were prepared in a similar way as mentioned, previously the EPA (equivalent to 5, 10, 20 and 30 % w/w weight of polymer) was dissolved in 1 mL of organic solvent (40:60 dichloromethane: acetone) containing 10 mg of PLGA to form a primary emulsion.

2.2. Particle size and zeta potential measurement

Average diameter (D) and Zeta Potential of PLGA, and EPA-loaded PLGA nanoparticles, for different w/w % ratio of EPA with respect to the total amount of PLGA, were determined by dynamic light scattering (DLS) and electrophoretic mobility using a Zetasizer

Nano ZS (Malvern Instruments, Malvern, UK) with a red laser of wavelength $\lambda_0 = 633$ nm (He-Ne, 4.0 Mw) and detection angle of 173° . All the samples were maintained at a constant temperature of $24.0 \pm 0.1^\circ\text{C}$, in all experiments and each batch was analyzed in triplicates.

2.3. Assessing the encapsulated loads of EPA

The amount of EPA present inside the nanoparticles was estimated by Sulfo-Phospho-Vanillin (SPV) assay. The colorimetric SPV method developed by (Anschau, Caruso, Kuhn, & Franco, 2017) was performed with slight modifications. Phospho-vanillin (PV) reagent was prepared dissolving 6 mg of vanillin in 100 mL of water and subsequently diluting to 500 mL 85 % of phosphoric acid (H_2SO_4). The resulting PV reagent was stored in the dark until use. The sample was prepared as follow, 20 μL of sample (PLGA, PLGA-EPA and EPA as standard) were diluted in 180 μL of concentrated H_2SO_4 glass test tubes and incubated at 100°C per 10 min. Then, tubes were cooled at room temperature and 500 μL of PV reagent was added to every tube for color development; then, the mixture was incubated at 37°C for 15 min and after that, 100 μL of each mixture was transferred to polystyrene 96-well microplates and stored for 45 min in a dark environment. Finally, the absorbance was measured at 530 nm by a microplate reader (FLUOstar Omega, BMG Labtech Inc., Ortenberg, Germany). For the quantification of EPA a calibration curve was made using 12 concentrations of pure EPA (10 mg/mL to downward) standard; also, a reactive blank containing 0 mg/mL EPA is used as a negative control; PLGA particles without EPA were also used as a control (this to ensure that if the system has absorbance, subtract the absorbance). The encapsulation efficiency (EE), loading capacity (LC) and amount of EPA (yield) contained in the system of EPA-loaded PLGA-PVA nanoparticles in respect to the total amount of PLGA, were determined according to Sigma-Aldrich Staff, (2019) with the following the equations:

$$\text{EE (\%)} = \frac{\text{Total weight EPA added} - \text{unloaded weight of EPA}}{\text{Total weight EPA added}} \times 100$$

$$\text{LC (\%)} = \frac{\text{The amount of total loaded EPA}}{\text{Total nanoparticle weight}} \times 100$$

2.4. Atomic force microscopy (AFM) studies

The morphology of PLGA and EPA-loaded nanoparticle was examined by atomic force microscopy (AFM) (JSPM-4210/TM-4210BU, JEOL, Serving Advanced Technology, Tokyo,

Japan). Samples (nanoparticulate suspensions, 100 µg/ml) were dropped into freshly cleaved mica, and after complete drying, and observed in non-contact mode using a NCS15 silicon cantilever (MikroMasch, Oregon, USA); the micrograph of the samples was recorded and it was analyzed using a digital software for scanning probe microscopy and a tool for nanotechnology (WSxM 5.0 development 9.4) (Horcas et al., 2007).

2.5. Cell culture

22Rv1 (prostate carcinoma)] and [ARPE-19 (retinal pigmented epithelium)] cell lines were cultured in RPMI-1640 Medium and Dulbecco's modified Eagle's medium (DMEM) (Sigma Aldrich, St. Louis, MO, USA), supplemented with 10 % heat-inactivated fetal bovine serum (FBS) (Corning, NY, USA) and grown at 37 °C in an atmosphere of 5 % CO₂ and high humidity (85 – 95 %) in a cell culture incubator (VWR 2325 Water-Jacketed CO₂ Incubator, Pa, USA).

2.6. In vitro cell viability assay

Cell viability was evaluated using the MTT assay (Roche, cell proliferation kit I, Roche, Cat. No. 11-465-007-001), according to manufacturer's instructions. Briefly, 2 x 10⁴ cells/well were suspended in 100 µL of RPMI or DMEM medium at 10 % of supplemented of FSB, according to ATCC specifications (Boyd & Paull, 1995); 22Rv1 and ARPE-19 were seeded on a flat-bottom 96-well plate and incubated per 24 h. Then, cell cultures were incubated in 100 µL of medium containing different concentrations of each of the cells diluted in medium and incubated for another 24 h. Control cell cultures were incubated with medium. After 4 h of cell culture, 10 µL of MTT stock solution (5 mg/mL) were added to each well. Formazan crystals formed were dissolved with 100 µL sodium dodecyl sulfate (SDS) and the absorbance in each well was read overnight using an ELISA plate reader (Benchmark Microplate Reader; Bio-Rad, Hercules, CA, USA) at test wavelength of 570 nm and a reference wavelength of 650 nm. Three independent assays were made, and all testing concentrations were assayed in triplicate.

2.7. Statistical analysis

Data were analyzed using an analysis of variance (ANOVA) with Tukey multiple comparisons test (Tukey's post hoc test), at a 95 % confidence interval, and the level of

significance of $P \leq 0.05$, (SPSS). All data are the mean value with their standard deviation (mean \pm S.D.) of three determination.

3. Results and discussion

3.1. Average diameter (D) and Zeta Potential characterization of PLGA-EPA nanoparticles

The D of the PLGA-PVA nanoparticles with or without EPA is shown in **Table 1**. The PLGA-PVA nanoparticles have the smallest size (135.57 nm) establishing significant differences among EPA-loaded nanoparticles ($P \leq 0.05$). The amount of EPA encapsulated in PLGA nanoparticle at different weight % has influence in the diameter size of nanoparticles, being the EPA-loaded PLGA 30 % the largest size (155.33 nm). Currently, many studies support that the increase in size of nanoparticles is related to the encapsulated drug amount (I. Bala et al., 2005).

Furthermore, the PDI values of PLGA-PVA and EPA-loaded PLGA-PVA nanoparticles are considered highly monodispersed ($PDI < 0.1$) (Lancheros et al., 2014). Additionally, PDI values can also indicate that there is no aggregation (Hughes, Budd, Tiede, & Lewis, 2014).

The Zeta potential decreases at a higher % of incorporation of EPA (**Table 1**); being the greater value for the PLGA-PVA nanoparticles without EPA (EPA / PLGA at 0 Wt%) with - 32.37 mV and the lowest for the EPA-loaded PLGA-PVA nanoparticles synthesized with 30 % of EPA (EPA / PLGA at 30 Wt%) (-5.64 mV). While the Zeta potential values recorded for EPA-loaded nanoparticles (5, 10 and 20 %) were -20.50, -17.07, -13.17 mV, respectively. The reduction of the Zeta potential for EPA-loaded nanoparticles could be due to the interactions occurring between the matrix and the encapsulated compound. In addition, it is known that Zeta potential values reported for stable systems are close to - 30 or + 30 mV, this to avoid aggregations over time (Cho et al., 2013).

The average size obtained for all PLGA-PVA systems with and without EPA are considered appropriated, due to cells can internalize PLGA nanoparticles of under to 300 nm in diameter by unspecific endocytosis process such as clathrin-, caveolae-mediated endocytosis or macropinocytosis (Cho et al., 2013; Mahl, Diendorf, Meyer-Zaika, & Epple, 2011) and then release the drug or bioactive compound at intracellular locations (Xu et al., 2009). The macropinocytosis process, occurs because the cell membrane protrudes and fuses with another

part of the membrane, producing large vesicles around the nanoparticles (Cho et al., 2013; Mahl, Diendorf, Meyer-Zaika, & Epple, 2011). It is important to mention that particles with a larger size (which varies around 1 to 10 μm) depend on phagocytosis (Garnett & Kallinteri, 2006; Harush-Frenkel, Altschuler, & Benita, 2008), however, for drug delivering proposed purposes small nanoparticles sizes are desired to prevent mononuclear phagocyte recognition and clearance by the immune system.

3.2. Encapsulation efficiency (EE), loading capacity (LC) and amount of EPA (yield) characterization of PLGA-EPA nanoparticles

Encapsulation efficiency (EE), loading capacity (LC) and amount of EPA (yield) are shown in **Table 2**. The EE varied between each percentage of EPA-loaded in PLGA nanoparticles, showing that at lowest % of EPA, the greater is the EE; at 5% EPA during the synthesis showed 100 % of EE (this being the highest value), so consecutively the other syntheses; the synthesis with 10 % of EPA showed a significant difference with the other syntheses ($P \leq 0.05$), and an EE of 75.68 %. In addition, the synthesis with 20 and 30 % EPA showed no significant difference ($P \leq 0.05$), however these were below 50 %.

An opposite effect to that already mentioned in EE parameters is observed when analyzing the LC parameters; the trend being that the higher the percentage of EPA incorporated during the synthesis, the greater the LC; the lowest % of LC was observed for EPA/PLGA at 5 % Wt, and the highest for EPA/PLGA at 30 % Wt (5 and 9.9, respectively). Addressing the results of the yield parameters, EPA/PLGA at 5 % Wt showed the lowest yield (1.5 mg/mL), EPA/PLGA at 10 and 20 % Wt showed no significant difference between them (2.28 and 2.65, mg/mL, respectively) ($P \leq 0.05$), and EPA/PLGA at 30 % Wt was the one with the highest yield with 2.97 mg/mL encapsulation.

3.3. Morphology of the PLGA-EPA nanoparticles at different Wt % of EPA with respect to the total amount of PLGA by AFM micrographs

The Figure 1 shown the morphology obtained by AFM of PLGA-PVA nanoparticles with and without EPA. The PLGA-PVA nanoparticles without EPA showed homogeneous size and spherical shape. The PLGA-PVA nanoparticles with 5 & 10 % (wt.) of EPA apparently showed homogeneous size and spherical shape with respect of the nanoparticles without EPA.

However, when the amount of EPA was increased (20-30 % wt), the spherical shape became as irregular shape and apparently heterogeneous size between the nanoparticles. These results agree with the average diameter (D) characterization by DLS. The PLGA-PVA-EPA 10 % (wt.) nanoparticles was proposed as the system with the highest incorporation of EPA that does not lose its morphological integrity, in addition there is greater homogeneity between the particles previously confirmed with the PDI values.

3.4. Cellular viability of human epithelial cells treated with PLGA-EPA 10 %

Cellular assays were development to evaluate the biological activity of the nanoparticles monitoring the cell viability (%). The MTT test was used to determine the cell viability and results are shown in **Table 3**.

The cancer cell line (22Rv1) are sensitive to all treatments. PLGA nanoparticles reduces the cellular viability around 50 % for the higher concentration (3000 µg/mL). This reduction could be due to the high concentration of PLGA, due to the non-enzymatic degradation (hydrolysis of its ester bonds) of the PLGA to its acidic monomers (lactic acid and glycolic acid), decreasing the pH of cytosol affecting the physiological function of the cell (Makadia & Siegel, 2011). Albeit of PLGA has been considered a biodegradable and non-toxic synthetic polymer (depending on the concentration) (Panyam & Labhasetwar, 2003), there are many factors which could affect the cellular viability (cytotoxicity), such size distribution, surface charge and the presence of functional groups on the surface of the particle (Biazar et al., 2011; Donaldson, Stone, Tran, Kreyling, & Borm, 2004; Garnett & Kallinteri, 2006).

The pure EPA standard showed a reduction below 50 % viability when using concentrations greater than 57 µg/mL, and the lowest viability being 8.70 % with the concentration of 228 µg/mL. As previously was described, lipid peroxidation is the potential mechanism through EPA being cytotoxicity (Germain, Chajès, Cognault, Lheillery, & Bougnoux, 1998), as was earlier demonstrated in breast, lung and prostate cancer cells (Bégin, Das, Ells, & Horrobin, 1985). EPA encapsulation could overcome this barrier, this according to already described drug parameters (Andrei et al., 2020; Ehdaie, 2007; Gao, Zhang, & Sun, 2012; Parhi, Mohanty, & Sahoo, 2012).

According to the values obtained in the drug encapsulation trials, we were able to determine that the system developed with 10 % EPA presented the best results; this is because

it is optimum percentage of synthesis, this parameter indicates the percentage at which a maximum EE % can be obtained without wasting EPA reagent, that is, there is the minimum amount of non-encapsulated EPA (in the supernatant); this value was obtained from the average of 3 values (optimal amount of EPA on the synthesis of 10, 20 and 30 % of EPA), being 2.63 mg/mL of EPA, this would give us 100% of EE and 0% of EPA waste (in the supernatant), resulting in an optimal percentage of EPA during the synthesis of 8.8% (theoretically). Based on this, the practical synthesis of PLGA-PVA-EPA 10% was the closest to that percentage.

Conferring to the previous tests, by incorporating 10 % EPA during the synthesis of the PLGA-EPA nanoparticles, a yield of 2.28 mg/mL (or 228 µg/mL) is obtained; so in the table we indicate in a column the concentration of PLGA and the concentration of EPA; when the 10 % PLGA-EPA system is used as a treatment, it's observed that all concentrations decrease more than 50 % of the cell viability, this even at the lowest concentration; the cell viability of latter concentration of PLGA-EPA 10 % (39.89 %) being significantly different from the latest concentration of PLGA nanoparticle and the pure EPA standard (96.66 and 71.72, respectively) ($P \leq 0.05$). This indicates that the encapsulation of EPA in the nanoparticulate PLGA matrix enhances its activity on a cancer cell. This results is similar to previous studies, in where the EPA is encapsulated in chitosan system, have shown that biological activity can be improved (Kim, Lee, Jeong, Kim, & Lee, 2012).

With the objective of evaluating the cytotoxicity of the systems in a cancerous cell line and a non-cancerous cell line, the results of the percentage of cell viability on ARPE-19 (non-cancerous cells) will be presented below. These results are shown in **Table 3**. In general, all systems/treatments showed a dose-response effect, which means that the viability is dependent on the concentration. When evaluating PLGA particles without EPA, it was evident that ARPE-19 is more resistant to the exposure of this system than 22Rv1, this is because the % of viability is much higher in general at all concentrations; in addition, at the lowest concentration (375 µg/mL), the PLGA particles presented 100 % cell viability.

The treatment of the pure EPA standard showed the lowest viability values (19.33 %) by using the lowest concentration (228 µg/mL); however, this value was lower than that obtained with this same concentration on line 22Rv1 (8.70 %), showing that EPA is more cytotoxic for a cancerous cell line than for a non-cancerous cell line. Despite the self-oxidation barrier in the physiological environment, EPA has another challenge to overcome; Due to its large size (for

example, EPA: 302 g/mol), some drugs that circulate intravenously escape renal clearance, and unable to penetrate through tight endothelial junctions of normal blood vessels, their concentration builds up in the plasma rendering them long plasma half-life (Greish, 2010); that is why encapsulated in a polymer matrix could solve this barrier.

Finally, the results of cell viability of the PLGA-EPA 10 % particles pointed out that: the two highest concentrations had the lowest viability percentages (23.63 and 35.63 %), since there were no significant differences with the higher EPA concentration (19.33 %) ($P \leq 0.05$); however, when comparing the lower concentration between 22Rv1 and ARPE-19, it's shown as if there are significant differences between treatments ($P \leq 0.05$); This is due to the fact that when using the lowest contraction in ARPE-19, 100 % viability is shown, while in 22Rv1, 39.89 % is shown. This proves the ability of the PLGA-EPA 10 % nanoparticles system to be effective against a cancerous cell line and not on a non-cancerous cell line at this concentration (375 $\mu\text{g/mL}$ total mass, where 28.5 $\mu\text{g/mL}$ belong to EPA).

One way of explaining the successful achievement of the selective selection of nanoparticles-drug for tumor cancer cells is due to abnormalities in their vasculature (i.e., hyper-vascularization), aberrant vascular architecture / form, pro-production factors of vascular permeability that stimulate extravasation within cells and lack of lymphatic drainage (Greish, 2010); this process is known as the enhanced permeability and retention (EPR) effect (Maeda, 2010). Therefore, nanoparticles into tumor cancerous cells through a leaky tumor vasculature and are then retained in the tumor bed due to reduced lymphatic drainage unlike normal cells (non-cancerous-tumor cells) (Kobayashi, Watanabe, & Choyke, 2014). Therefore, useful design parameters of a nanoparticle include limiting the size to < 300 nm in diameter, and maintaining a net surface charge as close to neutral as possible, this to provide a hydrophilic surface (Maeda, Nakamura, & Fang, 2013); and according to this, our 10 % PLGA-EPA system meets the parameters.

This same effect (of reducing the cytotoxicity of a chemotherapeutic agent) has already been observed in previous reports when using matrices with PLGA; as well as increase bioavailability, stability and make cancer cells more sensitive (Siddharth, Nayak, Nayak, Bindhani, & Kundu, 2017); In addition to another study that also increases the bioavailability of a powerful free radical chain-breaking antioxidant with PLGA matrices (Simon, Stout, & Sabliov, 2016). For last, the nanoparticles can reduce immunogenicity and side effects; the

maximum tolerated dose of drugs (in this case EPA) can be increased, this is because the non-toxic (biocompatible at these concentrations assessed) polymer with which the nanoparticle is created, reduces exposure to the drug and becomes less toxic.

Conclusion

EPA-loaded nanoparticles have been synthesized using simple emulsion method, which proves to be a suitable method for obtaining an appropriate system to synthesize EPA; the characteristics that is determined if the method is adequate were that a maximum encapsulation is obtained by using an optimal percentage of EPA in the synthesis; which ensures that the entire drug is encapsulated, and because the percentage of synthesis of 10 % of EPA was the closest to the optimum, this is selected as recommended. In addition, they are biodegradable, too very preferred because they are promising in the drug delivery system.

In our case, the nanoparticle that was designed possesses the ability to decrease the degree of cytotoxicity of EPA on a non-cancer cell line; likewise, the effect was improved when compared to the pure EPA standard, making it more effective. However studies where the protection of the drug (EPA) against oxidation is proven should be carried out.

Acknowledgment

Authors wish to thank Consejo Nacional de Ciencia y Tecnología (CONACYT) Mexico for financing the project No. 241133 and for granting research scholarships and for funding this project.

Reference

- Andrei, L., Kasas, S., Ochoa Garrido, I., Stanković, T., Suárez Korsnes, M., Vaclavikova, R., ... Pešić, M. (2020). Advanced technological tools to study multidrug resistance in cancer. *Drug Resistance Updates*, 48. <https://doi.org/10.1016/j.drug.2019.100658>
- Anschau, A., Caruso, C. S., Kuhn, R. C., & Franco, T. T. (2017). Validation of the sulphovanillin (SPV) method for the determination of lipid content in oleaginous microorganisms. *Brazilian Journal of Chemical Engineering*, 34(1), 19–27. <https://doi.org/10.1590/0104-6632.20170341s20140222>
- Antal, O., Hackler, L., Shen, J., Mán, I., Hideghéty, K., Kitajka, K., & Puskás, L. G. (2014).

- Combination of unsaturated fatty acids and ionizing radiation on human glioma cells: cellular, biochemical and gene expression analysis.* <https://doi.org/10.1186/1476-511X-13-142>
- Arab-Tehrany, E., Jacquot, M., Gaiani, C., Imran, M., Desobry, S., & Linder, M. (2012, May). Beneficial effects and oxidative stability of omega-3 long-chain polyunsaturated fatty acids. *Trends in Food Science and Technology*. <https://doi.org/10.1016/j.tifs.2011.12.002>
- Aruoma, O. I. (1998). Free radicals, oxidative stress, and antioxidants in human health and disease. *JAOCs, Journal of the American Oil Chemists' Society*, 75(2), 199–212. <https://doi.org/10.1007/s11746-998-0032-9>
- Bala, I., Bhardwaj, V., Hariharan, S., Sitterberg, J., Bakowsky, U., & Ravi Kumar, M. N. V. (2005). Design of biodegradable nanoparticles: A novel approach to encapsulating poorly soluble phytochemical ellagic acid. *Nanotechnology*, 16(12), 2819–2822. <https://doi.org/10.1088/0957-4484/16/12/014>
- Bala, Indu, Hariharan, S., & Kumar, M. N. V. R. (2004). PLGA nanoparticles in drug delivery: The state of the art. *Critical Reviews in Therapeutic Drug Carrier Systems*. <https://doi.org/10.1615/CritRevTherDrugCarrierSyst.v21.i5.20>
- Bégin, M. E., Das, U. N., Ells, G., & Horrobin, D. F. (1985). Selective killing of human cancer cells by polyunsaturated fatty acids. *Prostaglandins, Leukotrienes and Medicine*, 19(2), 177–186. [https://doi.org/10.1016/0262-1746\(85\)90084-8](https://doi.org/10.1016/0262-1746(85)90084-8)
- Biazar, E., Majdi, Zafari, M., Avar, M., Aminifard, S., Zaeifi, D., ... Gh. (2011). Nanotoxicology and nanoparticle safety in biomedical designs. *International Journal of Nanomedicine*, 1117. <https://doi.org/10.2147/ijn.s16603>
- Boyd, M. R., & Paull, K. D. (1995). Some practical considerations and applications of the national cancer institute in vitro anticancer drug discovery screen. *Drug Development Research*, 34(2), 91–109. <https://doi.org/10.1002/ddr.430340203>
- Brouwer, I. A. (2008). Fish, omega-3 fatty acids and heart disease. In *Improving Seafood Products for the Consumer* (pp. 165–181). <https://doi.org/10.1533/9781845694586.2.165>
- Carocho, M., Morales, P., & Ferreira, I. C. F. R. (2018). Antioxidants: Reviewing the chemistry, food applications, legislation and role as preservatives. *Trends in Food Science and Technology*. <https://doi.org/10.1016/j.tifs.2017.11.008>
- Cho, E. J., Holback, H., Liu, K. C., Abouelmagd, S. A., Park, J., & Yeo, Y. (2013, June 3).

- Nanoparticle characterization: State of the art, challenges, and emerging technologies. *Molecular Pharmaceutics*. <https://doi.org/10.1021/mp300697h>
- Ciavatta, M. L., Lefranc, F., Carbone, M., Mollo, E., Gavagnin, M., Betancourt, T., ... Kiss, R. (2017, July 1). Marine Mollusk-Derived Agents with Antiproliferative Activity as Promising Anticancer Agents to Overcome Chemotherapy Resistance. *Medicinal Research Reviews*. John Wiley & Sons, Ltd. <https://doi.org/10.1002/med.21423>
- Colquhoun, A. (2009). Mechanisms of Action of Eicosapentaenoic Acid in Bladder Cancer Cells In Vitro: Alterations in Mitochondrial Metabolism, Reactive Oxygen Species Generation and Apoptosis Induction. *Journal of Urology*, 181(4), 1885–1893. <https://doi.org/10.1016/j.juro.2008.11.092>
- Colquhoun, A., & Schumacher, R. I. (2001). γ -Linolenic acid and eicosapentaenoic acid induce modifications in mitochondrial metabolism, reactive oxygen species generation, lipid peroxidation and apoptosis in Walker 256 rat carcinosarcoma cells. *Biochimica et Biophysica Acta - Molecular and Cell Biology of Lipids*, 1533(3), 207–219. [https://doi.org/10.1016/S1388-1981\(01\)00136-6](https://doi.org/10.1016/S1388-1981(01)00136-6)
- Conner, S. D., & Schmid, S. L. (2003). Regulated portals of entry into the cell. *Nature*. <https://doi.org/10.1038/nature01451>
- Das, U. N. (1990). Gamma-linolenic acid, arachidonic acid, and eicosapentaenoic acid as potential anticancer drugs. *Nutrition*.
- Donaldson, K., Stone, V., Tran, C. L., Kreyling, W., & Borm, P. J. A. (2004, September). Nanotoxicology. *Occupational and Environmental Medicine*. <https://doi.org/10.1136/oem.2004.013243>
- Ehdaie, B. (2007). Application of nanotechnology in cancer research: Review of progress in the National Cancer Institute's alliance for nanotechnology. *International Journal of Biological Sciences*. Ivyspring International Publisher. <https://doi.org/10.7150/ijbs.3.108>
- Ferrari, M. (2005, March). Cancer nanotechnology: Opportunities and challenges. *Nature Reviews Cancer*. <https://doi.org/10.1038/nrc1566>
- Gao, Z., Zhang, L., & Sun, Y. (2012, August 20). Nanotechnology applied to overcome tumor drug resistance. *Journal of Controlled Release*. <https://doi.org/10.1016/j.jconrel.2012.05.051>
- Garnett, M. C., & Kallinteri, P. (2006). Nanomedicines and nanotoxicology: some physiological

- principles. *Occupational Medicine*, 56(5), 307–311.
<https://doi.org/10.1093/occmed/kql052>
- Germain, E., Chajès, V., Cognault, S., Lhcillery, C., & Bougnoux, P. (1998). Enhancement of doxorubicin cytotoxicity by polyunsaturated fatty acids in the human breast tumor cell line MDA-MB-231: Relationship to lipid peroxidation. *International Journal of Cancer*, 75(4), 578–583.
[https://doi.org/10.1002/\(SICI\)1097-0215\(19980209\)75:4<578::AID-IJC14>3.0.CO;2-5](https://doi.org/10.1002/(SICI)1097-0215(19980209)75:4<578::AID-IJC14>3.0.CO;2-5)
- Gerwick, W. H., & Moore, B. S. (2012, January 27). Lessons from the past and charting the future of marine natural products drug discovery and chemical biology. *Chemistry and Biology*. Cell Press. <https://doi.org/10.1016/j.chembiol.2011.12.014>
- Gottesman, M. M., & Pastan, I. (1993). Biochemistry of Multidrug Resistance Mediated by the Multidrug Transporter. *Annual Review of Biochemistry*, 62(1), 385–427.
<https://doi.org/10.1146/annurev.bi.62.070193.002125>
- Greish, K. (2010). Enhanced permeability and retention (EPR) effect for anticancer nanomedicine drug targeting. *Methods in Molecular Biology (Clifton, N.J.)*, 624, 25–37.
https://doi.org/10.1007/978-1-60761-609-2_3
- Gullapalli, R. P. (2010). Soft gelatin capsules (softgels). *Journal of Pharmaceutical Sciences*. John Wiley and Sons Inc. <https://doi.org/10.1002/jps.22151>
- Hans, M. L., & Lowman, A. M. (2002). Biodegradable nanoparticles for drug delivery and targeting. *Current Opinion in Solid State and Materials Science*, 6(4), 319–327.
[https://doi.org/10.1016/S1359-0286\(02\)00117-1](https://doi.org/10.1016/S1359-0286(02)00117-1)
- Harris, W. S., Miller, M., Tighe, A. P., Davidson, M. H., & Schaefer, E. J. (2008, March). Omega-3 fatty acids and coronary heart disease risk: Clinical and mechanistic perspectives. *Atherosclerosis*. <https://doi.org/10.1016/j.atherosclerosis.2007.11.008>
- Harush-Frenkel, O., ... Y. A.-C. R. in, & 2008, undefined. (n.d.). Nanoparticle-cell interactions: drug delivery implications. *DL.Begellhouse.Com*. Retrieved from <http://www.dl.begellhouse.com/journals/3667c4ae6e8fd136,6d9016640bf024d0,5544e9c7743829ac.html>
- Harush-Frenkel, O., Altschuler, Y., & Benita, S. (2008). Nanoparticle-cell interactions: Drug delivery implications. *Critical Reviews in Therapeutic Drug Carrier Systems*, 25(6), 485–544. <https://doi.org/10.1615/CritRevTherDrugCarrierSyst.v25.i6.10>
- Horcas, I., Fernández, R., Gómez-Rodríguez, J. M., Colchero, J., Gómez-Herrero, J., & Baro,

- A. M. (2007). WSXM: A software for scanning probe microscopy and a tool for nanotechnology. *Review of Scientific Instruments*, 78(1). <https://doi.org/10.1063/1.2432410>
- Huang, R. B., Mocherla, S., Heslinga, M. J., Charoenphol, P., & Eniola-Adefeso, O. (2010, August 8). Dynamic and cellular interactions of nanoparticles in vascular-targeted drug delivery (review). *Molecular Membrane Biology*. <https://doi.org/10.3109/09687688.2010.499548>
- Hughes, J. M., Budd, P. M., Tiede, K., & Lewis, J. (2014). Polymerized high internal phase emulsion monoliths for the chromatographic separation of engineered nanoparticles. *Journal of Applied Polymer Science*, 132(1). <https://doi.org/10.1002/app.41229>
- Igarashi, M., & Miyazawa, T. (2000). Do conjugated eicosapentaenoic acid and conjugated docosahexaenoic acid induce apoptosis via lipid peroxidation in cultured human tumor cells? *Biochemical and Biophysical Research Communications*, 270(2), 649–656. <https://doi.org/10.1006/bbrc.2000.2484>
- Jacobsen, C., Hartvigsen, K., Lund, P., Thomsen, M. K., Skibsted, L. H., Hølmer, G., ... Meyer, A. S. (2001). Oxidation in fish oil-enriched mayonnaise: 4. Effect of tocopherol concentration on oxidative deterioration. *European Food Research and Technology*, 212(3), 308–318. <https://doi.org/10.1007/s002170000251>
- Johnson, D. R., & Decker, E. A. (2015). The Role of Oxygen in Lipid Oxidation Reactions: A Review. *Annual Review of Food Science and Technology*, 6(1), 171–190. <https://doi.org/10.1146/annurev-food-022814-015532>
- Kampa, M., Nifli, A. P., Notas, G., & Castanas, E. (2007). Polyphenols and cancer cell growth. *Reviews of Physiology, Biochemistry and Pharmacology*, 159, 79–113. https://doi.org/10.1007/112_2006_0702
- Kim, J., Lee, C. M., Jeong, H. J., Kim, D. W., & Lee, K. Y. (2012). Elevated anti-inflammatory effects of eicosapentaenoic acid based self-aggregated glycol chitosan nanoparticles. *Journal of Nanoscience and Nanotechnology*, 12(3), 2672–2678. <https://doi.org/10.1166/jnn.2012.5685>
- Kim, J., Lee, C. M., Jeong, H. J., & Lee, K. Y. (2011). In vivo tumor accumulation of nanoparticles formed by ionic interaction of glycol chitosan and fatty acid ethyl ester. In *Journal of Nanoscience and Nanotechnology* (Vol. 11, pp. 1160–1166).

- <https://doi.org/10.1166/jnn.2011.3569>
- Kobayashi, H., Watanabe, R., & Choyke, P. L. (2014). Improving conventional enhanced permeability and retention (EPR) effects; What is the appropriate target? *Theranostics*. <https://doi.org/10.7150/thno.7193>
- Kris-Etherton, P. M., Harris, W. S., & Appel, L. J. (2003, February 1). Omega-3 fatty acids and cardiovascular disease: New recommendations from the American Heart Association. *Arteriosclerosis, Thrombosis, and Vascular Biology*. <https://doi.org/10.1161/01.ATV.0000057393.97337.AE>
- Lancheros, J. C., Beleño, R. J. ;, Ángel, J., Guerrero, ;, Arturo, C., Godoy-Silva, ;, & Darío, R. (2014). Producción de nanopartículas de PLGA por el método de emulsión y evaporación para encapsular N-Acetilcisteína (NAC). *Universitas Scientiarum*, 19(2), 162–168. <https://doi.org/10.11144/Javeriana.SC19-2.mpre>
- Lobo, V., Patil, A., Phatak, A., & Chandra, N. (2010, July). Free radicals, antioxidants and functional foods: Impact on human health. *Pharmacognosy Reviews*. <https://doi.org/10.4103/0973-7847.70902>
- M.S. Tokumoto, V. Briois, C. V. S. and S. H. P. (2003). Preparation of ZnO nanoparticles: structural study, 547–551.
- Maeda, H. (2010, May 19). Tumor-selective delivery of macromolecular drugs via the EPR effect: Background and future prospects. *Bioconjugate Chemistry*. <https://doi.org/10.1021/bc100070g>
- Maeda, H., Nakamura, H., & Fang, J. (2013, January). The EPR effect for macromolecular drug delivery to solid tumors: Improvement of tumor uptake, lowering of systemic toxicity, and distinct tumor imaging in vivo. *Advanced Drug Delivery Reviews*. <https://doi.org/10.1016/j.addr.2012.10.002>
- Mahl, D., Diendorf, J., Meyer-Zaika, W., & Eppel, M. (2011). Possibilities and limitations of different analytical methods for the size determination of a bimodal dispersion of metallic nanoparticles. *Colloids and Surfaces A: Physicochemical and Engineering Aspects*, 377(1–3), 386–392. <https://doi.org/10.1016/j.colsurfa.2011.01.031>
- Makadia, H. K., & Siegel, S. J. (2011). Poly Lactic-co-Glycolic Acid (PLGA) as biodegradable controlled drug delivery carrier. *Polymers*, 3(3), 1377–1397. <https://doi.org/10.3390/polym3031377>

- Malam, Y., Loizidou, M., & Seifalian, A. M. (2009, November). Liposomes and nanoparticles: nanosized vehicles for drug delivery in cancer. *Trends in Pharmacological Sciences*. <https://doi.org/10.1016/j.tips.2009.08.004>
- Motaung, E., Prinsloo, S. E., Van Aswegen, C. H., Du Toit, P. J., Becker, P. J., & Du Plessis, D. J. (1999). Cytotoxicity of combined essential fatty acids on a human prostate cancer cell line. *Prostaglandins Leukotrienes and Essential Fatty Acids*, 61(5), 331–337. <https://doi.org/10.1054/plef.1999.0107>
- Nair, V., Cooper, C. S., Vietti, D. E., & Turner, G. A. (1986). The chemistry of lipid peroxidation metabolites: Crosslinking reactions of malondialdehyde. *Lipids*, 21(1), 6–10. <https://doi.org/10.1007/BF02534294>
- Panyam, J., & Labhasetwar, V. (2003, February 24). Biodegradable nanoparticles for drug and gene delivery to cells and tissue. *Advanced Drug Delivery Reviews*. Elsevier. [https://doi.org/10.1016/S0169-409X\(02\)00228-4](https://doi.org/10.1016/S0169-409X(02)00228-4)
- Parhi, P., Mohanty, C., & Sahoo, S. K. (2012, September). Nanotechnology-based combinational drug delivery: An emerging approach for cancer therapy. *Drug Discovery Today*. <https://doi.org/10.1016/j.drudis.2012.05.010>
- Park, J. W. (2002). Liposome-based drug delivery in breast cancer treatment. *Breast Cancer Research*, 4(3), 95–99. <https://doi.org/10.1186/bcr432>
- Polo, S., & Di Fiore, P. P. (2006, March 10). Endocytosis conducts the cell signaling orchestra. *Cell*. <https://doi.org/10.1016/j.cell.2006.02.025>
- Romeu-Nadal, M., Castellote, A. I., & López-Sabater, M. C. (2004). Headspace gas chromatographic method for determining volatile compounds in infant formulas. In *Journal of Chromatography A* (Vol. 1046, pp. 235–239). <https://doi.org/10.1016/j.chroma.2004.06.032>
- Ryan, A. S., Astwood, J. D., Gautier, S., Kuratko, C. N., Nelson, E. B., & Salem, N. (2010). Effects of long-chain polyunsaturated fatty acid supplementation on neurodevelopment in childhood: A review of human studies. *Prostaglandins Leukotrienes and Essential Fatty Acids*, 82(4–6), 305–314. <https://doi.org/10.1016/j.plefa.2010.02.007>
- Sahoo, S. K., & Labhasetwar, V. (2005). Enhanced antiproliferative activity of transferrin-conjugated paclitaxel-loaded nanoparticles is mediated via sustained intracellular drug retention. *Molecular Pharmaceutics*, 2(5), 373–383. <https://doi.org/10.1021/mp050032z>

- Salminen, H., Helgason, T., Kristinsson, B., Kristbergsson, K., & Weiss, J. (2013). Formation of solid shell nanoparticles with liquid ω -3 fatty acid core. *Food Chemistry*, 141(3), 2934–2943. <https://doi.org/10.1016/j.foodchem.2013.05.120>
- Shahidi, F., & Zhong, Y. (2010, November). Lipid oxidation and improving the oxidative stability. *Chemical Society Reviews*. <https://doi.org/10.1039/b922183m>
- Siddharth, S., Nayak, A., Nayak, D., Bindhani, B. K., & Kundu, C. N. (2017). Chitosan-Dextran sulfate coated doxorubicin loaded PLGA-PVA-nanoparticles caused apoptosis in doxorubicin resistance breast cancer cells through induction of DNA damage. *Scientific Reports*, 7(1). <https://doi.org/10.1038/s41598-017-02134-z>
- Sigma-Aldrich Staff. (2019). Drug Delivery FAQs |. Retrieved January 27, 2020, from <https://www.sigmaaldrich.com/technical-documents/articles/materials-science/drug-delivery/drug-delivery-questions.html>
- Simon, L. C., Stout, R. W., & Sabliov, C. (2016, April 15). Bioavailability of Orally Delivered Alpha-Tocopherol by Poly(Lactic-Co-Glycolic) Acid (PLGA) Nanoparticles and Chitosan Covered PLGA Nanoparticles in F344 Rats. *Nanobiomedicine*. SAGE Publications Ltd. <https://doi.org/10.5772/63305>
- Sisein, E. A. (2014). Biochemistry of Free Radicals and Antioxidants. *Scholars Academic Journal of Biosciences (SAJB)*, 2(2), 110–118. https://doi.org/10.5822/978-1-59726-228-6_3_WATER
- Steele, D., & Dietel, G. (1993). Softgel Manufacturing Process. *U.S. Patent*. Retrieved from <https://patents.google.com/patent/US5200191A/en>
- Szakács, G., Paterson, J. K., Ludwig, J. A., Booth-Genthe, C., & Gottesman, M. M. (2006, March). Targeting multidrug resistance in cancer. *Nature Reviews Drug Discovery*. <https://doi.org/10.1038/nrd1984>
- Tsuzuki, T., Igarashi, M., & Miyazawa, T. (2004). Conjugated Eicosapentaenoic Acid (EPA) Inhibits Transplanted Tumor Growth via Membrane Lipid Peroxidation in Nude Mice. *The Journal of Nutrition*, 134(5), 1162–1166. <https://doi.org/10.1093/jn/134.5.1162>
- Tsuzuki, T., Kambe, T., Shibata, A., Kawakami, Y., Nakagawa, K., & Miyazawa, T. (2007). Conjugated EPA activates mutant p53 via lipid peroxidation and induces p53-dependent apoptosis in DLD-1 colorectal adenocarcinoma human cells. *Biochimica et Biophysica Acta - Molecular and Cell Biology of Lipids*, 1771(1), 20–30.

<https://doi.org/10.1016/j.bbalip.2006.11.006>

- Wang, J. J., Zeng, Z. W., Xiao, R. Z., Xie, T., Zhou, G. L., Zhan, X. R., & Wang, S. L. (2011). Recent advances of chitosan nanoparticles as drug carriers. *International Journal of Nanomedicine*. <https://doi.org/10.2147/ijn.s17296>
- Xu, P., Gullotti, E., Tong, L., Highley, C. B., Errabelli, D. R., Hasan, T., ... Yeo, Y. (2009). Intracellular drug delivery by poly(lactic-co-glycolic acid) nanoparticles, revisited. *Molecular Pharmaceutics*, 6(1), 190–201. <https://doi.org/10.1021/mp800137z>

Table 1. Z-Average diameter (D-z), polydispersion index (PDI) and zeta potential of PLGA-EPA nanoparticles at different Wt % of EPA with respect to the total amount of PLGA.

EPA/PLGA	D _z	PDI	Zeta Potential
----------	----------------	-----	----------------

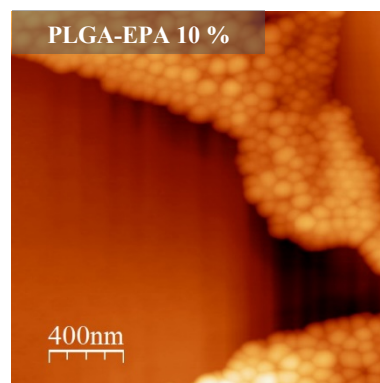
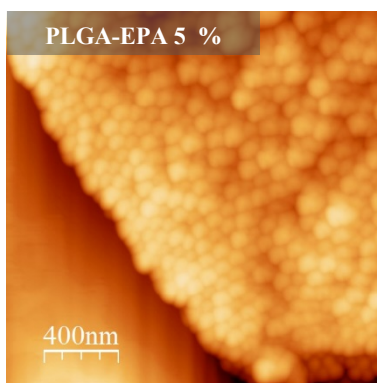
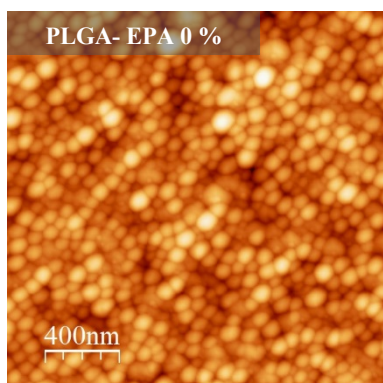
(Wt %)	(nm)		(mV)
0	135.57 ± 1.19 a	0.09 ± 0.008 a	-32.37 ± 0.71 e
5	137.33 ± 0.76 a	0.05 ± 0.03 a	-20.50 ± 2.05 d
10	143.87 ± 0.21 b	0.07 ± 0.027a	-17.07 ± 0.43 c
20	144.43 ± 0.41 b	0.06 ± 0.017 a	-13.17 ± 1.00 b
30	155.33 ± 1.10 c	0.07 ± 0.023 a	-5.64 ± 0.23 a

Values presented as mean ± S.D. indicate the replicates of three experiments. Values with different letters are significantly different ($P \leq 0.05$); Tukey significant difference test.

Table 2. Encapsulation efficiency (EE), loading capacity (LC) and amount of EPA (yield) contained in the system of PLGA-EPA nanoparticles at different Wt % of EPA with respect to the total amount of PLGA.

EPA/PLGA (Wt %)	EE (%)	LC (%)	Yield (mg/mL)
5	100 ± 3.8 c	5.0 ± 0.34 a	1.50 ± 0.103 a
10	75.68 ± 9.5 b	7.6 ± 0.87 ab	2.28 ± 0.263 b
20	44.17 ± 4.0 a	8.83 ± 0.36 ab	2.65 ± 0.109 bc
30	33.05 ± 4.6 a	9.9 ± 0.42 b	2.97 ± 0.126 c

Values presented as mean ± S.D. indicate the replicates of three experiments. Values with different letters are significantly different ($P \leq 0.05$); Tukey significant difference test.



PLGA-EPA 30 %

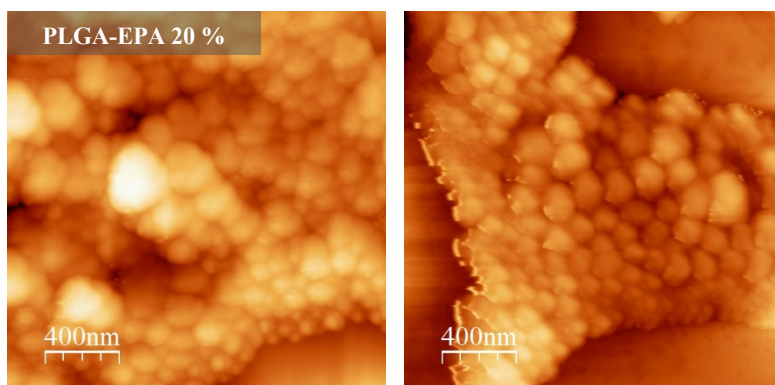


Figure 1. AFM micrographs of PLGA-EPA nanoparticles at different Wt % of EPA with respect to the total amount of PLGA.

Table 3. Percentage of cell viability of human epithelial cells treated with PLGA-EPA 10 % nanoparticles at 24 h

		Concentration ($\mu\text{g/mL}$)		Cell viability (%)	
		PLGA	EPA	22Rv1	ARPE-19
PLGA particles	3000			52.13 ± 1.29 cA	69.69 ± 1.57 cB
	1500			68.08 ± 8.62 deA	73.75 ± 1.05 cA
	750			75.49 ± 6.69 eA	88.54 ± 3.81 dB
	375			96.66 ± 7.60 fA	100.00 ± 5.11 eA
Pure EPA			228	8.70 ± 2.59 aA	19.33 ± 3.13 aB
			114	22.07 ± 1.53 aA	53.39 ± 2.53 bB

		57	54.55 ± 7.21 cdA	89.90 ± 2.38 dB
		28.5	71.72 ± 2.36 eA	92.36 ± 5.01 deB
PLGA-EPA 10 % particles	3000	*228	7.65 ± 1.40 aA	23.63 ± 4.36 aB
	1500	*114	9.72 ± 1.39 aA	25.63 ± 3.64 aB
	750	*57	24.09 ± 5.95 abA	58.95 ± 1.81 bB
	375	*28.5	39.89 ± 8.37 bcA	100.00 ± 1.11 eB

Values presented as mean ± S.D. indicate the replicates of three experiments. Values with different letters are significantly different ($P \leq 0.05$); lowercase letters represent differences between the entire column (all concentrations of all treatments on only one cell line), and capital letters represent a difference between the line (cell viability of 22Rv1 vs ARPE-19 with the same concentration); Tukey significant difference test. * This value represents the EPA content within the system, this according to the performance results

CONCLUSIONES GENERALES

Se logró obtener e identificar una fracción constituyente principalmente con tres lípidos (entre ellos, de importancia bioactiva: un ácido graso poliinsaturado y un nuevo indolocarbazole derivado de alcaloide), presentando propiedades quimioprotectoras (anti-proliferativa/pro-apoptótica, anti-oxidante y anti-inflamatoria); además, la encapsulación nanotecnológica de uno de ellos logró mantener la actividad biológica; todo esto en un sistema *in vitro*.

RECOMENDACIONES

- Se recomienda sintetizar químicamente a partir de precursores orgánicos el nuevo indolocarbazole derivado de alcaloide, así mismo, evaluarlo de nuevo en los mismos ensayos *in vitro* para conocer el comportamiento aislado de los demás compuestos (evaluación en su forma pura).

- Realizar más ensayos bioquímicos de los ya utilizados (relacionados con anti-proliferación / pro-apoptosis) como: arresto del ciclo celular, activación de caspasas extrínsecas / intrínsecas, y regulación de proteínas pro- y anti- apoptóticas.
- Llevar a cabo estudios *in vivo* de anti-tumorigénesis, los cuales serán pertinentes para conocer si el compuesto pudiera tener utilidad como agente quimioterapéutico.
- Llevar a cabo estudios para profundizar más en pruebas relacionadas con el microambiente carcinogénico (anti-oxidante/cito-protector, anti-inflamatorio e inclusive anti-angiogénico), los cuales ayudarán a conocer más si este compuesto, además de detener la proliferación de las células cancerígenas por medio de apoptosis, de alguna forma interfiere de forma positiva en el ambiente carcinogénico (disminución del estrés oxidativo, procesos inflamatorios y restricción de nutrientes, respectivamente).
- Por último, con respecto a la posible aplicación nanotecnológica del ácido graso poliinsaturado, se recomienda hacer una completa caracterización físico-química del sistema de partícula, esto para conocer de qué forma está dada la posible interacción entre los componentes, además realizar ensayos de liberación de fármaco, mecanismos de internalización celular y mecanismo de acción apoptótica.